CHAPTER 1

INTRODUCTION

1.1 Micelle

1.1.1. Overview of Micelle

Micelle is one type of self-assembled amphiphiles with special ability to break and reform over a wide range of aggregation sizes from nano- to milimeters, as well as variation in its aggregation shape. The uniqueness of its ability with superior flexibility has brought it to everyone's attention and it has been successfully utilized in various branches of applications.[1-4] In conjunction to that, the basic understanding of the physicochemical properties of micelle has become a great necessity to all. Micelle is usually characterized by its shape, aggregation number, the critical micellar concentration (cmc) and its degree of ionization (for ionic micelles only) by a number of approaches such as NMR study,[5] neutron or X-ray scattering,[5,6] chemical probes manipulation,[7,8] electrochemical methods[9] and electrophoresis[10].

1.1.2 Structure of Micelles

Micelle-forming surfactant consists of the hydrophilic head and hydrophobic tail of carbon atoms usually 8 to 18 in number.[11] The hydrophilic head can be nonionic, positive or negative in charge, or simultaneously having both positive and negative groups. Aggregation of micelle in polar solvent results in the formation of "normal" micelle in which the head groups remain exposed to the bulk polar solvent while the hydrophobic tail groups comprise the interior region of the micelle as the general structure shown by the Stigter model[12] in **Figure 1.1**.

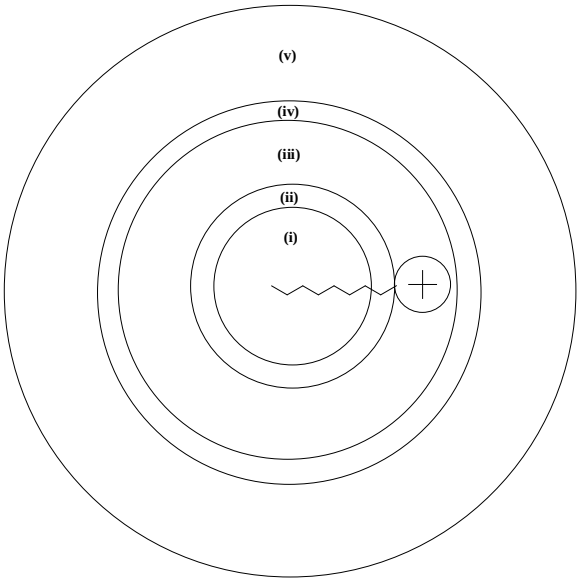

Figure 1.1 : Stigter Model for micellar structure.

Each aggregation as pictured in **Figure 1.1** unites a polar/ionic head and a nonpolar tail within the same molecule due to the simultaneous hydrophilic and hydrophobic behavior of each molecule. The nonpolar part, which is typically made up of one or more alkyl chains, causes these compounds to be sparingly soluble in water, whereas the polar or ionic part interacts strongly with water. It can be said that the core **(i)** (**Figure 1.1**) of the micelle is composed mainly of the uncharged carbon chains. Surrounding the core is a layer called Stern layer or palisade layer **(iii**) with a Core-Stern layer boundary **(ii)** as a separator. Here, in the Stern layer, the charged hydrophilic heads are placed adjacent to each other to maximize the interaction with water. A certain number of counterions will also inhibit this layer and might be able to neutralize 50 - 70 percent of the surface charges. Addition of counterions with increasing concentration and/or increasing hydrophobicity will eventually increase the fraction of neutralized charges at the micellar surface due to the polar head groups-counterions interaction. The shear layer **(iv)** binds the core and Stern layer inside and finally on the outer side is the Guoy Chapman Diffuse layer **(v)** which could be several hundred angstroms in thickness.

To discuss in depth understanding of micellar aggregation, it is worthwhile to quote the main characteristics of micellar packing aggregation pointed out by Hassan and his coworkers as the following.[13]

(a) The micelles are stabilized by hydrophobic forces and head group repulsion (electrostatic and steric forces).

(b) Each surfactant molecule moves in a fluid and the size, shape and aggregation numbers are decided by the packing parameter for the individual surfactant.

(c) Length scales of these micelles are in 10-1000 Å.

(d) The life time of these micelles are in milliseconds. On dilution below critical micelle concentration the aggregates disappear in milliseconds.

The research development and recent discoveries has proven that micellar aggregation can occur in many different ways, even controlled and designed wisely, for example by adding cosurfactant[14] or salts,[7,16] thus forming aggregates of micelles which are non spherical. However, typically at a surfactant concentration just above the critical micelle concentration (cmc), micelles are usually spherical in shape.

The flexibility of micellar aggregation is because of the dynamic nature of micellar aggregates and many factors that would influence the surfactant molecules ability and ways to self-assemble in forming aggregates of different microstructures and shapes depending on the composition, temperature and type of micelle-forming surfactant. However, there is attractive force that favor micellar growth as well as the repulsive force limiting the aggregation size, and the competition of these two forces are the main contributor in determining the characteristic of a micellar aggregation. The hydrophobic attractive interaction arises from the tail group-tail group interaction of the surfactant molecules in one micelle aggregation, favoring more surfactant molecules to aggregate together. Such

interaction depends highly on the characteristic of the hydrocarbon tail of that particular surfactant molecule. On the other hand, the electrostatic and steric repulsion between the similar charged head of micelle-forming surfactant are limiting the number of surfactant molecules in one micelle aggregation. Therefore, it is clear on how important is the architecture (i.e. tail length, head group area, and the molecular volume) of the micelle-forming-surfactant molecule in determining the micellar size and shape.

1.1.3 Factors Affecting Micellization

The process of micellization is a unique self-assembly process and will only occur in the conditions above the critical micelle concentration (cmc) and the Kraft temperature. Critical micelle concentration is the definite concentration where the monomers start to aggregate together forming micelle. It can be determined by various ways, in fact Mukerjee and Mysels[17] have reported about 71 methods of cmc determination at that time. The methods of determination arise from the fact that the cmc can be closely reflected by the surface and interfacial activity of the monomers in the aggregation of micelle. It is interesting that eventhough the value of cmc can be determined precisely, it can also be lowered and controlled accordingly by manipulating the condition of the aggregation. Kraft temperature or also known as critical micelle temperature is the minimum temperature when the aggregation started to take place. Both conditions (i.e. cmc and Kraft temperature) are crucial to the micellization process and will not take place without any one of it. Thus, all of the factors affecting micellization may be explained as below.

The first factor affecting micellization is the nature of the hydrophobic group of the micelle forming surfactant. The value of cmc will decrease by the increasing number of carbon in a straight chain manner but, the cmc will increase if branching exists. This is due

to the decrease in the free energy arising from the aggregation of branch chain molecules is less that that obtained with linear molecules with the same number of carbon atoms.[18]

The second factor is the nature of the hydrophilic group. It has been reported that groups with more charged head will posses higher cmc because it is harder to overcome the charged head group-head group repulsion, thus the non-ionic micelle-forming surfactant will posses much lower cmc.[19] Another related factor is the number of hydrophilic groups in one aggregation of micelle. As the number of hydrophilic group increases, the possibility of it to become soluble is more, thus the need of higher concentration to form micelle is also increased.[20]

Apart from the factors mentioned above, the counterion has a prominent effect in micellization process as well. Counterions with higher polarizability will result in less cmc required as well as more aggregation number allowed.[21] Electrolyte and non-electrolyte additive will also alter the cmc value. Again, the electrical work required to overcome the head group-head group repulsion is considered. The additives with the ability to reduce the repulsion will lower down the cmc, whilst the cmc will be increased if the additives result in greater repulsion.[22] These factors are crucially important and will definitely allow a better precision in controlling the ability of micelle.

1.1.4 The Viscoelasticity of Micellar Systems

Aqueous solutions of micellar system with viscoelastic behavior have been actively studied due to their remarkable rheological properties and large variation of potential applications[3,4,14b] especially in petrochemical[24], health and pharmaceutical area.[25] The viscoelasticity arises due to the formation of elongated flexible self-assembly structures aggregation of amphiphiles termed as “wormlike micelles”. Such aggregations of micelles

occur when small micellar aggregates of some surfactants exhibit enormous growth in one dimension and form very long and flexible network. This only occurs above a defined concentration in which they entangled into a dynamic network, overlapping with each other, thus displaying a remarkable viscoelastic properties similar to a solution of flexible polymers.[26] However, unlike polymers in solution, wormlike micelle posses a special ability that it can break and reform under shear or heat applied, thus considered to be "living polymers" [3,27] and making them stable in conditions where high shear rates as well as large amount of heat energy may be encountered.[14b,28]

Although micelles can self assemble forming viscoelastic wormlike micelles in aqueous solutions of cationic surfactants without added salt,[29] the addition of strongly binding counterions such as tosylate or salicylate can make the process be much easier.[30] The micelle forming surfactant, investigated in this study, CTABr is one of the most well known surfactant with the ability to form wormlike micelles over different addition of strongly binding counterions.[7,16,26,31] Inclusion of counterions between the head-groups that penetrate deep into micellar surface, screening of the electrostatic repulsion as well as neutralizing the charged micellar head will eventually promote micellar growth. [26]

1.2 Kinetic of Micellar-Mediated Reactions

Micellar pseudophase offers a reaction environment different from bulk water, leading to a kinetic medium effect. Hence, addition of micelle-forming surfactant above its cmc to a reaction mixture is able to accelerate or inhibit the rate of that particular reaction and this has been an active area of research for more than past 50 years.[7,16,32] Addition of micelles will inhibit the reaction if the rate of reaction in micellar phase is lower than in the aqueous phase. On the other hand, if the rate of reaction in micellar phase is higher than

that in the aqueous phase, the rate of reaction will be enhanced by the addition of micelle-forming surfactant. Change of the rate of reaction, generated in micellar phase, is due to two factors which are the electrostatic interaction and hydrophobic interaction between the micellar phase and reactants, transition state and products.[33] Electrostatic effect is certainly caused by the charged hydrophilic head group of micelle. It will affect the transition state which posses a charge or partial charge opposite to that of the micellar surface relative to the reactant state. This will directly affecting the rate of product formation, thus affecting the rate of reaction. The hydrophobic effect aroused due to the nature of the hydrophobic tails which are positioned towards the centre of the micellar aggregation. Thus, the hydrophobic nature of the reactants and the transition state will determine their position during the course of the reaction, and consequently will also affecting the rate of reaction.

1.3 Occurrence of Ion-Exchange in Micellar System

The occurrence of ion-exchange between counterions and ionic reactants of charge similar to the charge of counterions of micellar-mediated ionic reactions or semi-ionic bimolecular reactions has been known to enhance the rate of chemical reactions in certain cases as well as inhibiting the rate of reaction in the other cases.[7,16,34] It is possible to describe the occurrence of ion-exchange between the aqueous and micellar phases by an equilibrium process described as below.

$$[Y_M] + [X_W] \underset{}{\overset{K_X^Y}{\rightleftharpoons}} [Y_W] + [X_M] \qquad \textbf{Eq. 1.1}$$

where Y_M and Y_W are the Y counterionic species in micellar pseudophase and in bulk aqueous phase respectively, whilst X_W and X_M represents respective counterionic X species in bulk aqueous phase and micellar pseudophase as well. The corresponding selectivity coefficient or ion exchange constant may be be given by

$$K_X^Y = \frac{[Y_W][X_M]}{[Y_M][X_W]} \qquad \textbf{Eq. 1.2}$$

Srinivasan and coworkers[35] and many other researchers have strongly pointed out that the micellar properties of ionic surfactants are strongly affected not only by the overall counterion concentration but also by the specific type of counterions of the surfactant head groups and the counterions added to the solution. The ion-exchange process that occurs in the aqueous micellar system result in significant effect towards the micellar aggregation behavior, thus, it has become crucial to study such phenomena. Number of models had been proposed in discussing the condition and properties of such micellar solution.[36] Two extensively discussed and applied models are the Pseudophase Micellar (PM) model and Pseudophase Ion-Exchange (PIE) model as reviewed below.

1.3.1 Pseudophase Micellar Model

Micellar aggregation in an aqueous system should not be regarded as a real phase with real boundaries due to the invisibility towards UV-visible radiation at $[micelle]_T$ less and greater than its cmc. Instead, in serving the purpose of representing the phases, the term "pseudophase" might be the best, thus giving rise to the Pseudophase Micellar (PM) model of the micelle.

In PM, the micelles and bulk aqueous solvents are regarded as distinct reaction region, thus there are two different reaction domains with each one offering a new reaction medium that alters the distribution of reactants in solution. Hence, it may also be called the 'two-domain pseudophase" model of micelles. On the other hand, when the bulk aqueous region, the Stern region and the hydrophobic micellar core are considered to be three different reaction regions instead of only two, the PM model is termed the "three-domain pseudophase" model of micelles.[33]

The rate constant of a micellar-mediated reaction is governed by the micellar binding constants of reactants as well as the rates for the reaction that occur in micellar pseudophase. Polar/ionic and van der Waals forces between solubilizate and micelles that control the micellar binding constant of a solubilizate, are largely influenced by the structural features of the solubilizate and micelle-forming surfactant molecules; and not affected by the size and shape of the micelle. On the other hand, medium characteristics of the micro micellar reaction environment in which the reaction occurs that control the rate constant for the reaction of micellized reactant (k_M) is not expected to vary with the change in size and shape of the micelles. Since both factors are independent towards the changes in the size and shape of micelle, thus it can be conluded that the micellar effects on reaction rates and equilibria are insensitive as well.[32]

Apart of what were discussed, the PM model also suggested another three assumptions. The first assumption is when k_S and k_{-S} are the respective rate constants for micellar incorporation and micellar exit of solubilizate/substrate S and k_W and k_M are the rate constants for reaction involving S in respective aqueous phase and micellar pseudophase, $k_S >> k_W$ and $k_{-S} >> k_M$. Thus, $K_S = k_S/k_{-S}$ where K_S is the equilibrium constant for micellization of S. In simpler explanation, the micellization of substrate S is much faster than the reaction of S in aqueous phase, whilst the release of substrate S into aqueous phase is much faster than the reaction of S in micellar pseudophase that it is considered as constant. Thus, the reaction rates under the condition of both phases, k_W and k_M are independent of the micellar incorporation and micellar release of substrate S. Second assumption is the equilibrium constants for micellar incorporation of different solubilizates are independent of each other. The third assumption considers the equilibrium constant for micelle formation, K_M as represented by **Eq. 1.3**.

$$\{(n\text{-}N)/N_A\} \text{ monomers} \underset{}{\overset{K_M}{\rightleftharpoons}} (N/rN_A) \text{ micelles} \qquad \textbf{Eq. 1.3}$$

where n is the total number of surfactant molecules, N is the total number of surfactant molecules used up in the formation of number of micelles (N/r), r is the mean aggregation number of micelle and N_A is the Avogadro's number. K_M is assumed to be independent of equilibrium constants, K_S for micellar solubilization of different solubilizate and rate constants k_M for micellar-mediated reactions. This is because the rates of formation and disintegration of micelle are independent of the corresponding micellar intake and exit of a solubilizate: $k_f^M >> k_W$ and $k_d^M >> k_M$ where k_f^M and k_d^M represent respective rate constants for micelle formation and micelle disintegration, therefore $k_f^M/k_d^M = K_M$.[33] When the reaction is very fast, the three assumptions elaborated may easily collapsed due to the dynamics of micelle formation and disintegration. Such reaction will lead to further complication where the reaction does not follow simple first- or second-order rate law anymore.[33]

The last assumption in PM model is that for a bimolecular reaction between reactants R and S, only reactants within the same phase will react (i.e. R_M with S_M and R_W with S_W, where M represents micellar pseudophase whilst W represents aqueous phase). Cross-interface reactions such as between R_M and S_W or R_W and S_M do not occur.[33]

1.3.2 Pseudophase Ion-Exchange Model

The Pseudophase Ion-Exchange (PIE) model is a theoretical model developed by Romsted[37] which provides semiquantitative interpretation of the ion-exchange involving the competition between counterions (X) and another counterions (Y) of similar charges at ionic micellar surface. It contains the following basic assumptions[38]:

(i) The micelles act as a separate phase from water,

(ii) Changes in the rate constants due to added surfactant and salt depend on the distribution of the reactants between the micellar and bulk water phases, and

(iii) This model assumes that the degree of dissociation of the ionic micelle can be considered constant.[39]

This model has been repetitively applied to many bimolecular reactions between an organic substrate and univalent ion of charge opposite to that of the interphase such as in aqueous ionic micelles,[38] reversed micelles,[39] and cosurfactant-modified micelles[40]. Instead of considering the details of the micellar structure, this model treated the total volume of the aggregates in solution as a separate pseudophase and counterions are assumed to be either bound to the aggregate or free in the surrounding aqueous system.[38,41]

Since PIE model is the extension of PM model with the inclusion of ion-exchange consideration, the assumptions of PIE model also cover all of the assumptions in PM model with the additions listed below as discussed elsewhere.[33]

1. The degree of counterion ionization remains constant (i.e., there is a strictly 1:1 ion-exchange) irrespective of ion type or surfactant concentration.
2. The micellar surface region can be thought of as an ion-exchange resin in which ion-exchange processes occur in the same way as for a resin.

The details concepts and theories of PIE can be found elsewhere. [33,42]

Applicability of PIE model has been proven by its successes in the treatment of reactions at varying concentrations of micelles ($[D_n]$) as well as its ability to predict the maxima in the plots of k_{obs} vs $[D_n]$ under experimental conditions where PM model is no longer applicable.[33,39,43,44] But, failures in the application of PIE model has been observed in a few cases where reactive counterion surfactants are involved or at high detergent or salt concentration as well as in the presence of an excess of very hydrophilic counterions such as HO^- and F^-.[44] These failures were related to the breakdown of the assumption involving

the constant degree of counterion dissociation, α where α = 1- β.[38] Assumption of the occurrence of strictly 1:1 ion-exchange turned out to be invalid, as suggested by Bunton and coworkers, when α is large and concentration of added counterion is high or both.[45] Due to the large magnitude of α in such cases, it can be no longer neglected or considered as unchanged. Therefore, in explaining the ion-exchange competition between counterions X and another counterions Y in an aqueous micellar system by using PIE model treatment, α value should also be considered in the equation. [46] Thus, the concentration of Y_M will be denoted as **Eq. 1.4** where the ionic reagent Y is the counterion of the surfactant and no other counterions are present.[33]

$$[Y_M] = [(1-\alpha)/V_M] + [Y_M] \qquad \textbf{Eq. 1.4}$$

Unfortunately still, due to some physical and chemical reasons, PIE model is less reliable for use than the PM model if the ion-exchange process could not be detected kinetically.[33]

1.3.3 Methods to Study the Ion-Exchange in Micellar System

The study on counterion binding towards ionic micellar surface has become crucial for the advancement of chemical kinetics and industrial processes due to its importance in designing micellar aggregation as well as stabilizing viscoelastic micellar aggregate structures.[38,43,47] Bachofer and Simonis[48] has generalized the methodologies to study the counterion binding to micellar interfaces into two:

(i) Methods such as conductivity,[9,49] potentiometry and ion selective electrode (ISE)[9,50] to determine fractional ionization constants, α of the micelle; and

(ii) UV-visible spectroscopy,[51] ^{1}H NMR,[52] light scattering,[53] ultrafiltration[51a] and fluorescence quenching[54] measurements to study the fraction of either an inorganic anion in competition with another interface.

The second group manipulates the competition between two ions for the micellar interface, and in turns result in the ion-exchange constants. Such experimental methods has been applied to the determination of ion-exchange constant even in systems other than micelles[38,51b,55] such as air/solution interfaces[56]. Here, a few methods are compared in terms of their advantages and disadvantages over the determination of ion-exchange constant.

One of the most common method in the determination of ion-exchange constant is the manipulation of ^{1}H NMR and conductivity method.[48] The changes of the chemical shift of the ^{1}H NMR is used to detect the characteristic changes thus allowing the fractions of micellar bound anions to be measured whilst the conductivity data will be used to determine the fractional ionization constant, α as well as providing further insight into the micellar aggregate structures. The combination of both makes it possible to determine the concentration of anions in both micellar pseudophase and bulk aqueous phase as well as to calculate the ion-exchange constants. Furthermore, eventhough this method has been proven to be effective for the calculation of ion-exchange constant in few cases,[57] the uses are limited to only small aromatic organic ions. Apart from the limited cases applicable, this method is only usable under the assumption that the α remains essentially constant, thus applies only to spherical or prolate micellar aggregates.

Another widely used method is the flotation technique. It was first used in 1967 and known as the "batch flotation technique" to determine the selectivity among a few anions. Grieves and coworkers[58] has refined the method for the ion-exchange measurement involving pairs of univalent anions as well as the alkali-metal cations. This method was later reapplied by other researchers for divalent/univalent anion exchange. In 1992 Galvin[59] published a paper on his attempt to modify the technique to a more rapid batch flotation technique to measure the selectivity of $Au(CN)_2^-$ over $Ag(CN)_2^-$ at cetyltrimethylammonium films but the error was too high (~ 25%) to be accepted. The

technique was in favor because the foam generated is providing sufficiently large interfacial areas for the conventional mass balance technique to determine the composition of the surface phase. But, the disadvantage was obvious that the method was laborious and more robust toward the presence of impurities than other method such as surface tension measurements.

Fluorescence quenching technique has also been repetitively applied in ion-exchange measurement but the value is doubted because it only respond to counterions at the immediate micelle interface, while the ions in the diffuse part of the double layer escape detection because the fluorophore is located at the plane of the surfactant head groups.[60]

1.4 Scope and Significance of Study

For the last more than five decades, it has been discovered that the addition of salts to aqueous cationic surfactant weakens electrostatic interactions and enhances micellar growth due to their specific ion effects and hydrophobicity.[61-64] The mixing ratio of hydrophobic counterion/surfactant, degree of hydrophobicity and particular geometry of the hydrophobic counterions are the important factors that directly affect the physical properties of ionic surfactant micellar solutions.[65] There have been many attempts to investigate further on this, but qualitative observations and speculative predictions do not offer deep understanding to the phenomena. Thus, the quantitative value of the thermodynamic ion-exchange constant, K_X^Y for ion-exchange process X^-/Y^- on cationic micellar surface in aqueous solution has become an interest to many researchers in this area. But, since the of ion-exchange constant might differ with different technique used in its determination, there will be obstacles in correlating the counterion binding to the possible micellar structures.[5]

Due to the above mentioned problem, in this study the ion-exchange constant, K_X^{Br} for the ion-exchange processes involving different halo-substituted organic salts, MX and cetyltrimethylammonium bromide (CTABr) micelles in aqueous system were determined by a new semiempirical kinetic approach with the interest of investigating the relationship of the ion-exchange constant to the micellar aggregation behavior. The main objectives of this study are:

1. Determination of the ion exchange constant for different counterions of a cationic surfactant by the use of an empirical kinetic technique.
2. A quantitative study on the penetration of counterions in micelles.
3. Comparing the behavior of relative counterions' penetration in the case of viscoelastic and nonviscoelastic cationic surfactant solution.

In this study, the concentrations of CTABr were fixed to be at 5, 6, 7, 10 and 15 mM for all set of experiments. These variations were chosen to get a more precise and reliable ion-exchange. The organic salts used are 3- and 4-$FC_6H_4CO_2Na$; 2-, 3- and 4-$ClC_6H_4CO_2Na$; 2-, 3- and 4-$BrC_6H_4CO_2Na$; and 2- and 4-$IC_6H_4CO_2Na$.

New methods will always need strong proves of justifications to be accepted. In realization to this fact, this study also includes a well known method to study the structures of micelle which is the rheological measurement. This is to support the proposed relation of ion-exchange occurrence towards the aggregation behavior of micelle. Each system with kinetically determined ion-exchange constant were studied rheologically and their behavior of plots of shear viscosity upon applied shear rate as well as the viscosity values as a function of [MX] are presented in this study.

1.5 References

(1) Davidson, M.; Dommersnes, P.; Makstrom, M.; Joanny, J-F.; Karisson, M.; Orwar, O. *J. American Chemical Society* **2005**, *127*, 1251-1257.

(2) Harada, M.; Satou, H.; Okada, T. *J. Physical Chemistry B* **2007**, *111*, 12136-12140.

(3) Yang, J. *Current Opinion Colloid Interface Science* **2002**, *7*, 276-281.

(4) Kefi, S.; Lee, J.; Pope, T. L.; Sullivsn, P.; Nelson, E.; Hernandez, A. N.; Olsen, T.; Parlar, M.; Powers, B.; Roy, A.; Wilson, A.; Twynam, A. *Oilfield Review* **Winter 2004/2005**.

(5) Magid, L. J.; Han, Z.; Warr, G. G.; Cassidy, M. A.; Butler, P. D.; Hamilton, W. A. *J. Physical Chemistry B* **1997**, *101*, 7919-7927.

(6) Aswal, V. K.; Kohlbrecher, J.; Goyal , P. S.; Amenitsh, H.; Bernstorff, S. *J. Physics Condensed Matter* **2006**, *18*, 11399-11410.

(7) (a) Yusof, N. S. M.; Khan, M. N. *Langmuir* **2010**, *26*, 10627-10635. (b) Yusof, N. S. M.; Khan, M. N. *J. Colloid Interface Sci.* **2011**. Online.

(8) (a) Asakawa, T.; Kitano, H.; Ohta, A.; Miyagishi, S. *J. Colloid Interface Sci*. **2001**, *242*, 284-287. (b) He, Z. M.; O'Connor, P. J.; Romsted, L. S.; Zanette, D. *J. Physical Chemistry B.* **1989**, *93*, 4219-4226.

(9) Zana, R. *J. Colloid Interface Sci.* **1980**, *78*, 330-337.

(10) Iso, K.; Okada, T. *Langmuir* **2000**, *16*, 9199-9204.

(11) Cordes, E. H., and Gitler, C. (1973). Reaction Kinetics in the Presence of Micelle Forming Surfactants.

(12) Stigter, D. *J. Colloid. Interface. Sci.* **1967**, *23*, 379-383.

(13) Hassan, P. A.; Narayanan, J.; Manohar, C. *Current Science* **2001**, *80*, 8, 980-989.

(14) (a) Rojas, M. R.; Muller, A. J.; Saez, A. E. *J. Colloid Interface Science* **2008**, *326*, 221-226. (b) Schubert, B. A.; Kaler, E. W. Wagner, N. J. *Langmuir* **2003**, *19*, 4079-4089.

(15) (a) Acharya, D. P.; Kuneida, H. *J. Physical Chemistry B* **2003**, *107*, 10168-10175. (b) Acharya, D. P.; Kunieda, H. *Advances Colloid Interface Science* **2006**, *123-126*, 401-413.

(16) (a) Khan, M. N.; Ismail, E.; Yusof, N. S. M. *Colloids and Surfaces A.* **2010**, *361*, 150-161. (b) Ruan, K.; Zhao, Z.; Ma, *J. Colloid Polymer Science* **2001**, *279*, 813-818.

(17) Mukerjee, P.; Mysels, K. J. Critical Micelle Concentration of Aqueous Surfactant System (1971) NSRDS-NBS 36, U.S. Govt. printing Office, Washington, D.C.

(18) Janjjap, H.; Nusselder; Degroot; Jan, T.; Michel, T. Engbert Jan, B. F. N. *J. Org. Chem.* **1992**, *11*, 53, 243-246.

(19) Anacker, E. W.; Ghose, H. M. *J. American Chemical Society* **1968**, *90*, 3161-3166.

(20) Evans, H. C. *J. Phys. Chem. Colloid. Chem.* **1956,** *60*, 576.

(21) Ruckerstein, E.; Beunen, J. A. *Langmuir* **1988**, *4*, 77-90.

(22) (a) Leszek, M. *Colloid Surface.* **1987**, *25*, 2-4. (b) Christine, H.; Francoise, C. *J. Colloid Interface Science* **1988**, *125*, 1, 97-110. (c) Panda, S.; Sinha, B. K. *J. Indian Chemical Society* **1990**, *67*, 3, 199-201. (d) Rao, I. V.; Ruckenstein, E. *J. Colloid Interface Science* **1987**, *119*, 1, 211-227.

(23) (a) Berret, J.-F. *Langmuir* **1997**, *13*, 2227- 2234. (b) Clausen, T. M.; Vinson, P. K.; Minter, J. R.; Davis, H. T.; Talmon, Y.; Miller, W. G. *J. Physical Chemistry* **1992**, *96*, 414. (c) Magid, L. *J. Physical Chemistry B* **1998**, *102*, 4064-4074. (d) Truong, M. T.; Walker, L. M. *Langmuir* **2000**, *16*, 7991-7998. (e) Bautista, F.; Soltero, F.

A.; Macias, E. R.; Puig, J. E.; Manero, O. J. *J. Physical Cbemistry B* **2002**, *106*, 13018−13026.

(24) Qi, Y.; Zakin, J. L. *Ind. Eng. Chem. Res.* **2002**, *41*, 6326-6336.

(25) (a) Nishiyama, N.; Bae, Y.; Miyata, K.; Fukushima, S.; Kataoka, K. *Drug Discovery Today: Technologies* **2005**, *2*, 1, 21-26. (b) Sutton, D.; Nasongkla, N.; Blanco, E.; Gao, *J. Pharmaceutical Research* **2007**, *24*, 6,1029-1046. (c) Ideta, R.; Yanagi, Y.; Tamaki, Y.; Tasaka, F.; Harada, A.; Kataoka, K. *FEBS Letters* **2004**, *557*, 21-25. (d) Rangel-Yagui, C.; Pessoa-Jr, A.; Tavares, L. S. *J. Pharmacy Pharmaceutical Science* **2005**, *8*, 2, 147-163. (e) Kabanov, A. V.; Batrakova, E. V.; Alakhov, V. Y. *J. Controlled Release* **2002**, *82*, 189-212. (f) Nishiyama, N.; Kataoka, K. *Pharmacology & Therapeutics* **2006**, *112*, 630-648. (g) Kataoka, K.; Harada, A.; Nagasaki, Y. *Adv. Drug Delivery Reviews* **2001**, *47*, 113-131.

(26) Dreiss, C. A. *Soft Matter* **2007**, *3*, 956-970.

(27) Ziserman, L.; Abezgauz, L.; Ramon, O.; Raghavan, S. R.; Danino, D. *Langmuir* **2009**, *25*, 10483-10489.

(28) Davies, T. S.; Ketner, A. M.; Raghavan, R. *J. Am. Chem. Soc*. **2006,** 128, 6669-6675.

(29) Gamez-Corrales, R.; Berret, J.-F.; Walker, L. M.; Oberdisse, J. *Langmuir* **1999**, *15*, 6755-6763.

(30) (a) Ali, A. A.; Makhloufi, R. *Physical Review E* **1997**, *56*, 4, 4474-4478. (b) Soltero, J. F. A.; Puig, J. E.; Manero, O. *Langmuir* **1996**, *12*, 2654-2662. (c) Shikata, T.; Hirata, H.; Kotaka, T. *Langmuir* **1987**, *3*, 1081-1086.

(31) Candau, S. J.; Hirsch, E.; Zana, R. *J. Colloid Interface Science* **1985**, *105*, 521-528.

(32) (a) Khan, M. N. Ahmad, F. B. H. *Colloids Surfaces A* **2001**, *181*, 11-18. (b) Khan, M. N.; Ahmad, F. B. H. *Reaction Kinetic Catalysis Letters* **2001**, *72*, 2, 321-329.

(33) Khan, M. N. Micellar Catalysis. In Surfactant Science Series; CRC Press; Taylor & Francis Group. Boca Raton, FL, 2006: vol. 133.

(34) (a) Khan, M. N.; Arifin, Z.; Yusoff, M. R.; Ismail, E. *J. Colloid Interface Science* **1999**, *220*, 474-476. (b) Khan, M. N.; Ismail, E. *J. Physical Chemistry A* **2009**, *113*, 6484-6488. (c) Khan, M. N.; Ismail, E. *Indian J. Chemistry* **2009**, *48A*, 781-787. (d) Khan, M. N. *J. Chem. Soc Perkin Trans. II* **1989**, 199-207. (e) Khan, M. N.; Arifin, Z.; Lasidek, M. N.; Hanifiah, M. A. M.; Alex, G. *Langmuir* **1997**, *13*, 3959-3964. (f) Khan, M. N. *J. Organic Chemistry* **1997**, *62*, 3190-3193.

(35) Srinivasan, V.; Blankschtein, D. *Langmuir* **2003**, *19*, 9932-9945.

(36) (a) Minero, C.; Pelizetti, E. *Pure & Applied Chemistry* **1993**, *65*, 12, 2573-2582. (b) Yunes, S. J.; Nicholas, D. G.; Bunton, C. A. *J. Colloid Interface Science* **2005**, *281*, 482-487. (c) Khan, M. N.; Naaliya, J.; Dahiru, M. *J. Chemical Research(s)* **1988**, 1168-1176.

(37) Romsted, L. S. In *Surfactant in Solutions*; Mittal, K. L., Lindmann, B., Eds.; Plenum: New York, 1984; Vol. 2, pp 1015-1068.

(38) Bunton, C. A.; Nome, F.; Quina, F. H.; Romsted, L. S. *Acc. Chem. Res.* **1991**, *24*, 357-364.

(39) Quina, F. H.; Chaimovich, H. *J. Physical Chemistry* **1979**, *83*, 1844-1850.

(40) (a) El Seoud, O. A.; Chinelatto, A. M. *J. Colloid Interface Science* **1983**, *95*, 163-171. (b) Vishal, S. P. G.; Gandhi, K. S.; Ayappa, K. G. *Langmuir* **2005**, *21*, 767-778.

(41) El Seoud, O. A. *Adv. Colloid Interface Science* **1989**, *30*, 1-2, 1-30.

(42) Bunton, C. A.; Savelli, G. *Advances Physical Organic Chemistry* **1986**, *22*, 213-309.

(43) (a) Pereira, R. D. R.; Zanette, D.; Nome, F. *J. Physical Chemistry* **1990**, *94*, 356-361. Quina, F. H.; Chaimovich, H. *J. Physical Chemistry* **1979**, *83*, 14, 1844-1854. (b) Cheong, M.-Y.; Ariffin, A.; Khan, M. N. *Bull. Korean Chem. Soc.* **2007**, *28*, 7, 1135-1139.

(44) Khan, M. N.; Ismail, E. *J. Chem. Soc. Perkin Trans* **2001**, *2*, 1346-1350.

(45) Abuin, E.; Lissi, E.; Araujo, P. S.; Aleixo, R. M.V. *J. Colloid Interface Science* **1983**, *96*, 1, 293-295.

(46) Blasko, A.; Bunton, C. A. Cerichelli, G.; McKenzie, D. C. *J. Physical Chemistry* **1993**, *97*, 43, 11324-11331.

(47) Rehage,H.; Hoffmann, H. *Rheologica Acta* **1982**, *21*, 561-563.

(48) Bachofer, S. J.; Simonis, U. *Langmuir* **1996**, *12*, 1744-1754.

(49) Sepulveda, L.; Cortes, J. *J. Physical Chemistry* **1985**, *89*, 5322-5324.

(50) Abuin, E. B.; Lissi, E. A.; Nunex, R.; Olea, A. *Langmuir* **1989**, *5*, 753-757.

(51) (a) Gamboa, C.; Sepulveda, L.; Soto, R. *J. Physical Chemistry* **1981**, *85*, 1429-1434. (b) Sepulveda, L.; Bartet, D.; Gamboa, C. *J. Physical Chemistry* **1980**, *84*, 272-275.

(52) (a) Olsson, U.; Soderman, O.; Guering, P. *J. Physical Chemistry* **1986**, *90*, 5223-5232. (b) Hirata, H.; Shikata, T.; Kotaka, T. *Langmuir* **1988**, *4*, 354-359.

(53) Underwood, A. L.; Anacker, E. W. *J. Colloid Interface Science* **1985**, *106*, 86-93.

(54) Abuin, E. B.; Lissi, E.; Bianchi, N.;Miola, L.; Quina, F. H. *J. Physical Chemistry* **1983**, *87*, 5166-5172.

(55) (a) Loughlin, J. A.; Romsted, L. S. *Colloids Surfaces* **1990**, *48*, 123-137. (b) Drummond, C. J.; Grieser, F. *J. Colloid Interface Science* **1989**, *127*, 281-291.

(56) (a) Abuin, E. B.; Lissi, E. *J. Physical Chemistry* **1989**, *93*, 4886- 4890. (b) Romsted, L. S.; Zanette, D. *J. Physical Chemistry* **1989,** *93*, 4219-4226.

(57) Trainer, C.; Makayssi, A. *Langmuir* **1992**, *69*, 375-378.

(58) Grieves, R. B.; The, P. J. *J. Inorganic Nucl. Science* **1974**, *36*, 1391-1396.

(59) Galvin, K. P.; Nicol, S. K.; Waters, A. G. *Colloids Surfaces* **1992**, *64*, 21-33.

(60) Abuin, E.; Lissi, E. *J. Coll. Interface Science* **1991**, *143*, 1, 97-102.

(61) (a) Cates, M. E. *Macromolecules* **1987**, *20*, 2289-2296. (b) Cates, M. E. *J. Phyical Chemistry* **1988**, *49*, 1593-1600.

(62) Jager, C. M.; Hirsh, A.; Schade, B.; Ludwig, K.; Bottcher, C.; Clark, T. *Langmuir* **2009**, *26*, 10460-10466.

(63) Vermathen, M.; Stiles, P.; Bachofer, S. J.; Simonis, U. *Langmuir* **2002**, *18*, 1030-1042.

(64) Abdel-Rahem, R. *Advances in Colloid and Interface Sci.* **2008**, *141*, 24-36.

(65) Shikata, T.; Hirata, H.; Kotaka, T. *Langmuir* **1987**, *3*, 1081-1086.

CHAPTER 2

MATERIALS AND

EXPERIMENTAL METHODS

2.1 Materials

2.1.1 Major Chemicals

The following major chemicals have been used in the present study.

Hexadecyltrimethylammonium bromide, represented as CTABr, was purchased from Fluka with ≥ 99% purity. The stock solution (0.2 M) was prepared in purified water. Phenyl salicylate (PSH) was bought from Fluka with ≥ 98% purity. The concentration of 0.01 M was prepared in acetonitrile which was also an A.R. Grade chemical from Merck. The molarity of PSH was kept constant at 2.0×10^{-4} M for all kinetic and rheological measurements. Piperidine was one of the reactants in the reaction of piperidinolysis of phenyl salicylate. It was bought from Merck with ≥ 99% purity. Stock solution of 1 M was prepared in purified/distilled water and a concentration of 0.1 M was generated to each sample for kinetic and rheological studies.

2.1.2 Inert Organic Acids

There were 11 inert organic acids used in this study and these acids are listed in **Table 2.1**

Table 2.1 : Inert Organic Acids Used in the Study

Chemical	Manufacturer	Purity
o-fluorobenzoic acid	Merck	≥ 97%
m-fluorobenzoic acid	Merck	≥ 98%
p-fluorobenzoic acid	Merck	≥ 97%
o-chlorobenzoic acid	Merck	≥ 98%
m-chlorobenzoic acid	Merck	≥ 98%

p-chlorobenzoic acid	Merck	≥ 95%
o-bromobenzoic acid	Fluka	≥ 97%
m-bromobenzoic acid	Fluka	≥ 98%
p-bromobenzoic acid	Merck	≥ 99%
o-iodobenzoic acid	Merck	≥ 98%
p-iodobenzoic acid	Merck	≥ 99%

Some of the organic acids such as *o*-, *m*- and *p*-fluorobenzoic acids were recrystallized using distilled water as recrystallizing solvents. The preparation of stock solution (w M) of each organic salt was carried out by adding (w + 0.05) M NaOH to w M halo-substituted benzoic acid in order to completely convert them to sodium salts.

2.2 Experimental Details

This study consists of two parts of experiments. The first and the main part is the kinetic measurements of the piperidinolysis of phenyl salicylate where the disappearance of anionic phenyl salicylate was monitored using a UV-spectrophotometer.[1,2] The second part is the supporting experiment where the rheological measurements were carried out using a rheometer.[2]

2.2.1 Kinetic Measurements

The kinetic measurements were carried out using SHIMADZU UV-Visible Spectrophotometer Double Beam Model UV-1650 and UV-1800 along with its electronically temperature controlled cell compartment. The wavelength was fixed at 350 nm and temperature at 35^{o}C. For each kinetic run, a volume of 5 mL with specific measured concentrations of reaction ingredients except the substrate (i.e. phenyl salicylate)

was prepared and equilibrated in the water bath at 35^{o}C for at least 15 minutes. For samples, with the addition of sodium 4-iodobenzoate, total volume of 10 mL instead of 5 ml was prepared to minimize the problem occurred while transferring the solution into quartz cell for the UV-spectrophotometer measurement. This was because of the very high viscosity shown by these samples.

The UV-Visible spectrophotometer was calibrated with distilled water before use. The reaction was then initiated by adding the known volume of substrate and simultaneously starting the kinetic measurement on the UV-1650 PC software. The mixture was shaken and transferred to the quartz cuvette which then placed in the cell compartment as fast as possible. Minimum time taken for these processes can assure higher reliability of the data collected. The reactions were carried out for the reaction period of more than 6 half-lives.

2.2.2 Kinetic Equation of Simple First-Order Reaction.

The kinetic measurements for this study were designed to be under pseudo-first-order condition by fixing the concentration of piperidine ($[Pip]_T$) 500 times larger than the concentration of phenyl salicylate ($[PSH]_T$). The reaction step for first-order reaction is expressed below

$$S \xrightarrow{k_{obs}} P \qquad \textbf{Eq. 2.1}$$

where S and P represent respective reactant and the product and k_{obs} is the pseudo-first-order rate constant for the reaction (i.e. $k_{obs} = k_n$ [Pip] with k_n represesnting nucleophilic second-order rate constant). The rate law of the reaction illustrated by **Eq. 2.1** can be written as:

$$\text{Rate} = \frac{-d[S]}{dt} = \frac{-d[Pip]}{dt} = \frac{+d[P]}{dt} = k_{obs}[S] \qquad \textbf{Eq. 2.2}$$

or

$$\text{Rate} = \frac{-d[S]}{dt} = k_{obs}[S] \qquad \textbf{Eq. 2.3}$$

The integration of **Eq. 2.3** gives **Eq. 2.4**.

$$[S] = [S_0] \exp(-k_{obs}t) \qquad \textbf{Eq. 2.4}$$

where $[S_0]$ is the initial concentration of S and [S] is the concentration of S at any reaction time, t. If A_{obs} is the observed absorbance of the reaction mixture then

$$A_{obs} = \delta_S[S] + \delta_P[P] \qquad \textbf{Eq. 2.5}$$

where the δ_S and δ_P represent the molar extinction coefficient of S and P, respectively. From **Eq. 2.2**, it can be shown that

$$[S_0] = [S] + [P] \qquad \textbf{Eq. 2.6}$$

thus

$$[P] = [S_0] - [S] \qquad \textbf{Eq. 2.7}$$

Eqs. 2.5 and **2.7** results in

$$A_{obs} = \delta_S[S] + \delta_P ([S_0] - [S])$$

$$= (\delta_S - \delta_P)[S] + \delta_P [S_0] \qquad \textbf{Eq. 2.8}$$

If $\delta_P [S_0] = A_\infty$ and $\delta_S - \delta_P = \delta_{app}$, **Eq. 2.8** can be simplified to

$$A_{obs} = \delta_{app}[S] + A_\infty \qquad \textbf{Eq. 2.9}$$

Substitution of **Eq. 2.4** into **Eq. 2.9** results in

$$A_{obs} = \delta_{app}[S_0] \exp(-k_{obs}t) + A_\infty \qquad \textbf{Eq. 2.10}$$

The observed data (A_{obs} vs t) seem to fit to **Eq. 2.10** where δ_{app} is the apparent molar extinction coefficient of the reaction mixture and A_∞ is the absorbance at $t = \infty$. If the rate

of reaction was studied by monitoring the appearance of product (P) as a function of t, then **Eq. 2.11** should be used.

$$A_{obs} = \delta_{app} [S_0] [1-\exp(-k_{obs}t)] + A_0 \qquad \textbf{Eq. 2.11}$$

In **Eq. 2.11**, $A_0 = A_{obs}$ at t = 0.

2.2.3. Rheological Measurements

The rheological part was aimed to provide the supporting data as the justification to the result and conclusion drawn from the kinetic data. It was carried out by the R/S+ rotational Brookfield rheometer with double gap coaxial cylinder (CC-DG). The total volume was 16 mL for one run. The sample was poured into the cylinder and left connected to the temperature controller at 35^{o}C for at least 15 minutes before starting the measurement. By fixing the shear rate (γ) range 1.0 – 15 s^{-1} in 2400 s and 1.0 – 1000 s^{-1} in 8000 s, the dependent shear stress (τ) and shear viscosity (η), detected by the machine, were recorded after each 80 s.

2.3 References

(1) (a) Khan, M. N.; Ismail, E.; Yusof, N. S. M. *Colloids and Surfaces A* **2010**, *361*, 150-161. (b) Khan, M. N. Ahmad, F. B. H. *Colloids Surfaces A* **2001**, *181*, 11-18. (c) Khan, M. N.; Ahmad, F. B. H. *Reaction Kinetic Catalysis Letters* **2001**, *72*, 2, 321-329. (d) Khan, M. N.; Arifin, Z.; Yusoff, M. R.; Ismail, E. *J. Colloid Interface Science* **1999**, *220*, 474-476. (e) Khan, M. N.; Ismail, E. *J. Physical Chemistry A* **2009**, *113*, 6484-6488. (f) Khan, M. N.; Ismail, E. *Indian J. Chemistry* **2009**, *48A*, 781-787. (g) Khan, M. N. *J. Chem. Soc Perkin Trans. II* **1989**, 199-207. (h) Khan, M. N.; Arifin, Z.; Lasidek, M. N.; Hanifiah, M. A. M.; Alex, G. *Langmuir* **1997**, *13*, 3959-3964.

(2) (a) Yusof, N. S. M.; Khan, M. N. *Langmuir* **2010**, *26*, 10627-10635. (b) Yusof, N. S. M.; Khan, M. N. *J. Colloid Interface Sci* (2011), doi: 10.1016/j.jcis.2011.01.061.

Chapter 3: RESULTS

In this chapter, the results of the kinetic experiments of the piperidinolysis of anionic phenyl salicylate (PS^-) and the rheological measurement of aqueous mixtures containing a constant concentration of cetyltrimethylammonium bromide (CTABr) and different concentrations of organic salts, MX (MX = *m*- and *p*-$FC_6H_4CO_2Na$; *o*-, *m*- and *p*-$ClC_6H_4CO_2Na$; *o*-, *m*- and *p*-$BrC_6H_4CO_2Na$; and *o*- and *p*-$IC_6H_4CO_2Na$) are presented. The observed kinetic data (A_{obs} versus t) were found to fit **Eq. 2.10** for reaction period ≥ 6 half-lives of the reaction. The data treatment was carried out by the use of nonlinear least-squares technique in determining the three kinetic parameters: k_{obs}, δ_{app} and A_∞. The observed data fit to **Eq. 2.10** was found to be good in terms of the percent residual errors ($RE = 100\times(A_{obs\,i} - A_{calc\,i})/A_{obs\,i}$ where $A_{obs\,i}$ and $A_{calc\,i}$ represent observed and least-squares calculated values of absorbance at the i-th reaction time, t_i) as well as the standard deviations associated with the calculated parameters: k_{obs}, δ_{app} and A_∞.

3.1 Effects of the Concentrations of Various Halo-Substituted Benzoate Salts on the Rate of Piperidinolysis of PS^- in the Absence of CTABr at 35°C.

3.1.1 Rate of Piperidinolysis of PS^- at $[CTABr]_T = 0$ and Varying Concentrations of 3- and 4-FBzNa.

To investigate the probability of any effect of inert salts 3- and 4-FBzNa on the reaction rate under the condition of this study, a few kinetic runs were carried out in the absence of CTABr micelle with 0.1 M Pip, 0.2 mM PSH and with different concentrations of 3- or 4-FBzNa ranging from 0.0 to 0.3 M. The values of [NaOH] were within the range of 0.03 to ≤ 0.06 M. The calculated kinetic parameters k_{obs}, δ_{app} and A_∞ are listed in **Table 3.1**.

3.1.2 Rate of Piperidinolysis of PS^- at $[CTABr]_T = 0$ and Varying Concentrations of 2-FBzNa.

A few kinetic runs for 2-FBzNa were also carried out within [2-FBzNa] range 0.0 to 0.035 M. Rather low concentration range was achieved due to the solubility problem of 2-FBzNa faced initially with uncrystallized 2-FBzH. The calculated values of k_{obs}, δ_{app} and A_∞ are shown in **Table 3.2**. However, recrystallization of 2-FBzH has overcome the low solubility problem, but another obstacle that concerns with the reactivity of 2-FBz^- with ionized phenyl salicylate discouraged the attempt to proceed further with 2-FBzNa.

3.1.3 Rate of Piperidinolysis of PS^- at $[CTABr]_T = 0$ and Varying Concentrations of 2-, 3- and 4-ClBzNa.

Kinetic measurements under the kinetic conditions as set for 3-and 4-FBzNa, were carried out for 2-, 3- and 4-ClBzNa. The values of [2-ClBzNa], [3-ClBzNa] and [4-ClBzNa] varied within the respective range of 0.0 – 0.6 M, 0.0 – 0.3 M and 0.0 – 0.7 M. The values of [NaOH] varied from 0.03 to $\leq$ 0.06 M, 0.03 to $\leq$ 0.06 M and 0.0 to $\leq$ 0.65 M for 2-ClBzNa, 3-ClBzNa and 4-ClBzNa respectively. The least-squares calculated values of kinetic parameters, k_{obs}, δ_{app} and A_∞ are summarized in **Table 3.3**.

3.1.4 Rate of Piperidinolysis of PS^- at $[CTABr]_T = 0$ and Varying Concentrations of 2-, 3- and 4-BrBzNa.

Several kinetic runs were carried out at different concentrations of 2-BrBzNa, 3-BrBzNa and 4-BrBzNa under the reaction conditions similar to that for F-BzNa or Cl-BzNa. The values of [2-BrBzNa], [3-BrBzNa] and [4-BrBzNa] varied within the range of 0.0 – 0.5 M, 0.0 – 0.7 M and 0.0 – 0.5 M, respectively. The concentrations of NaOH were

fixed to be within $0.03 \leq [NaOH] \leq 0.055$, $0.03 \leq [NaOH] \leq 0.065$ and $0.03 \leq [NaOH] \leq 0.055$ M for 2-BrBzNa, 3-BrBzNa and 4-BrBzNa, respectively. The calculated values of k_{obs}, δ_{app} and A_∞, obtained under such conditions, are listed in **Table 3.4**.

3.1.5 Rate of Piperidinolysis of PS^- at $[CTABr]_T = 0$ and Varying Concentrations of 2- and 4-IBzNa.

The effects of [2-IBzNa] and [4-IBzNa] on k_{obs} for piperidinolysis of PS^- were studied by carrying out several kinetic runs under kinetic conditions similar to those for substituted bromobenzoates with the concentration range $0.0 \leq$ [2-IBzNa] and [4-IBzNa] $\leq$ 0.3 M. The concentrations of NaOH varied within the range of 0.03 to 0.06 M. The calculated kinetic parameters for each kinetic runs are listed in **Table 3.5**.

3.2 Effects of the Concentrations of Various Halo-Substituted Benzoate Salts on the Rate of Piperidinolysis of PS^- at Constant $[CTABr]_T$ and 35°C.

3.2.1 Rate of Piperidinolysis of PS^- at Constant Values of $[CTABr]_T$ and Varying Concentrations of 3- and 4-FBzNa.

Several kinetic runs were carried out within concentration range $0.0 - \leq 0.30$ M of 3- or 4-FBzNa at 0.1 M Pip, 0.2 mM PSH, 0.03 - 0.06 M NaOH and constant $[CTABr]_T$ at 35°C. The constancies of $[CTABr]_T$ were varied at 5, 6, 7, 10 and 15 mM. The values of k_{obs} versus [MX] are graphically represented by **Figure 3.1** for 3-FBzNa and **Figure 3.2** for 4-FBzNa. These data are also summarized in Tables I and II in Appendix A. The values of δ_{app} were discovered to be independent of the concentrations of 3- and 4-FBzNa. The mean values of δ_{app} ($= \delta_{app}^{av}$) are shown in Tables I and II of Appendix A. The calculated A_∞ values were found to show mild absorption of 3- or 4-FBzNa at 350 nm and the δ value (δ

= A_∞/([3-FBzNa] or [4-FBzNa])) is ~10-14 $M^{-1}cm^{-1}$ with δ representing the molar absorptivity of 3-FBz^- or 4-FBz^-. The values of δ remained unchanged within the $[CTABr]_T$ range of 5-15 mM.

3.2.2 Effects of [2-FBzNa] on k_{obs} for the Reaction of Piperidine with PS^- at Constant $[CTABr]_T$.

The effect of [2-FBzNa] on the rate of reaction between piperidine and PS^- were also studied by carrying out several kinetic runs at 0.2 mM PSH, 0.1 M Pip, 5 mM CTABr and within [2-FBzNa] range 0.0 to 0.05 M at 35°C. The values of [NaOH] were within the range of 0.03 to ≤ 0.035 M. The calculated values of k_{obs}, δ_{app}, A_∞ and A_0 are presented in **Table 3.6** where A_0 (= δ_{app} $[Sub]_T$ + A_∞) is the absorbance at t = 0.

Despite the plausible increase of k_{obs} versus [2-FBzNa], the calculated values of A_0 seem to increase rapidly with increasing [MX] (**Table 3.6**) until the point when the reaction rate could not be studied at > 0.05 M 2-FBzNa due to A_{obs} value > 2.4. The reaction mixtures with all reaction ingredients except the substrate (i.e. phenyl salicylate) showed visible characteristic colour changes from clear to yellowish. This led to a perception that there are other reaction(s) along with the known nucleophilic substitution reaction between piperidine and phenyl salicylate that are taking place in the reaction mixture. Thus, a few kinetic runs with modified reactions were carried out as an attempt to prove such possibility. The first set of kinetic measurements, i.e. (i), was carried out with the reaction conditions similar to that for 3- and 4-FBzNa, but, the addition of piperidine was carried out right before the addition of phenyl salicylate. To investigate the individual effects of piperidine and phenyl salicylate, second (ii) and third (iii) sets of kinetic measurements were carried out in the presence of all reaction ingredients except respective Pip and PSH.

The calculated values of k_{obs}, δ_{app} and A_∞, obtained under conditions (i), (ii) and (iii) are presented in **Table 3.7**.

The values of k_{obs}, shown in **Table 3.7** indicate the occurrence of reactions under all three different reaction conditions. Furthermore, the ability of the reaction under condition (i) **(**where piperidine was added right before the addition of PSH) to provide plausible A_∞ values as compared to the reaction shown in **Table 3.6** (where piperidine was added long before the addition of phenyl salicylate) supports the proposal that 2-FBzNa is showing mild reactivity towards both piperidine and phenyl salicylate.

3.2.3 Rate of Piperidinolysis of PS^- at Constant Values of $[CTABr]_T$ and Varying Concentrations of 2-, 3- and 4-ClBzNa.

Several kinetic runs were carried out at different concentrations of 2-, 3- and 4-ClBzNa under kinetic conditions similar with those 3- and 4-FBzNa at 35^{o}C. The values of [2-ClBzNa], [3-ClBzNa] and [4-ClBzNa] varied within the respective range of 0.0 to 0.6 M, 0.0 to 0.3 M and 0.0 to 0.2 M. The concentration of NaOH was within the range of 0.0 to 0.06 M, 0.0 to 0.06 M and 0.0 to 0.04 M for 2-ClBzNa, 3-ClBzNa and 4-ClBzNa respectively. The values of k_{obs}, at $[CTABr]_T$ = 5, 6, 7, 10 and 15 mM, are represented graphically by **Figures 3.3**, **3.4** and **3.5** for respective 2-, 3- and 4-ClBzNa. The data are also given in Tables III to V in Appendix A. The δ_{app} values were found to be almost independent of the concentrations of 2-, 3- and 4-ClBzNa, and the mean values, δ_{app}^{av} are shown in Tables III - V of Appendix A. The calculated values of A_∞ were found to increase mildly with the increase of [MX] (MX = 2-ClBzNa and 3-ClBzNa) at 350 nm due to the molar absorptivity (δ) of the inert organic salts. The δ value is ≤ 13 $M^{-1}cm^{-1}$ 2-$ClBz^-$, ≤ 11 $M^{-1}cm^{-1}$ for 3-ClBzNa and almost none for 4-ClBzNa.

3.2.4 Rate of Piperidinolysis of PS^- at Constant Values of $[CTABr]_T$ as well as Varying Concentrations of 2-, 3- and 4-BrBzNa.

A few kinetic runs were carried out at a constant $[CTABr]_T$ and within [MX] range from 0.0 to 0.5 M where MX = 2-, 3- or 4-BrBzNa under similar reaction condition as that for chlorobenzoates at 35°C. The values of [NaOH] varied from 0.03 to 0.055 M. The values of k_{obs}, obtained under such conditions for 2-, 3- and 4-BrBzNa are shown graphically in respective **Figures 3.6**, **3.7** and **3.8**. These observed data are also shown in Tables VI to VIII in Appendix A. The δ_{app} values turned out to be almost independent of the concentrations of 2-, 3- and 4-BrBzNa, and the mean values, δ_{app}^{av} at $[CTABr]_T$ range 5-15 mM are shown in Tables VI - VIII of Appendix A. The calculated values of A_∞ revealed mild absorption due to these organic salts at 350 nm. The molar absorptivity, δ value is ≤ 10 $M^{-1}cm^{-1}$ for $2\text{-}BrBz^-$ and ≤ 13 $M^{-1}cm^{-1}$ for 3- and $4\text{-}BrBz^-$. These values remain constant at varying $[CTABr]_T$.

3.2.5 Rate of Piperidinolysis of PS^- at Constant Values of $[CTABr]_T$ and Varying Concentrations of 2- and 4-IBzNa.

Kinetic measurements were carried out under the kinetic conditions as set for chloro- and bromobenzoates, for 2- and 4-IBzNa at 35°C. The values of [2-IBzNa] and [4-IBzNa] were varied within the respective range 0.0 to 0.3 M and 0.0 to 0.1 M. The concentration of NaOH varied within the range of 0.03 to ≤ 0.06 M for 2-IBzNa and 0.03 to ≤ 0.04 M for 4-IBzNa. The values of k_{obs} at different values of [2-IBzNa] and [4-IBzNa] are shown graphically by respective **Figures 3.9** and **3.10** as well as in the Tables IX - X of the Appendix A. The calculated values of δ_{app} turned out to be independent towards the

concentrations of 2- and 4-IBzNa. The mean values, δ_{app}^{av} are given in Tables IX to X in Appendix A. The calculated A_∞ values revealed mild absorption caused by the molar absorptivities, $\delta = \leq 1$ and ≤ 3 $M^{-1}cm^{-1}$ for respective 2-IBz^- and 4-IBz^- at 350 nm. Under variation values of $[CTABr]_T$, the δ values remained constant.

3.3 Rheological Properties of CTABr/MX with MX = 3-FBzNa, 4-FBzNa, 2-ClBzNa, 3-ClBzNa, 4-ClBzNa, 2-BrBzNa, 3-BrBzNa, 4-BrBzNa, 2-IBzNa and 4-IBzNa.

The investigation on rheological behavior of CTABr/MX where MX are 3- and 4-FBzNa; 2-, 3- and 4-ClBzNa; 2-, 3- and 4-BrBzNa as well as 2- and 4-IBzNa were carried out under steady-shear rheological response at the respective 34.3 ± 0.5, 34.0 ± 2.0; 33.2 ± 2.3 and 33.9 ± 1.6 ^oC. The aqueous micellar solution contains 0.2 mM PS^-, 2% v/v CH_3CN, 0.1 M Pip, constant known values of [NaOH], 15 mM CTABr and varying concentration of respective inert organic salts (i.e. [MX]).

The data of apparent shear viscosity, η versus shear rate, γ (≥ 0.5 - ≤ 1000 s^{-1}) are graphically represented by the log-log plots of **Figures 3.11** to **3.20**. In all figures, except **Figure 3.13**, the viscosity (η) values were showing shear thinning behavior upon the increasing values of shear rate (γ). This is a typical characteristic of elongated wormlike micelles.[2] For micellar system with spherical micellar aggregates, the rheological response towards shear rate will show Newtonian behavior as in **Figure 3.13**. Thus, it can be predicted that wormlike micelles exist in all systems studied except for the system of CTABr/2-ClBzNa.

Another indicator of the existence of wormlike micellar system is the presence of maxima in the plots of shear viscosity value at fixed shear rate (η_γ) versus concentration of MX. This is shown by **Figure 3.21** for 3- and 4-FBzNa at $\gamma = 100$ s^{-1}; **Figure 3.22** for 2-, 3-

and 4-ClBzNa at $\gamma = 0.5\ s^{-1}$; **Figure 3.23** for 2-, 3- and 4-BrBzNa at $\gamma = 1.0\ s^{-1}$; and **Figure 3.24** for 2- and 4-IBzNa at $\gamma = 2.5\ s^{-1}$. The maxima are observable in the plots for all systems except for CTABr/2-ClBzNa (**Figure 3.22**). This supports the prediction that only spherical micellar aggregation exist in such system. The plots for CTABr/2-BrBzNa (**Figure 3.23**) revealed an almost constant apparent viscosity values at shear rate $1.0\ s^{-1}$ despite the shear thinning behavior shown in **Figure 3.16**. It is predicted that there were a mixture of spherical and vesicles micellar aggregations in the system which can only be detected specifically by cryo-TEM study.

Table 3.1 Kinetic Parameters, k_{obs}, δ_{app} and A_∞, Calculated from **Eq 2.10** for Reaction of Pip with PS^- in the Presence of 3- or 4-FBzNa and Absence of CTABr.[a]

[MX] =	3-$FC_6H_4CO_2Na$			4-$FC_6H_4CO_2Na$		
10^2 [MX] M	10^4 k_{obs} s^{-1}	10^{-1} δ_{app} $M^{-1}cm^{-1}$	10^2 A_∞	10^4 k_{obs} s^{-1}	10^{-1} δ_{app} $M^{-1}cm^{-1}$	10^2 A_∞
0.0	340 ± 1.0[b]	671 ± 1	1.8 ± 0.0	340 ± 0.4[b]	705 ± 1	1.9 ± 0.1
0.2	338 ± 1.8	682 ± 2	1.6 ± 0.1	329 ± 0.3	695 ± 2	1.9 ± 0.3
0.5	342 ± 1.7	671 ± 2	1.6 ± 0.1	305 ± 0.9	707 ± 3	2.2 ± 0.2
0.8	324 ± 1.7	678 ± 5	1.1 ± 0.3	334 ± 0.8	708 ± 2	2.1 ± 0.1
1.0	345 ± 1.6	679 ± 2	1.9 ± 0.1	332 ± 0.7	717 ± 7	2.5 ± 0.3
1.5	332 ± 1.5	675 ± 2	1.6 ± 0.1	310 ± 1.0	697 ± 3	4.5 ± 0.8
2.0	333 ± 1.8	671 ± 2	1.7 ± 0.1	313 ± 0.8	701 ± 2	5.2 ± 0.3
2.5	317 ± 1.2	666 ± 1	2.1 ± 0.1	318 ± 0.3	711 ± 2	5.9 ± 0.8
3.0	329 ± 1.3	669 ± 1	1.9 ± 0.1	340 ± 0.9	699 ± 7	6.7 ± 0.9
4.0	322 ± 1.2	671 ± 1	1.7 ± 0.1	327 ± 1.0	682 ± 9	8.9 ± 0.3
5.0	321 ± 1.3	675 ± 1	2.0 ± 0.1	333 ± 0.1	712 ± 1	11 ± 0.1
7.0	305 ± 1.1	675 ± 1	1.9 ± 0.1	323 ± 0.8	702 ± 1	16 ± 0.3
10	304 ± 1.6	679 ± 2	2.1 ± 0.1	314 ± 0.5	702 ± 1	23 ± 0.1
15	278 ± 1.2	687 ± 1	2.6 ± 0.1	313 ± 1.4	711 ± 1	27 ± 0.1
20	340 ± 1.0	671 ± 1	1.8 ± 0.0	294 ± 0.4	704 ± 1	35 ± 0.1
30	338 ± 1.8	682 ± 2	1.6 ± 0.1	285 ± 0.9	706 ± 2	43 ± 0.2

[a] $[\text{phenyl salicylate}]_0$ = 0.2 mM, 35 ^oC, λ = 350 nm, $[\text{piperidine}]_T$ = 0.1 M, $[\ ]_T$ represents total concentration and the aqueous reaction mixture for each kinetic run contained 2 % v/v CH_3CN. The required amounts of 3- or 4-$FC_6H_4CO_2Na$ ([MX]) were generated into the reaction mixture by using the stock solution (w M) of 3- or 4-$FC_6H_4CO_2H$ prepared in (w + 0.05) M aqueous NaOH. The stock solution of NaOH was used to produce a fixed known concentration (0.03 M) of NaOH into the reaction mixture for each kinetic run. Thus, the maximum concentration of added NaOH was 0.06 M. [b] Error limits are standard deviations.

Table 3.2. Kinetic Parameters, k_{obs}, δ_{app} and A_∞ Calculated from **Eq. 2.10** for Reaction of Pip with PS^- in the Presence of 2-FBzNa and Absence of CTABr.[a]

[MX] =	**2-$FC_6H_4CO_2Na$**		
10^2 [MX]	**10^4 k_{obs}**	**10^{-1} δ_{app}**	**10^2 A_∞**
M	**s^{-1}**	**$M^{-1}cm^{-1}$**	
0.0	333 ± 1.8[b]	614 ± 2	2.3 ± 0.1
0.2	343 ± 1.5	622 ± 2	4.0 ± 0.1
0.4	333 ± 0.2	621 ± 2	3.9 ± 0.0
0.6	341 ± 1.6	635 ± 2	4.4 ± 0.1
0.8	334 ± 1.0	643 ± 1	7.1 ± 0.1
1.0	342 ± 1.2	627 ± 1	9.4 ± 0.1
1.2	335 ± 1.4	636 ± 2	10 ± 0.1
1.4	341 ± 1.1	630 ± 1	12 ± 0.1
1.6	330 ± 1.2	633 ± 2	13 ± 0.1
2.0	348 ± 1.6	629 ± 2	21 ± 0.1
2.5	335 ± 1.3	647 ± 2	28 ± 0.2
3.0	331 ± 1.9	633 ± 2	31 ± 0.1
3.5	346 ± 1.3	622 ± 2	41 ± 0.1

[a] $[\text{phenyl salicylate}]_0$ = 0.2 mM, 35 ^oC, λ = 350 nm, $[\text{piperidine}]_T$ = 0.1 M, $[\ ]_T$ represents total concentration and the aqueous reaction mixture for each kinetic run contained 2 % v/v CH_3CN. The required amounts of 2-$FC_6H_4CO_2Na$ were generated into the reaction mixture by using the stock solution (w M) of 2-$FC_6H_4CO_2H$ prepared in (w + 0.05) M aqueous NaOH. The stock solution of NaOH was used to produce a fixed known concentration (0.03 M) of NaOH into the reaction mixture for each kinetic run. Thus, the maximum concentration of added NaOH was 0.035 M. [b] Error limits are standard deviations.

Table 3.3. Kinetic Parameters, k_{obs}, δ_{app} and A_∞, Calculated from **Eq 2.10** for Reaction of Pip with PS^- in the Presence of 2-, 3- or 4-ClBzNa and Absence of CTABr.[a]

[MX] =	**2-$ClC_6H_4CO_2Na$**			**3-$ClC_6H_4CO_2Na$**			**4-$ClC_6H_4CO_2Na$**		
10^2 [MX]	**10^4 k_{obs}**	**10^{-1} δ_{app}**	**10^2 A_∞**	**10^4 k_{obs}**	**10^{-1} δ_{app}**	**10^2 A_∞**	**10^4 k_{obs}**	**10^{-1} δ_{app}**	**10^2 A_∞**
M	**s^{-1}**	**$M^{-1}cm^{-1}$**		**s^{-1}**	**$M^{-1}cm^{-1}$**		**s^{-1}**	**$M^{-1}cm^{-1}$**	
0	309 ± 2.8[b]	607 ± 4	2.0 ± 0.2	310 ± 2.4[b]	642 ± 4	2.3 ± 0.2	304 ± 2.4[b]	597 ± 5	2.2 ± 0.1
0.1	305 ± 3.6	637 ± 6	1.9 ± 0.2	326 ± 2.2	640 ± 3	2.6 ± 0.1	304 ± 1.5	600 ± 3	2.7 ± 0.1
0.2	294 ± 3.1	629 ± 5	2.0 ± 0.2				307 ± 1.8	597 ± 4	2.7 ± 0.1
0.3	317 ± 3.0	620 ± 5	2.1 ± 0.1	318 ± 1.5	640 ± 2	2.6 ± 0.1	296 ± 5.1	597 ± 10	3.3 ± 0.2
0.4	308 ± 2.1	650 ± 5	2.5 ± 0.9				299 ± 4.0	605 ± 8	3.2 ± 0.2
0.5	311 ± 2.9	625 ± 5	2.0 ± 0.2	326 ± 1.5	630 ± 2	2.7 ± 0.1	290 ± 1.7	617 ± 4	3.4 ± 0.1
0.7				326 ± 1.3	627 ± 2	2.8 ± 0.1			
0.8				314 ± 2.4	645 ± 3	2.7 ± 0.2			
0.9				333 ± 1.5	631 ± 2	3.3 ± 0.1			
1.0	299 ± 2.7	627 ± 4	2.5 ± 0.2	322 ± 1.4	644 ± 2	3.1 ± 0.1	298 ± 1.6	599 ± 4	2.7 ± 0.1
1.5				321 ± 1.5	634 ± 2	3.0 ± 0.1	307 ± 1.7	616 ± 4	3.0 ± 0.1
2.0	315 ± 2.7	618 ± 4	2.5 ± 0.1	317 ± 1.4	640 ± 2	3.0 ± 0.1	303 ± 1.7	615 ± 4	3.1 ± 0.1
2.5				324 ± 1.0	635 ± 1	3.3 ± 0.7	299 ± 3.3	595 ± 7	3.3 ± 0.1
3.0	298 ± 3.0	634 ± 5	3.1 ± 0.2	316 ± 1.2	642 ± 2	3.5 ± 0.8	307 ± 4.0	606 ± 9	4.0 ± 0.1
4.0				309 ± 1.4	640 ± 2	3.5 ± 0.1	297 ± 3.1	585 ± 6	2.7 ± 0.1
5.0	304 ± 2.9	621 ± 5	3.7 ± 0.2	310 ± 0.14	643 ± 2	3.6 ± 0.1	298 ± 1.6	617 ± 4	5.6 ± 0.1

6.0				313 ± 1.7	642 ± 2	3.8 ± 0.1	286 ± 2.8	588 ± 6	2.9 ± 0.1
7.0	301 ± 2.0	628 ± 3	4.5 ± 0.1				280 ± 2.7	595 ± 6	2.8 ± 0.1
8.0				301 ± 1.6	644 ± 2	4.4 ± 0.1	274 ± 2.9	576 ± 6	2.9 ± 0.1
10	305 ± 2.7	617 ± 4	6.0 ± 0.2	296 ± 1.5	643 ± 2	4.5 ± 0.1	276 ± 2.0	608 ± 5	3.8 ± 0.1
15	304 ± 3.8	614 ± 5	7.8 ± 0.2	277 ± 1.6	641 ± 2	5.5 ± 0.2			
20	303 ± 0.8	623 ± 1	9.5 ± 0.1	272 ± 1.5	643 ± 2	6.7 ± 0.2	256 ± 2.0	604 ± 4	5.4 ± 0.1
30	306 ± 1.3	612 ± 2	13 ± 0.1	258 ± 0.8	641 ± 1	8.5 ± 0.8	233 ± 1.6	619 ± 4	6.4 ± 0.1
40	284 ± 0.1	608 ± 1	17 ± 0.1						
50	268 ± 1.3	632 ± 2	21 ± 0.1				190 ± 0.8	610 ± 2	7.7 ± 0.1
60	257 ± 0.1	629 ± 1	24 ± 0.1						
65							161 ± 0.9	611 ± 2	7.3 ± 0.1
70							145 ± 1.9	605 ± 5	8.3 ± 0.3

[a] $[\text{phenyl salicylate}]_0$ = 0.2 mM, 35 ^{o}C, λ = 350 nm, $[\text{piperidine}]_T$ = 0.1 M, $[\ ]_T$ represents total concentration and the aqueous reaction mixture for each kinetic run contained 2 % v/v CH_3CN. The required amounts of 2-, 3- or 4-$ClC_6H_4CO_2Na$ ([MX]) were generated into the reaction mixture by using the stock solution (w M) of 2-, 3- or 4-$ClC_6H_4CO_2H$ prepared in (w + 0.05) M aqueous NaOH. The stock solution of NaOH was used to produce a fixed known concentration (0.03 M) of NaOH into the reaction mixture for each kinetic run. Thus, the maximum concentrations of added NaOH were 0.06, 0.06 and 0.065 M for respective 2-, 3- and 4-$ClC_6H_4CO_2Na$. [b] Error limits are standard deviations.

Table 3.4. Kinetic Parameters, k_{obs}, δ_{app} and A_∞, Calculated from **Eq 2.10** for Reaction of Pip with PS^- in the Presence of 2-, 3- or 4-$BrC_6H_4CO_2Na$ and Absence of CTABr.[a]

[MX] =	**2-$BrC_6H_4CO_2Na$**			**3-$BrC_6H_4CO_2Na$**			**3-$BrC_6H_4CO_2Na$**		
10^2 [MX] M	**$10^4 k_{obs}$ s^{-1}**	**$10^{-1} \delta_{app}$ $M^{-1}cm^{-1}$**	**$10^2 A_\infty$**	**$10^4 k_{obs}$ s^{-1}**	**$10^{-1} \delta_{app}$ $M^{-1}cm^{-1}$**	**$10^2 A_\infty$**	**$10^4 k_{obs}$ s^{-1}**	**$10^{-1} \delta_{app}$ $M^{-1}cm^{-1}$**	**$10^2 A_\infty$**
0	316 ± 2.6[b]	606 ± 5	1.8 ± 0.3	319 ± 1.6[b]	678 ± 4	1.8 ± 0.2	313 ± 1.6[b]	586 ± 2	1.6 ± 0.1
0.2	321 ± 1.9	606 ± 4	1.8 ± 0.1	335 ± 2.1	673 ± 3	2.0 ± 0.1	303 ± 1.7	596 ± 2	1.8 ± 0.2
0.5	313 ± 2.1	616 ± 3	1.9 ± 0.2	324 ± 1.9	688 ± 4	2.4 ± 0.4	309 ± 1.3	586 ± 1	1.9 ± 0.3
0.8	324 ± 1.8	621 ± 3	2.0 ± 0.4				332 ± 1.1	583 ± 2	2.0 ± 0.2
1.0	333 ± 2.3	620 ± 4	1.9 ± 0.4	303 ± 15	647 ± 8	2.7 ± 0.2	315 ± 1.7	592 ± 1	2.0 ± 0.1
1.5	328 ± 1.6	603 ± 3	2.0 ± 0.2	319 ± 1.1	697 ± 4	2.8 ± 0.1	317 ± 1.2	598 ± 1	2.2 ± 0.4
2.0	340 ± 2.5	614 ± 3	2.1 ± 0.4	320 ± 0.9	675 ± 4	3.3 ± 0.3	310 ± 1.0	590 ± 2	2.4 ± 0.2
2.5	310 ± 3.3	599 ± 2	2.3 ± 0.2				313 ± 1.2	588 ± 2	2.8 ± 0.3
3.0	322 ± 3.1	609 ± 3	2.3 ± 0.5	330 ± 1.8	669 ± 1	3.3 ± 0.1	328 ± 1.1	600 ± 1	3.0 ± 0.2
3.5							316 ± 1.9	600 ± 1	3.4 ± 0.4
4.0	318 ± 2.9	625 ± 3	2.8 ± 0.2				340 ± 2.0	583 ± 2	3.7 ± 0.3
5.0	310 ± 1.5	618 ± 2	3.2 ± 0.5	310 ± 1.7	610 ± 2	4.9 ± 0.7	332 ± 1.7	586 ± 2	4.5 ± 0.1
6.0							324 ± 1.0	587 ± 2	4.5 ± 0.3
7.0	305 ± 1.9	619 ± 3	3.7 ± 0.7	316 ± 1.5	689 ± 4	5.4 ± 0.3			
8.0							318 ± 1.2	597 ± 1	5.8 ± 0.1

10	305 ± 2.9	596 ± 5	4.2 ± 0.4	306 ± 2.0	686 ± 3	6.5 ± 0.1	312 ± 1.6	608 ± 2	7.4 ± 0.2
15	299 ± 2.8	616 ± 6	5.2 ± 0.4	299 ± 1.6	688 ± 2	8.8 ± 0.1	296 ± 1.3	598 ± 1	9.8 ± 0.1
20	285 ± 1.5	620 ± 2	6.3 ± 0.1	283 ± 2.2	689 ± 4	14 ± 0.2	270 ± 1.0	603 ± 1	13 ± 0.1
30	273 ± 1.6	625 ± 2	9.2 ± 0.2	250 ± 1.5	697 ± 2	16 ± 0.2	250 ± 1.6	605 ± 2	18 ± 0.2
50	247 ± 0.9	640 ± 1	15 ± 0.1	178 ± 1.8	719 ± 4	23 ± 0.6	195 ± 0.7	621 ± 1	28 ± 0.1
70				148 ± 1.3	718 ± 2	32 ± 0.3			

[a] [phenyl salicylate]$_0$ = 0.2 mM, 35 ^oC, λ = 350 nm, [piperidine]$_T$ = 0.1 M, [ ]$_T$ represents total concentration and the aqueous reaction mixture for each kinetic run contained 2 % v/v CH_3CN. The required amounts of 2-, 3- or 4-$BrC_6H_4CO_2Na$ ([MX]) were generated into the reaction mixture by using the stock solution (w M) of 2-, 3- or 4-$BrC_6H_4CO_2H$ prepared in (w + 0.05) M aqueous NaOH. The stock solution of NaOH was used to produce a fixed known concentration (0.03 M) of NaOH into the reaction mixture for each kinetic run. Thus, the maximum concentrations of added NaOH were 0.055, 0.065 and 0.055 M for respective 2-, 3- and 4-$BrC_6H_4CO_2Na$. [b] Error limits are standard deviations.

Table 3.5. Kinetic Parameters, k_{obs}, δ_{app} and A_∞, Calculated from **Eq 2.10** for Reaction of Pip with PS^- in the Presence of 2- or 4-$IC_6H_4CO_2Na$ and Absence of CTABr.[a]

[MX] =	2-$IC_6H_4CO_2Na$			4-$IC_6H_4CO_2Na$		
10^2 [MX] M	$10^4 k_{obs}$ s^{-1}	$10^{-1} \delta_{app}$ $M^{-1}cm^{-1}$	$10^2 A_\infty$	$10^4 k_{obs}$ s^{-1}	$10^{-1} \delta_{app}$ $M^{-1}cm^{-1}$	$10^2 A_\infty$
0	321 ± 1.8[b]	695 ± 3	3.0 ± 0.1	309 ± 3.6[b]	682 ± 3	1.1 ± 0.3
0.2	306 ± 1.2	696 ± 2	2.8 ± 0	310 ± 2.4	692 ± 4	2.3 ± 0.2
0.5	300 ± 1.2	681 ± 2	3.4 ± 0.2	323 ± 1.8	714 ± 2	2.3 ± 0.1
0.7	341 ± 1.3	681 ± 2	3.7 ± 0	314 ± 2.9	682 ± 3	2.9 ± 0.2
1.0	304 ± 1.2	681 ± 2	4.2 ± 0.1	333 ± 1.5	682 ± 2	4.0 ± 0.1
1.5	340 ± 1.2	699 ± 2	4.7 ± 0.1	304 ± 1.5	690 ± 1	5.6 ± 0.1
2.0	310 ± 1.0	689 ± 1	5.5 ± 0.1	324 ± 1.0	643 ± 1	7.1 ± 0.1
3.0	328 ± 1.4	696 ± 2	6.1 ± 0.1	310 ± 2.1	699 ± 2	8.6 ± 0.2
5.0	309 ± 1.6	690 ± 2	8.6 ± 0.2	320 ± 1.2	683 ± 2	13 ± 0.1
7.0	317 ± 1.4	682 ± 2	10 ± 0.1	294 ± 3.3	700 ± 3	18 ± 0.3
10	316 ± 1.6	689 ± 3	13 ± 0.1	283 ± 3.1	703 ± 3	25 ± 0.3
15	309 ± 1.4	662 ± 2	18 ± 0.1	274 ± 2.8	662 ± 2	34 ± 0.4
20	308 ± 1.1	673 ± 2	23 ± 0.1	257 ± 3.6	698 ± 3	45 ± 0.3
30	285 ± 1.3	699 ± 2	33 ± 0.1	231 ± 2.9	689 ± 3	68 ± 0.4

[a] $[\text{phenyl salicylate}]_0$ = 0.2 mM, 35 ^oC, λ = 350 nm, $[\text{piperidine}]_T$ = 0.1 M, $[\ ]_T$ represents total concentration and the aqueous reaction mixture for each kinetic run contained 2 % v/v CH_3CN. The required amounts of 2- or 4-$IC_6H_4CO_2Na$ ([MX]) were generated into the reaction mixture by using the stock solution (w M) of 2- or 4-$IC_6H_4CO_2H$ prepared in (w + 0.05) M aqueous NaOH. The stock solution of NaOH was used to produce a fixed known concentration (0.03 M) of NaOH into the reaction mixture for each kinetic run. Thus, the maximum concentrations of added NaOH were 0.06 and 0.04 M for respective 2- and 4-$IC_6H_4CO_2Na$. [b] Error limits are standard deviations.

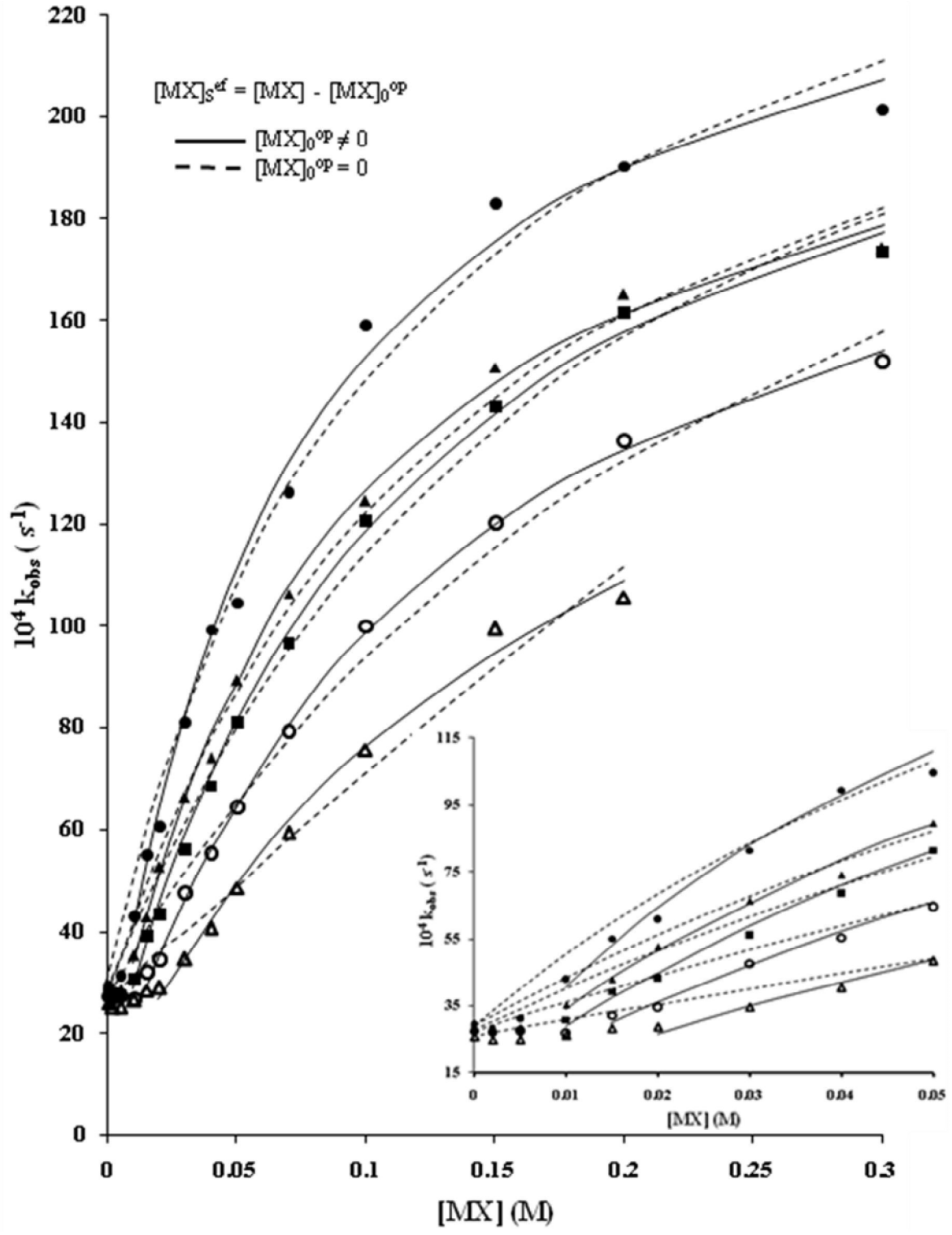

Figure 3.1. Effects of [3-FBzNa] on k_{obs} for the reaction of piperidine with PS^- at different constant $[CTABr]_T$ and 35°C. The $[3\text{-FBzNa}]_0^{op}$ for set with $[CTABr]_T$/mM = 5 (●), 6 (▲), 7 (■), 10 (○) and 15 (Δ) are 5.9 mM, 7.3 mM, 9.4 mM, 13.1 mM and 18.8 mM respectively.

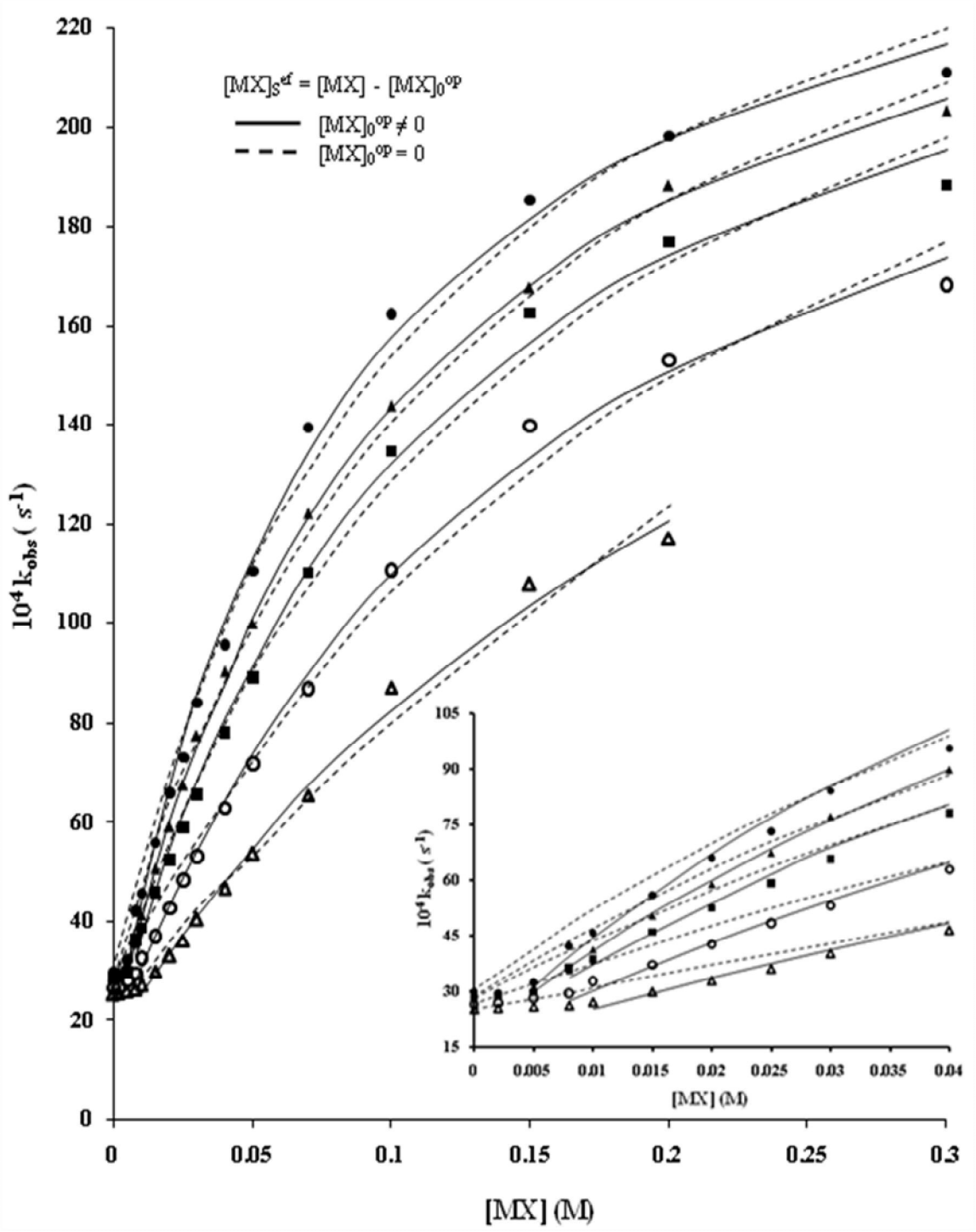

Figure 3.2. Effects of [4-FBzNa] on k_{obs} for the reaction of piperidine with PS^- at different constant $[CTABr]_T$ and 35°C. The $[4\text{-FBzNa}]_0^{op}$ for set with $[CTABr]_T$/mM = 5 (●), 6 (▲), 7 (■), 10 (○) and 15 (Δ) are 4.5 mM, 4.7 mM, 5.2 mM, 7.3 mM and 9.8 mM respectively.

Table 3.6. Kinetic Parameters, k_{obs}, δ_{app} and A_∞ Calculated from **Eq. 2.10** for Reactions of Pip with PS^- in the Presence of 2-FBzNa and 5 mM CTABr.[a]

10^2 MX M	10^4 k_{obs}[b] s^{-1}	10^{-1} δ_{app} $M^{-1}cm^{-1}$	10^1 A_∞	10^1 A_0[c]
0.0	29.1 ± 0.3	714 ± 3	0.16 ± 0.04	14.4
0.5	31.9 ± 0.2	727 ± 2	1.03 ± 0.03	15.6
1.0	34.2 ± 0.5	706 ± 4	1.87 ± 0.06	16.0
1.5	38.1 ± 0.3	705 ± 2	2.75 ± 0.04	16.8
2.0	42.9 ± 0.4	720 ± 3	3.76 ± 0.05	18.2
3.0	52.7 ± 0.7	726 ± 3	5.56 ± 0.06	20.1
5.0	66.2 ± 0.3	724 ± 5	8.89 ± 0.09	23.4

[a] $[\text{phenyl salicylate}]_0$ = 0.2 mM, 35 ^oC, λ = 350 nm, $[\text{piperidine}]_T$ = 0.1 M, $[\ ]_T$ represents total concentration and the aqueous reaction mixture for each kinetic run contained 2 % v/v CH_3CN. The required amounts of 2-$FC_6H_4CO_2Na$ ([MX]) were generated into the reaction mixture by using the stock solution (w M) of 2-$FC_6H_4CO_2H$ prepared in (w + 0.05) M aqueous NaOH. The stock solution of NaOH was used to produce a fixed known concentration (0.03 M) of NaOH into the reaction mixture for each kinetic run. Thus, the maximum concentration of added NaOH was 0.035 M. [b] Error limits are standard deviations. [c] $A_0 = \delta_{app}\,[\text{Sub}]_T + A_\infty$.

Table 3.7. Kinetic Parameters, k_{obs}, δ_{app} and A_∞ Calculated from **Eq. 2.10** for Conditions (i), (ii) and (iii) as listed in the Presence of 5 mM CTABr.[a]

(i) 0.2 mM PSH, 0.1 M Pip, $0.0 \leq [2\text{-}FC_6H_4CO_2Na] \leq 0.3$ M, 5 mM CTABr and $0.03 \leq [NaOH] \leq 0.06$ M with the addition of Pip right before the addition of PSH.

(ii) 0.2 mM PSH, $0.0 \leq [2\text{-}FC_6H_4CO_2Na] \leq 0.3$ M, 5 mM CTABr and $0.03 < [NaOH] \leq 0.06$ M

(iii) 0.1 M Pip, $0.0 \leq [2\text{-}FC_6H_4CO_2Na] \leq 0.3$ M, 5 mM CTABr and $0.03 < [NaOH] \leq 0.06$ M

Reaction		**(i)**			**(ii)**			**(iii)**	
10^2 [MX] M	**10^4 k_{obs} s^{-1}**	**10^{-1} δ_{app} $M^{-1}cm^{-1}$**	**10^2 A_∞**	**10^4 k_{obs} s^{-1}**	**10^{-1} δ_{app} $M^{-1}cm^{-1}$**	**10^2 A_∞**	**10^4 k_{obs} s^{-1}**	**δ_{app} $M^{-1}cm^{-1}$**	**10^2 A_∞**
0.0	29.6 ± 0.2	685 ± 2	2.2 ± 0.3						
0.5	32.4 ± 0.5	676 ± 4	8.1 ± 0.5	1.74 ± 0.0	661 ± 1	2.8 ± 0.1	11.3 ± 0.4	0.95 ± 0.01	2.5 ± 0.1
1.0	37.0 ± 0.5	650 ± 3	13 ± 0.5	1.90 ± 0.0	663 ± 1	2.7 ± 0.2	10.6 ± 0.1	1.79 ± 0.01	6.1 ± 0.1
1.5	41.4 ± 0.6	636 ± 3	16 ± 0.5	2.09 ± 0.0	675 ± 1	2.9 ± 0.2	9.64 ± 0.1	2.56 ± 0.01	5.5 ± 0.1
2.0	60.4 ± 1.0	603 ± 4	17 ± 0.6	2.24 ± 0.0	657 ± 5	3.9 ± 0.9	8.76 ± 0.1	3.18 ± 0.01	4.3 ± 0.1
3.0	71.2 ± 1.5	582 ± 4	21 ± 0.7	2.62 ± 0.0	615 ± 1	4.0 ± 0.1	7.48 ± 0.0	4.93 ± 0.03	5.0 ± 0.3
4.0	87.6 ± 1.4	598 ± 4	24 ± 0.5	2.79 ± 0.0	656 ± 1	5.4 ± 0.2	6.97 ± 0.0	6.57 ± 0.04	6.3 ± 0.4
5.0	96.9 ± 1.4	581 ± 3	25 ± 0.5	2.98 ± 0.0	654 ± 2	6.9 ± 0.2	6.09 ± 0.0	8.14 ± 0.09	9.8 ± 0.7
7.0	120 ± 2.4	581 ± 4	29 ± 0.6	3.34 ± 0.0	660 ± 2	8.4 ± 0.4	5.47 ± 0.0	11.6 ± 0.11	12 ± 0.9
10	148 ± 2.2	593 ± 3	33 ± 0.5	3.73 ± 0.0	676 ± 3	11 ± 0.5	3.74 ± 0.0	15.4 ± 0.05	12 ± 0.4
15	179 ± 2.0	580 ± 2	39 ± 0.4	4.57 ± 0.1	575 ± 3	14 ± 0.6	3.25 ± 0.1	22.8 ± 0.23	16 ± 1.6
20	218 ± 4.6	637 ± 5	45 ± 0.7	5.18 ± 0.1	668 ± 3	22 ± 0.5	3.21 ± 0.0	28.7 ± 0.05	21 ± 0.3
30	250 ± 5.6	613 ± 6	58 ± 0.7	6.11 ± 0.1	644 ± 2	32 ± 0.3	2.87 ± 0.3	31.1 ± 1.00	25 ± 6.9

[a] Rates of reactions were monitored spectrophotometrically at 350 nm.

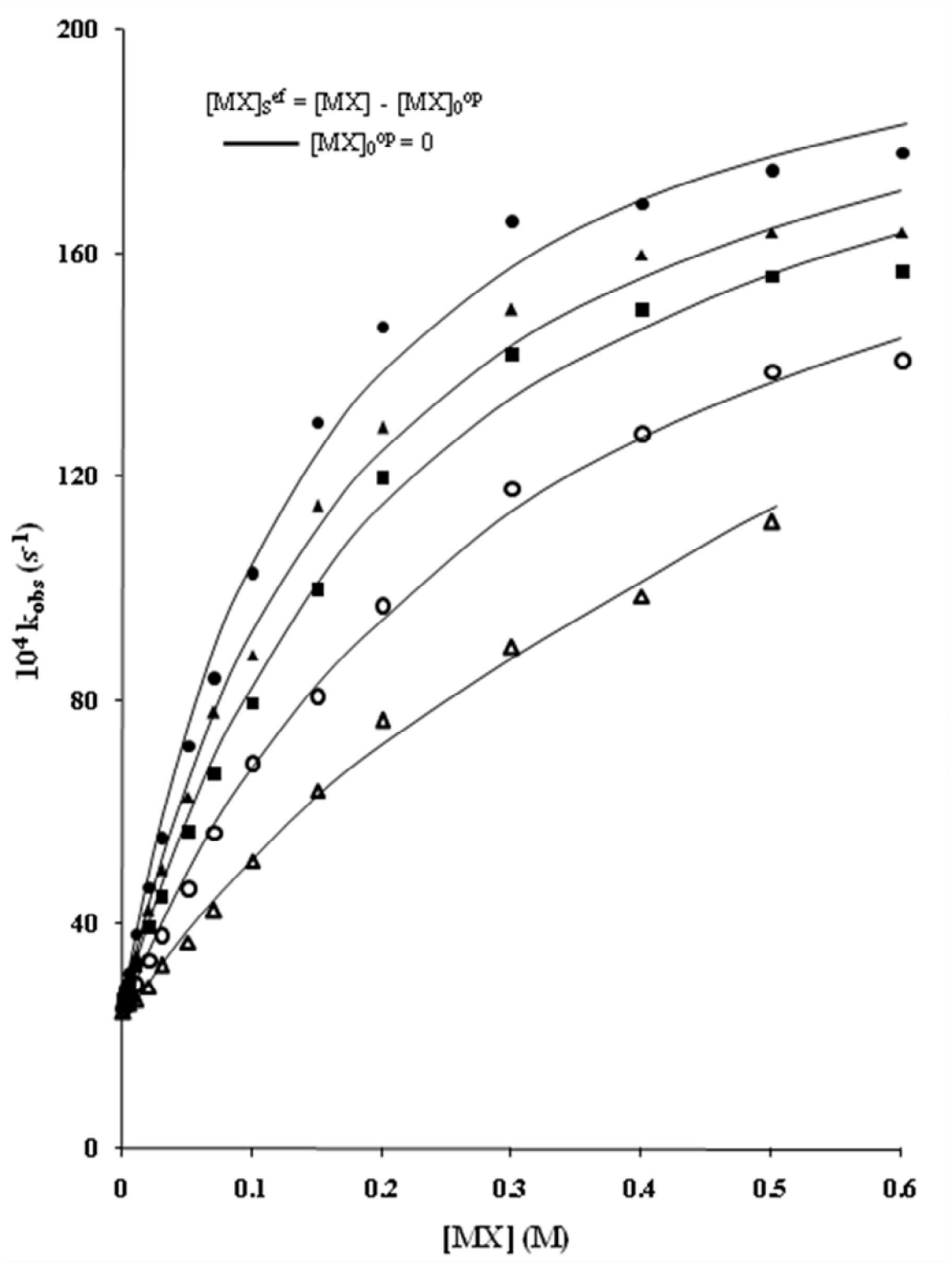

Figure 3.3 Effects of [2-ClBzNa] on k_{obs} for the reaction of piperidine with PS^- at different constant $[CTABr]_T$ and 35°C. The $[2\text{-ClBzNa}]_0^{op}$ for set with $[CTABr]_T$/mM = 5 (●), 6 (▲), 7 (■), 10 (○) and 15 (Δ) are all zeros.

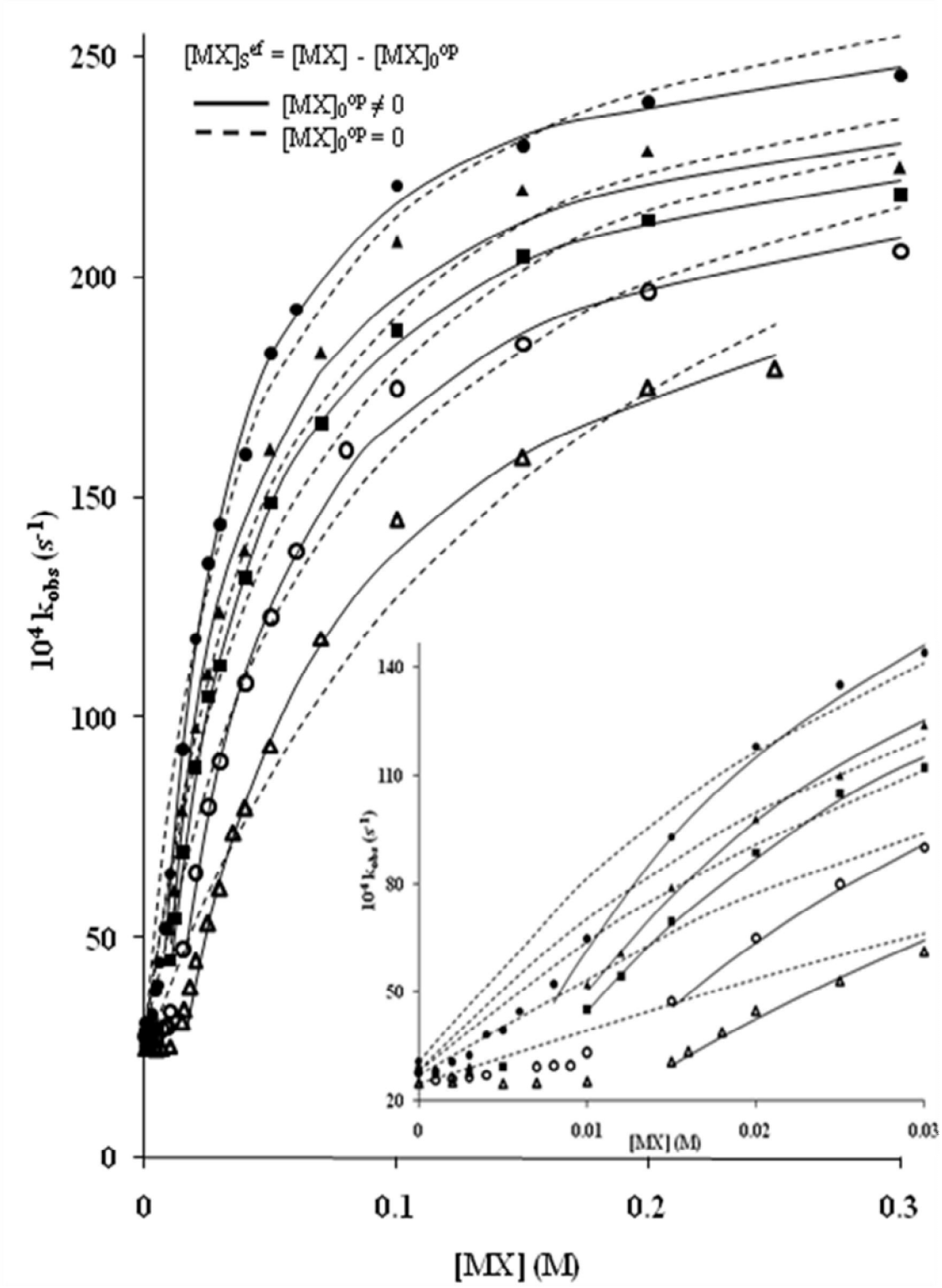

Figure 3.4 Effects of [3-ClBzNa] on k_{obs} for the reaction of piperidine with PS^- at different constant $[CTABr]_T$ and 35°C. The $[3\text{-ClBzNa}]_0^{op}$ for set with $[CTABr]_T$/mM = 5 (●), 6 (▲), 7 (■), 10 (○) and 15 (Δ) are 6.0 mM, 6.8 mM,7.1 mM, 10.8 mM and 13.3 mM respectively.

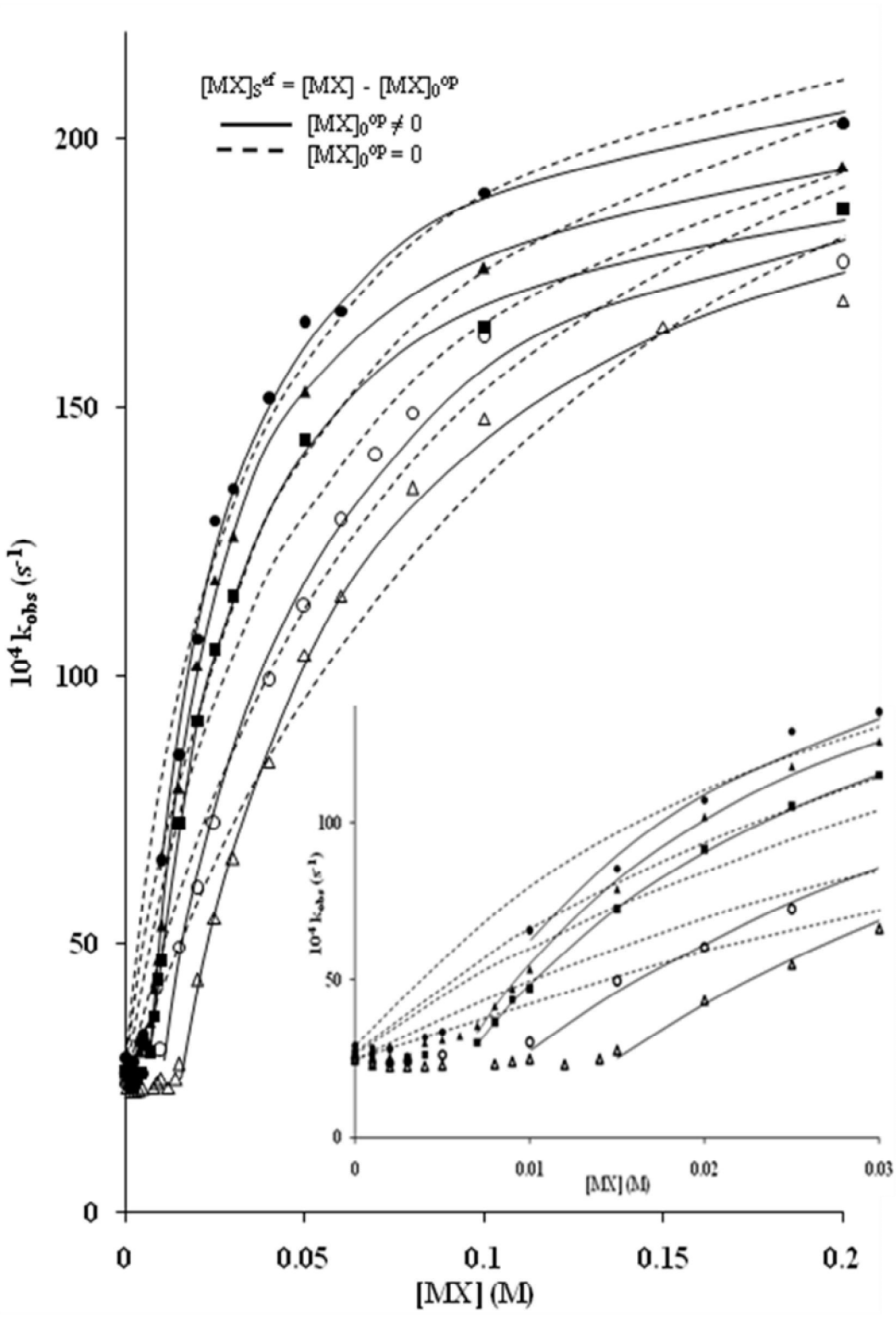

Figure 3.5 Effects of [4-ClBzNa] on k_{obs} for the reaction of piperidine with PS^- at different constant $[CTABr]_T$ and 35°C. The $[4\text{-ClBzNa}]_0^{op}$ for set with $[CTABr]_T$/mM = 5 (●), 6 (▲), 7 (■), 10 (○) and 15 (Δ) are 5.6 mM, 6.3 mM, 6.6 mM, 9.2 mM and 14.8 mM respectively.

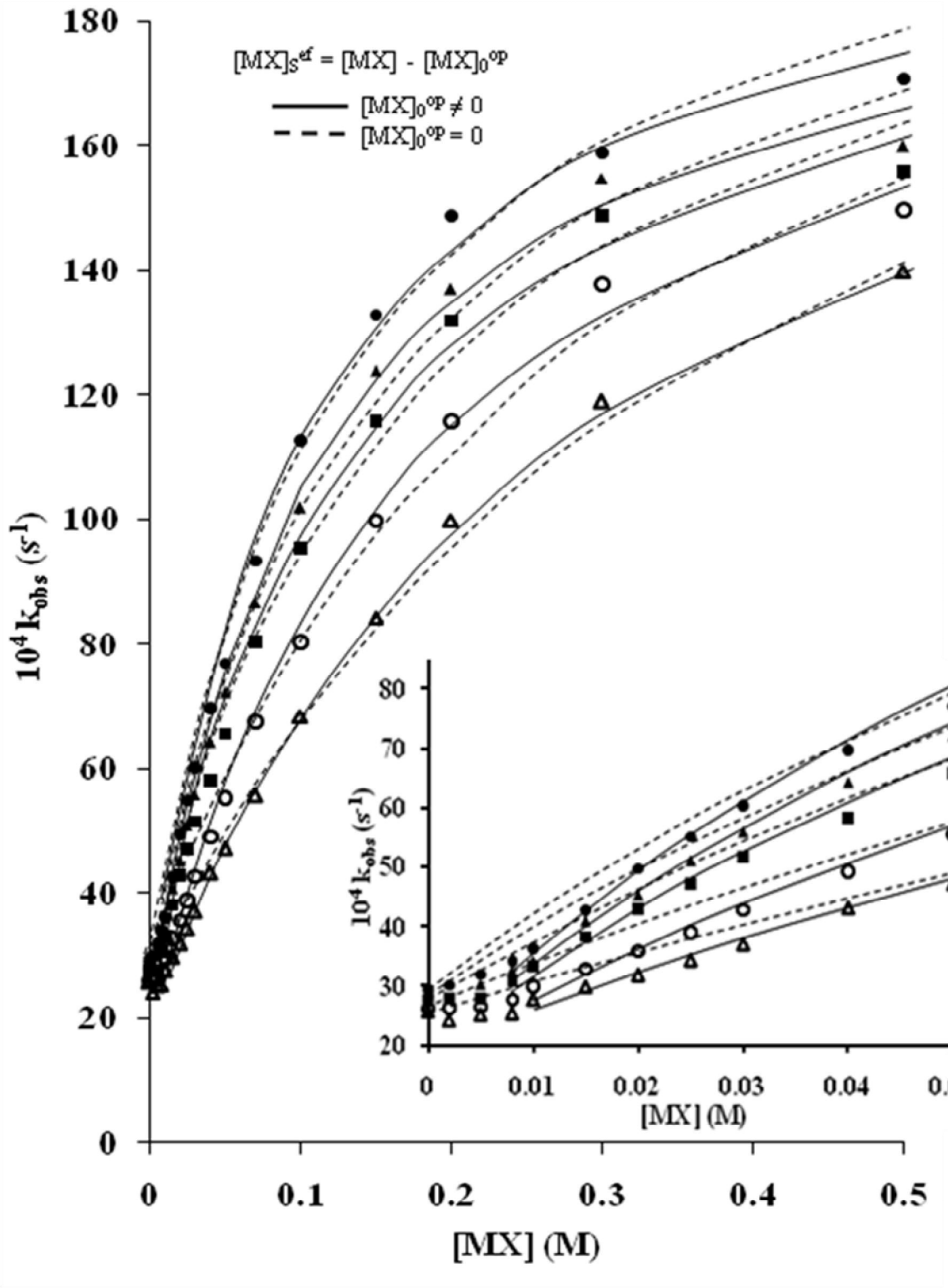

Figure 3.6. Effects of [2-BrBzNa] on k_{obs} for the reaction of piperidine with PS^- at different constant $[CTABr]_T$ and 35°C. The $[2\text{-BrBzNa}]_0^{op}$ for set with $[CTABr]_T$/mM = 5 (●), 6 (▲), 7 (■), 10 (○) and 15 (Δ) are 6.3 mM, 6.6 mM, 6.7 mM, 8.8 mM and 9.4 mM respectively.

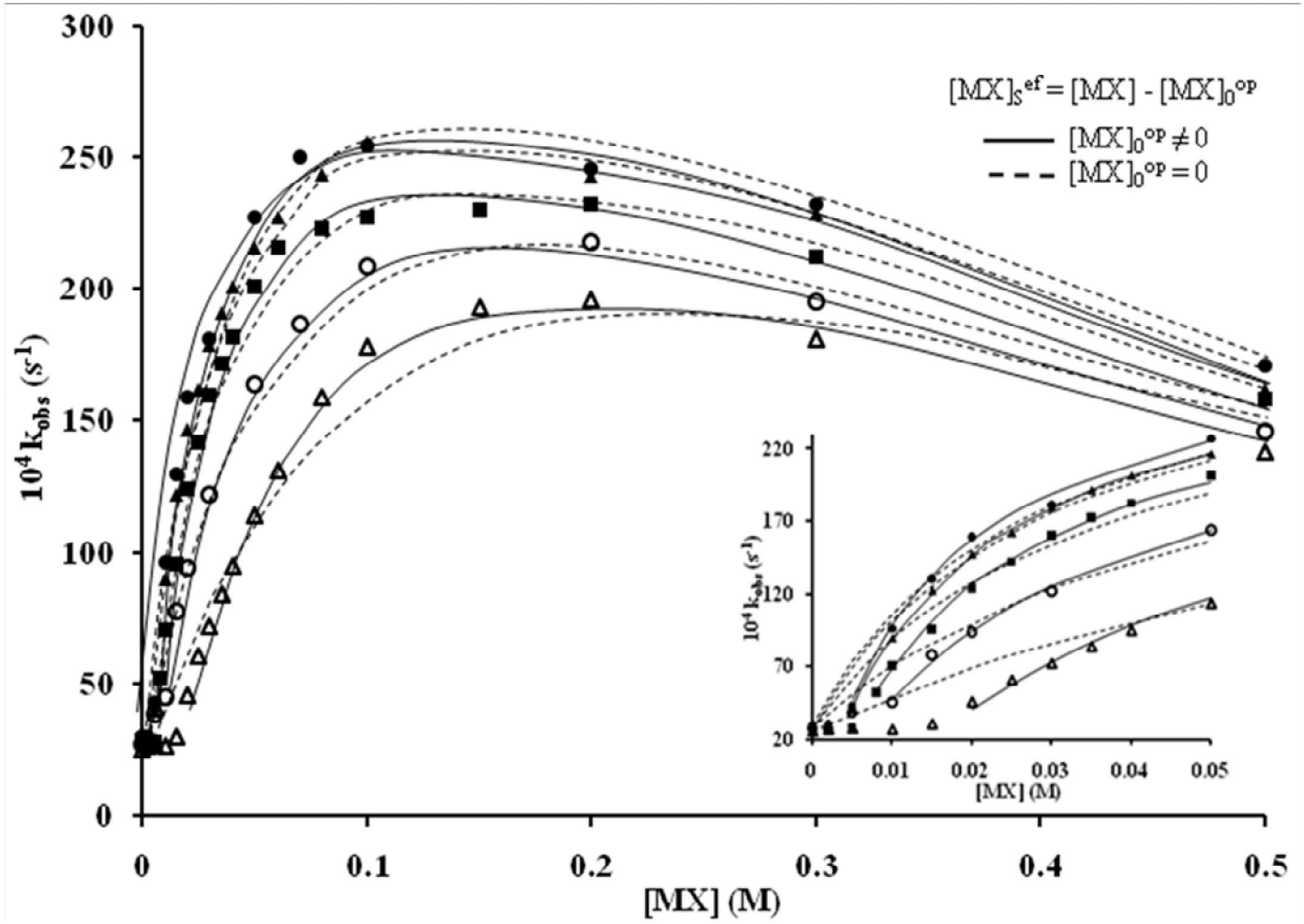

Figure 3.7. Effects of [3-BrBzNa] on k_{obs} for the reaction of piperidine with PS^- at different constant $[CTABr]_T$ and 35°C. The $[3\text{-}BrBzNa]_0^{op}$ for set with $[CTABr]_T$/mM = 5 (●), 6 (▲), 7 (■), 10 (○) and 15 (Δ) are 4.0 mM, 4.1 mM, 5.7 mM, 6.8 mM and 15.9 mM respectively.

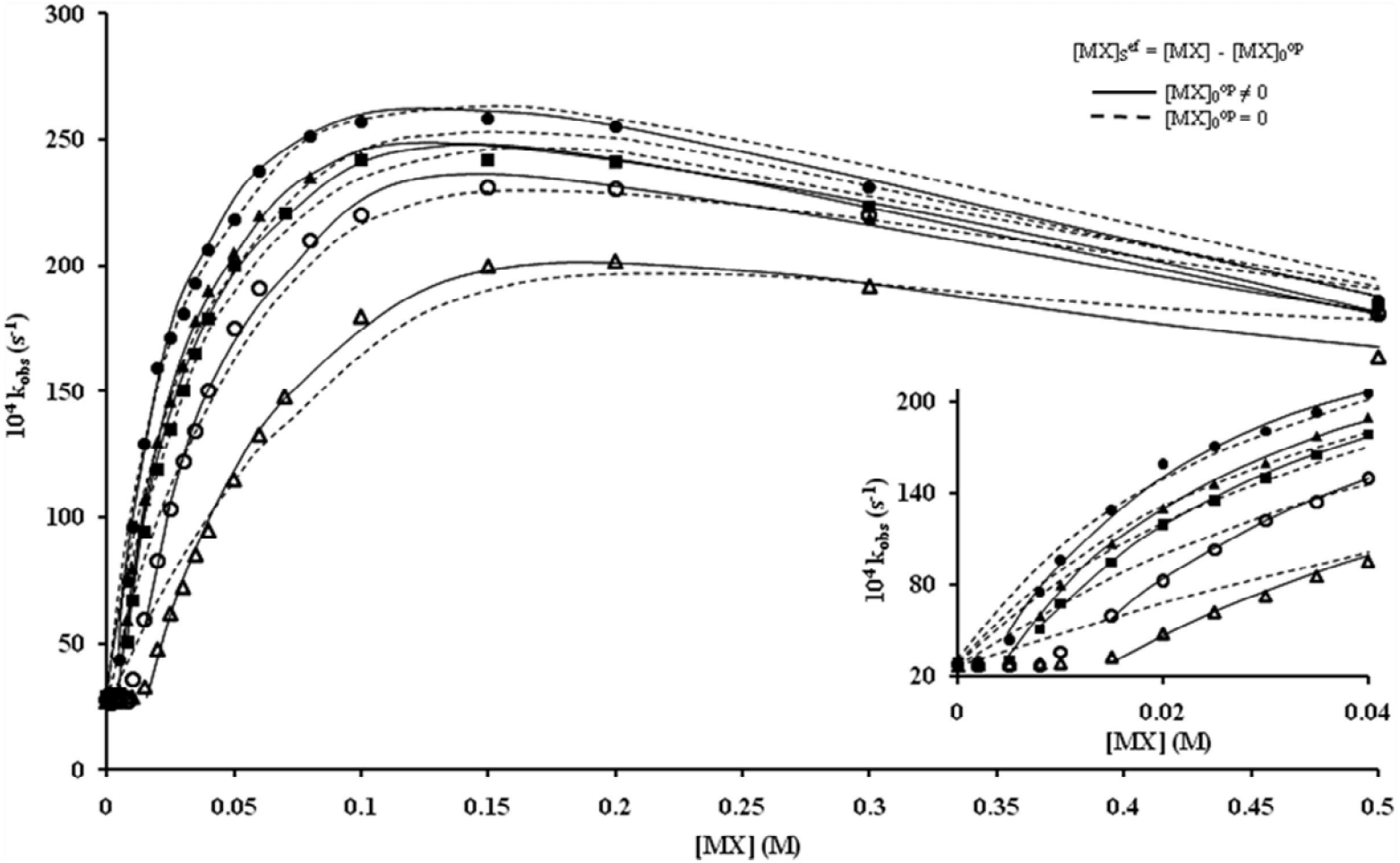

Figure 3.8. Effects of [4-BrBzNa] on k_{obs} for the reaction of piperidine with PS^- at different constant $[CTABr]_T$ and 35°C. The $[4\text{-}BrBzNa]_0^{op}$ for set with $[CTABr]_T$/mM = 5 (●), 6 (▲), 7 (■), 10 (○) and 15 (Δ) are 3.6 mM, 4.6 mM, 5.3 mM, 10.2 mM and 14.4 mM respectively.

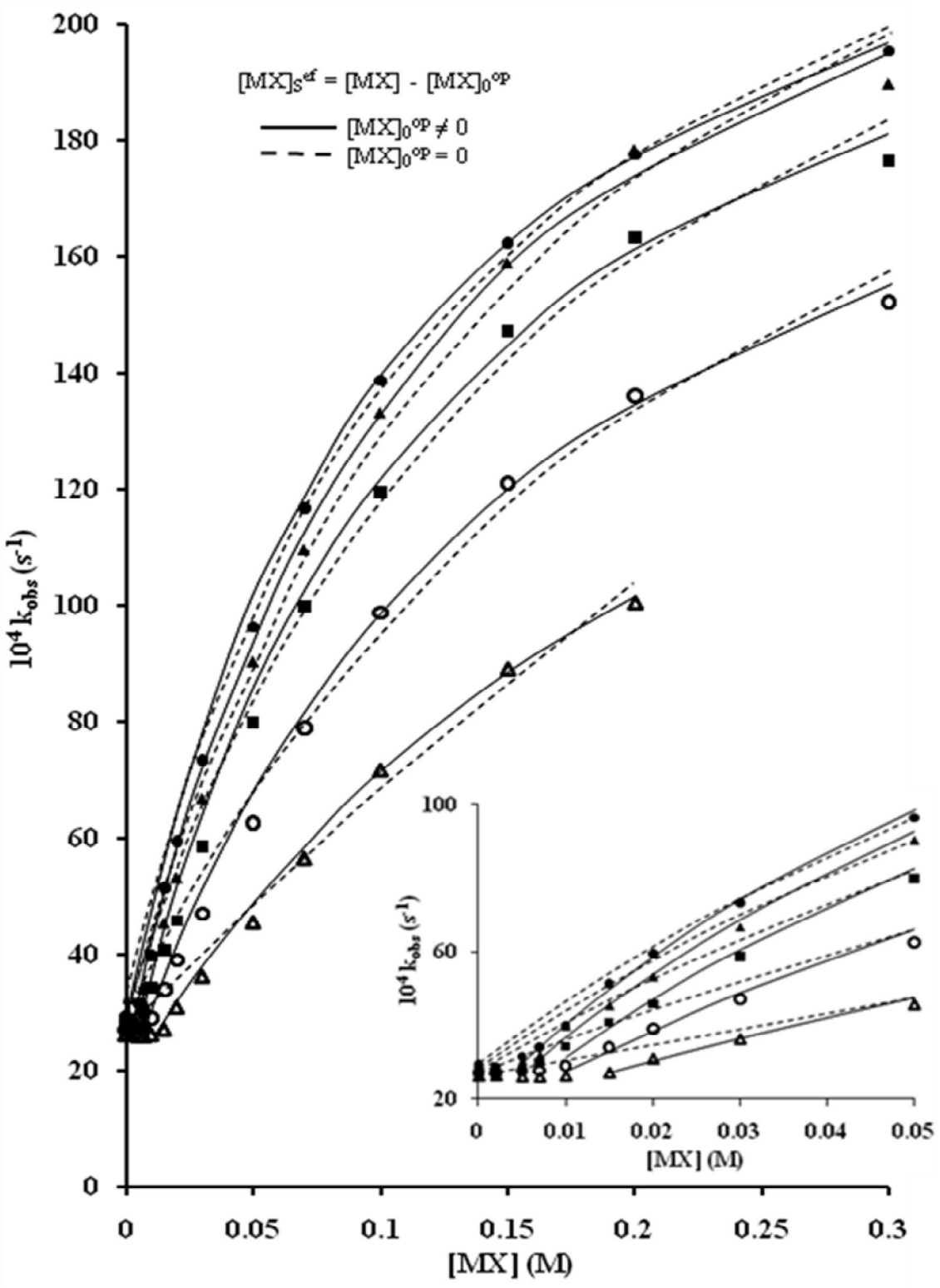

Figure 3.9. Effects of [2-IBzNa] on k_{obs} for the reaction of piperidine with PS^- at different constant $[CTABr]_T$ and 35°C. The $[2\text{-IBzNa}]_0^{op}$ for set with $[CTABr]_T$/mM = 5 (●), 6 (▲), 7 (■), 10 (○) and 15 (Δ) are 4.5 mM, 5.6 mM, 7.8 mM, 9.7 mM and 14.0 mM respectively.

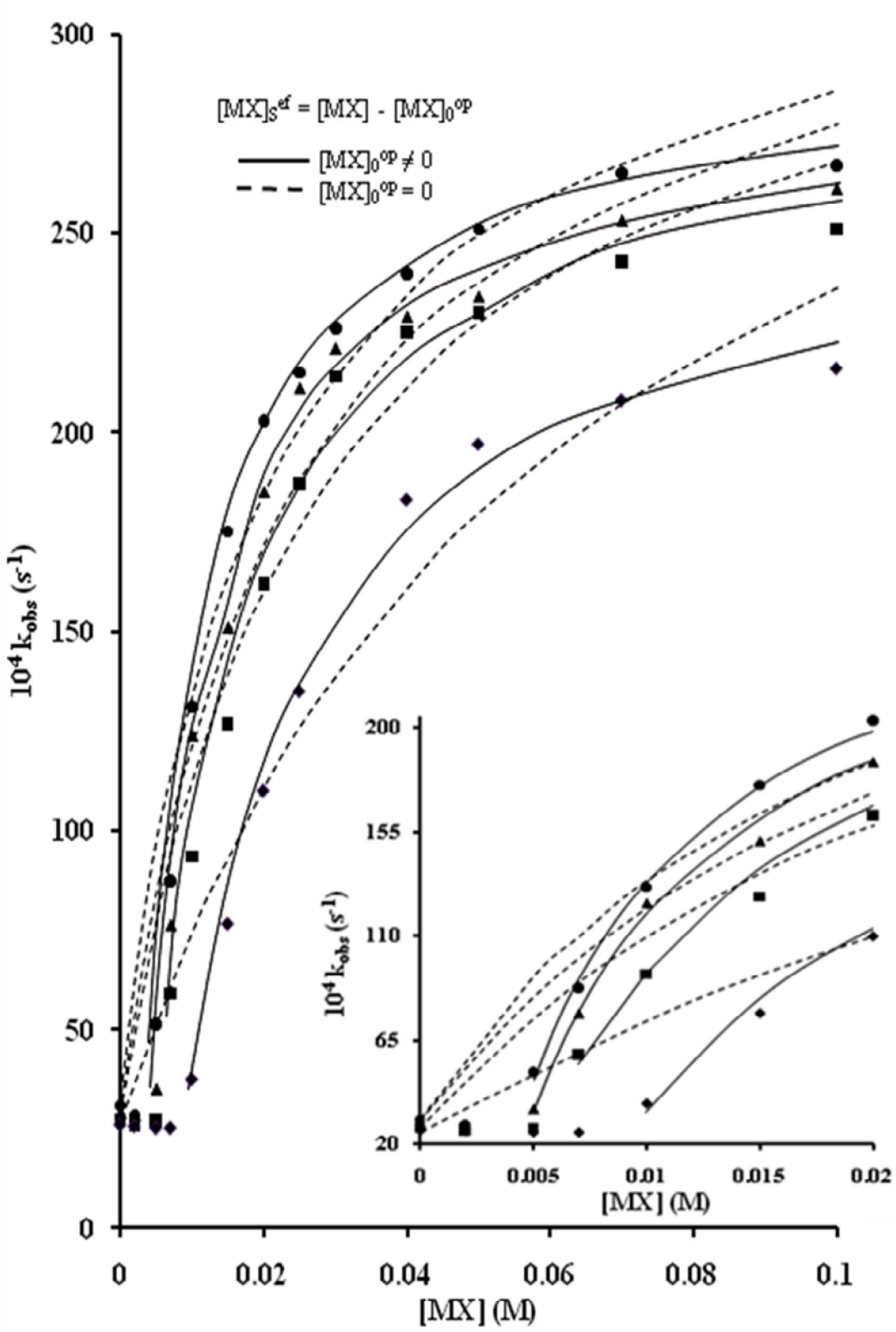

Figure 3.10. Effects of [4-IBzNa] on k_{obs} for the reaction of piperidine with PS^- at different constant $[CTABr]_T$ and 35°C. The $[4\text{-IBzNa}]_0^{op}$ for set with $[CTABr]_T$/mM = 5 (●), 6 (▲), 7 (■) and 10 (♦) are 4.4 mM, 4.8 mM, 5.5 mM and 9.4 mM respectively.

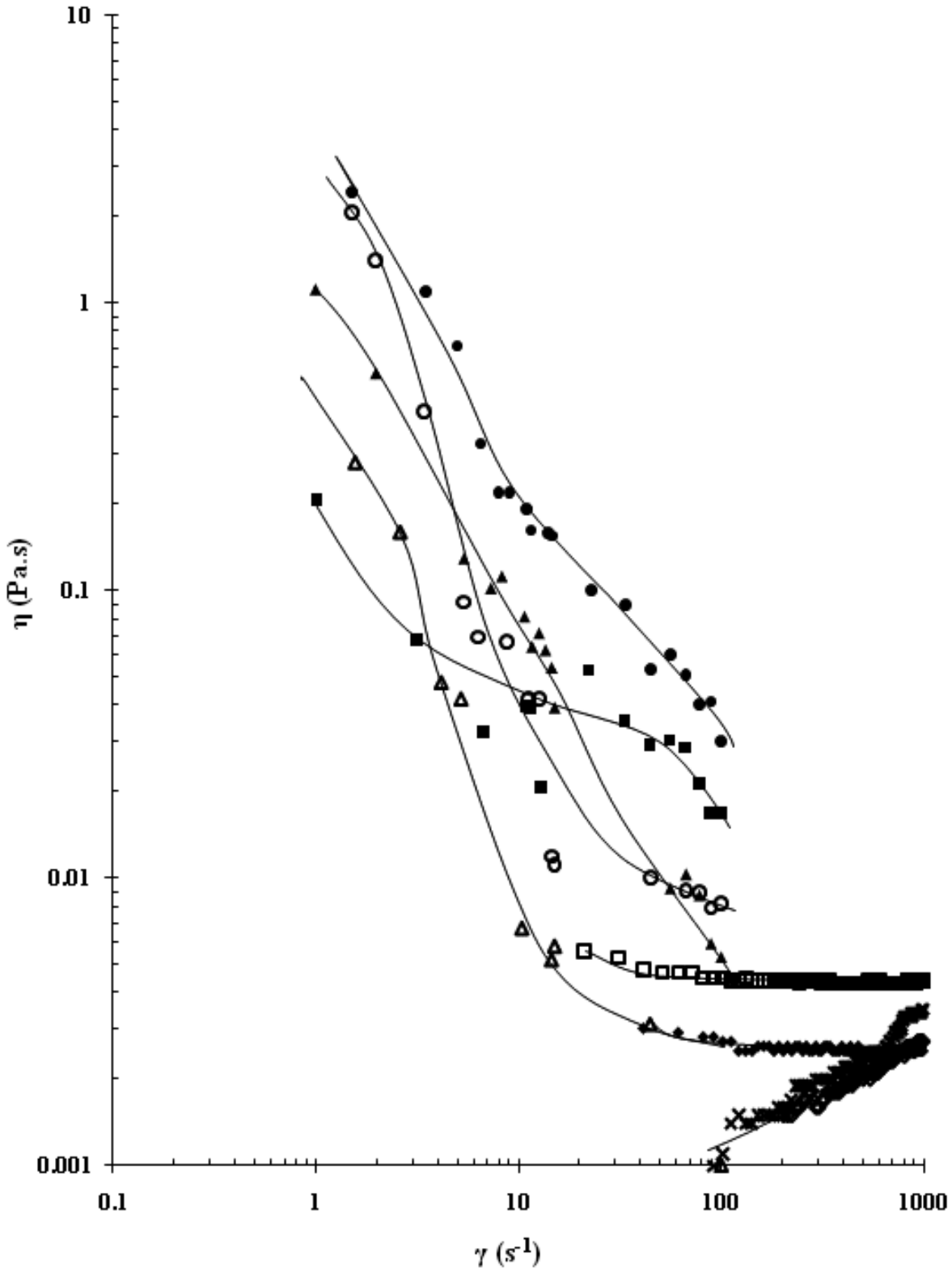

Figure 3.11. Rheological behavior shown by samples of kinetic measurements with $[CTABr]_T$ = 0.015 M and [3-FBzNa] = 0.0 M (◊), 0.03 M (♦), 0.05 M (■), 0.06 M (Δ), 0.07 M (●), 0.08 M (**O**) and 0.10 M (▲), 0.15 M (□) and 0.20 M (×).

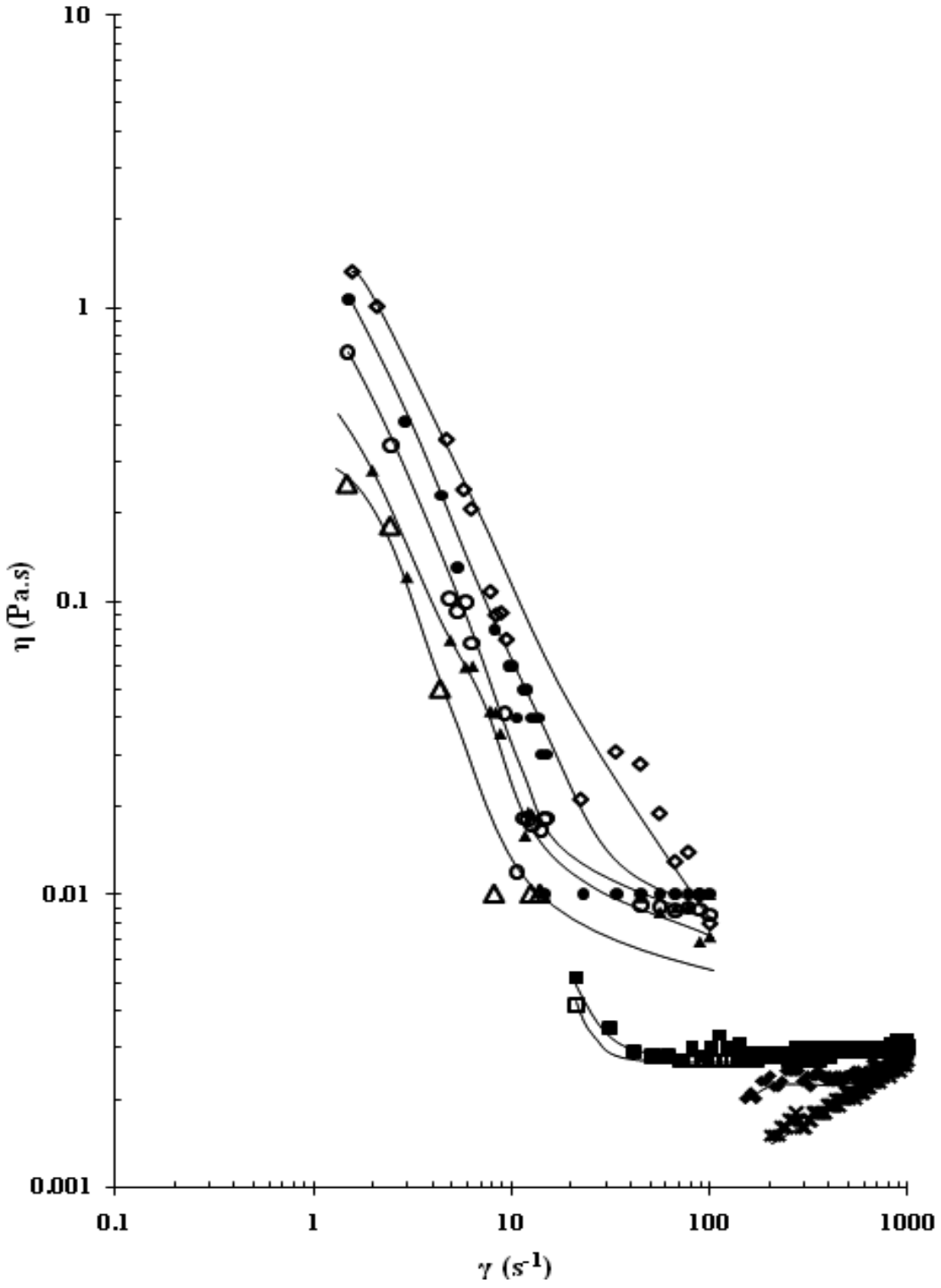

Figure 3.12. Plots showing the dependence of shear viscosity (η) upon shear rate (γ) for samples where [PSH] = 2.0×10^{-4} M, [NaOH] = 0.03 M, [Pip] = 0.1 M, [CTABr] = 0.015 M and [4-FBzNa] = 0.0 M (**x**), 0.02 M (□), 0.04 M (■), 0.06 M (Δ), 0.07 M (◊), 0.08 M (●), 0.10 M (**O**) and 0.15 M (▲) and 0.20 M (♦).

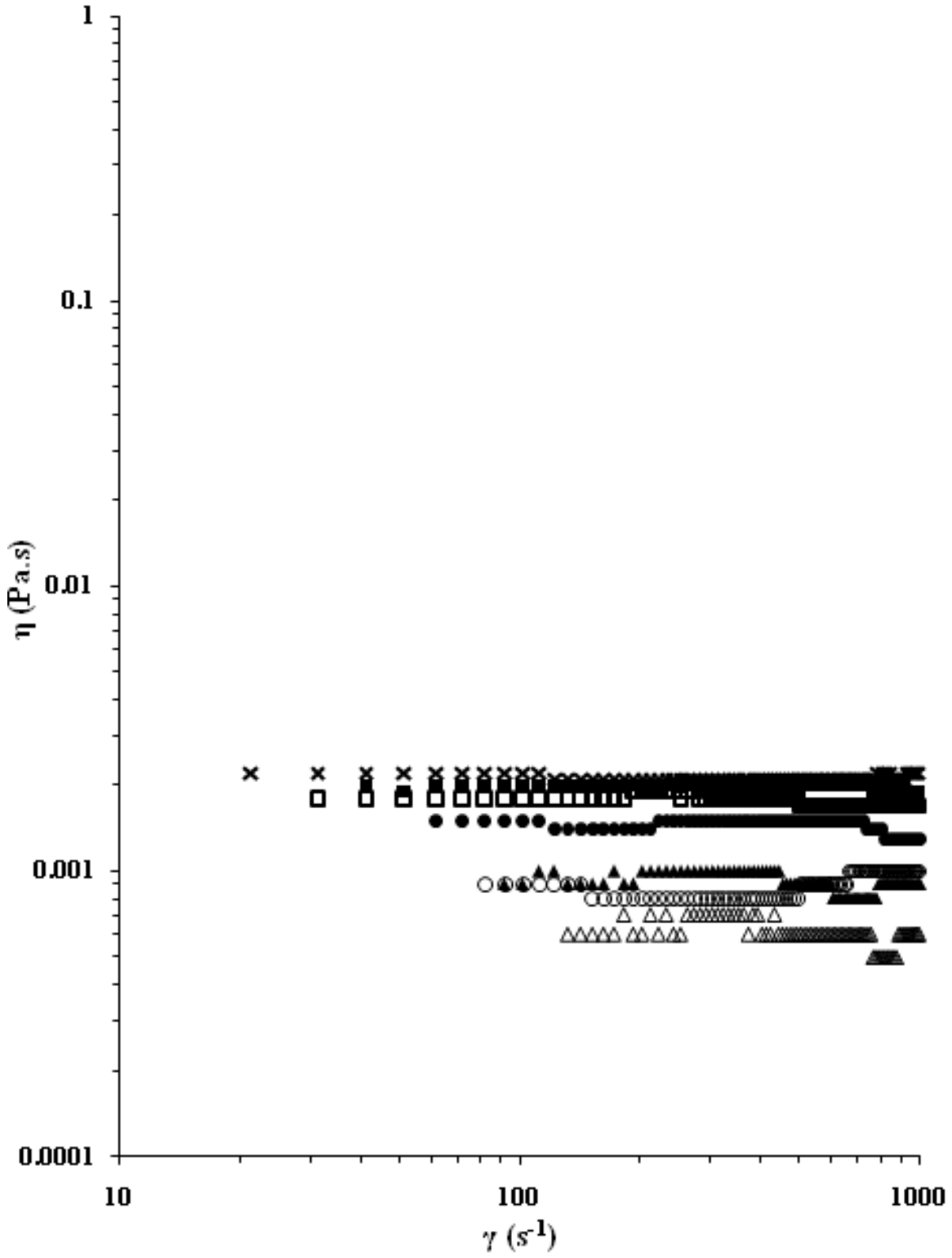

Figure 3.13. Rheologival behavior shown by samples of kinetic measurements with $[CTABr]_T$ = 0.015 M and [2-$ClC_6H_4CO_2Na$] = 0.01 M (Δ), 0.05 M (▲), 0.1 M (○), 0.3 M (●), 0.4 M (□), 0.5 M (■) and 0.6 M (×).

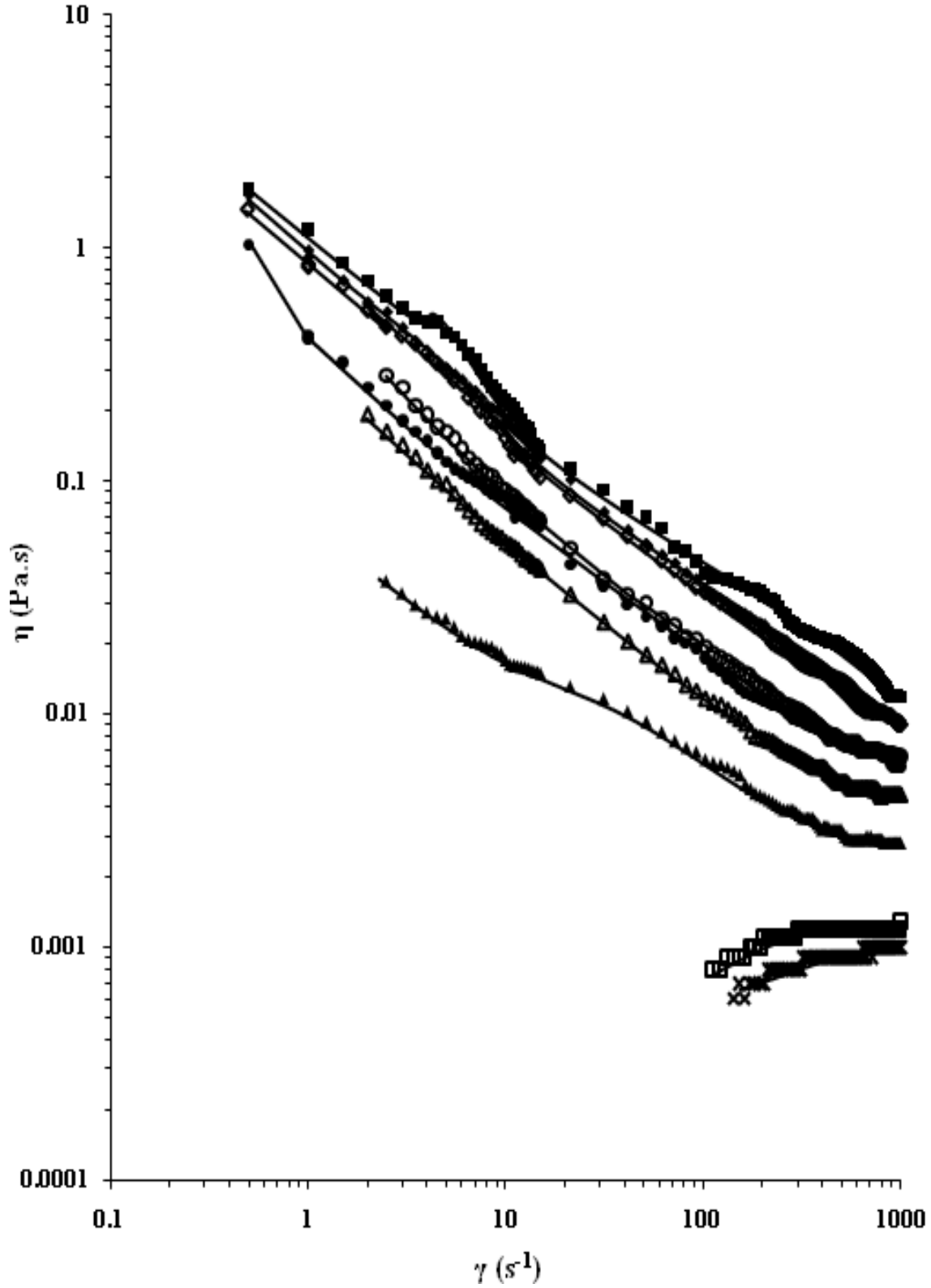

Figure 3.14. Rheological behavior shown by samples of kinetic measurements with $[CTABr]_T$ = 0.015 M and [3-ClBzNa] = 0.005 M (×), 0.01 M (□), 0.02 M (▲), 0.03 M (●), 0.04 M (♦), 0.05 M (■), 0.06 M (◊), 0.07 M (○) and 0.1 M (Δ).

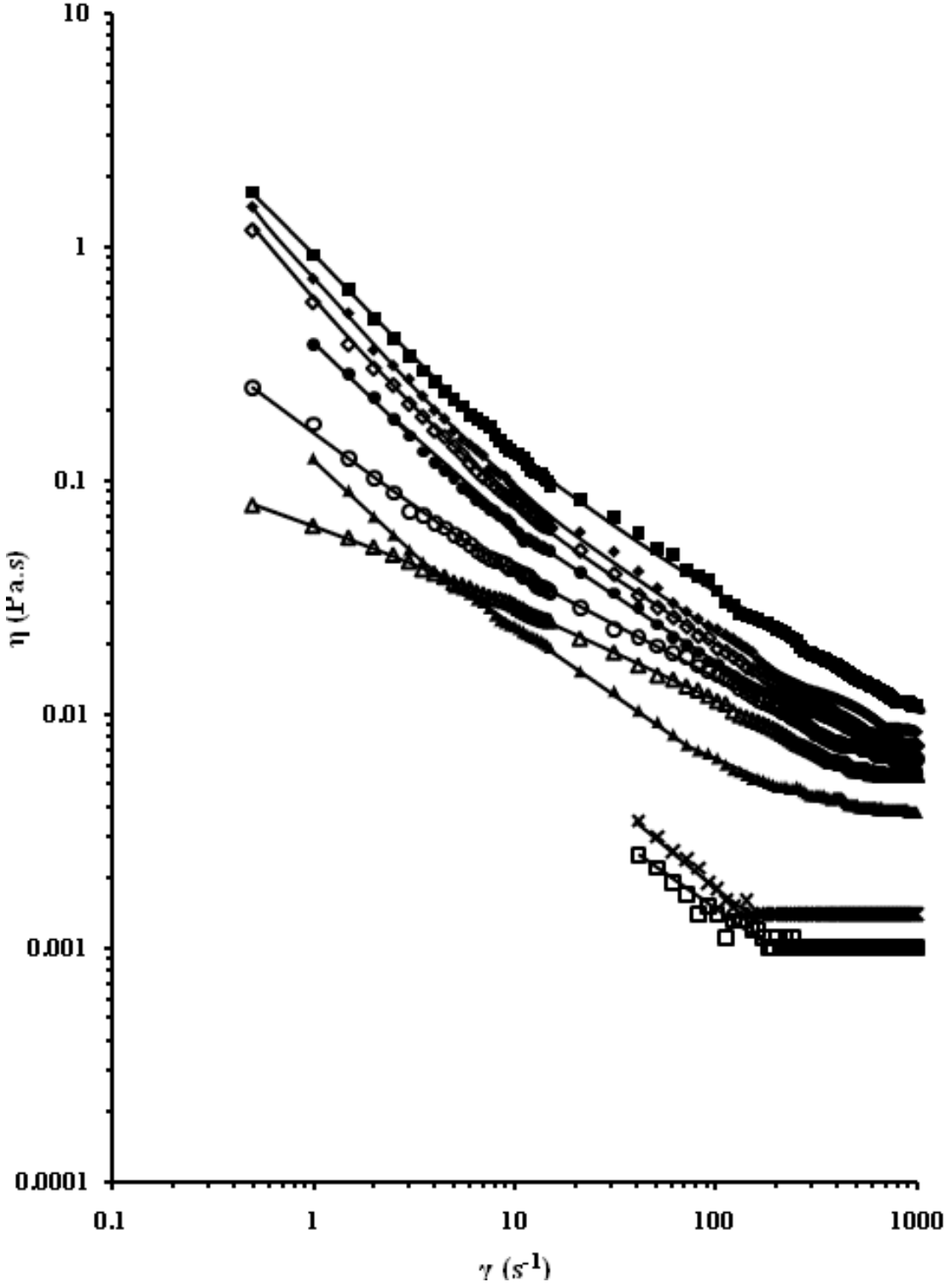

Figure 3.15. Rheological behavior shown by samples of kinetic measurements with $[CTABr]_T$ = 0.015 M and [4-$ClC_6H_4CO_2Na$] = 0.005 M (□), 0.01M (×), 0.02 M (▲), 0.03 M (●), 0.04 M (♦), 0.05 M (■), 0.06 M (◊), 0.07 M (○) and 0.1 M(Δ).

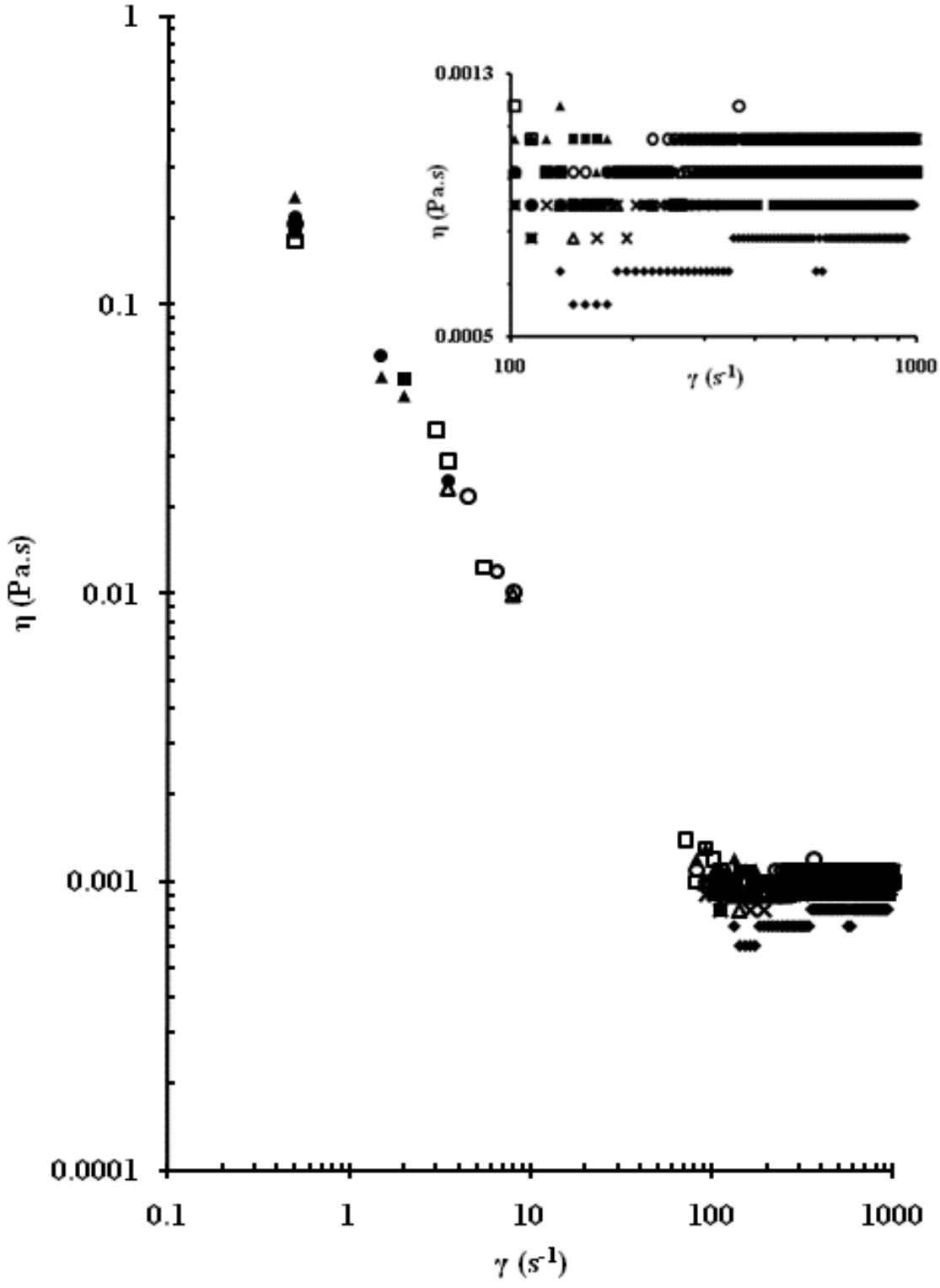

Figure 3.16. Rheological behavior shown by samples of kinetic measurements with $[CTABr]_T$ = 0.015 M and [2-$BrC_6H_4CO_2Na$] = 0.02 M (♦), 0.04 M (■), 0.06 M (▲), 0.08 M (●), 0.1 M (○), 0.2 M (Δ), 0.3 M (□) and 0.4 M (×).

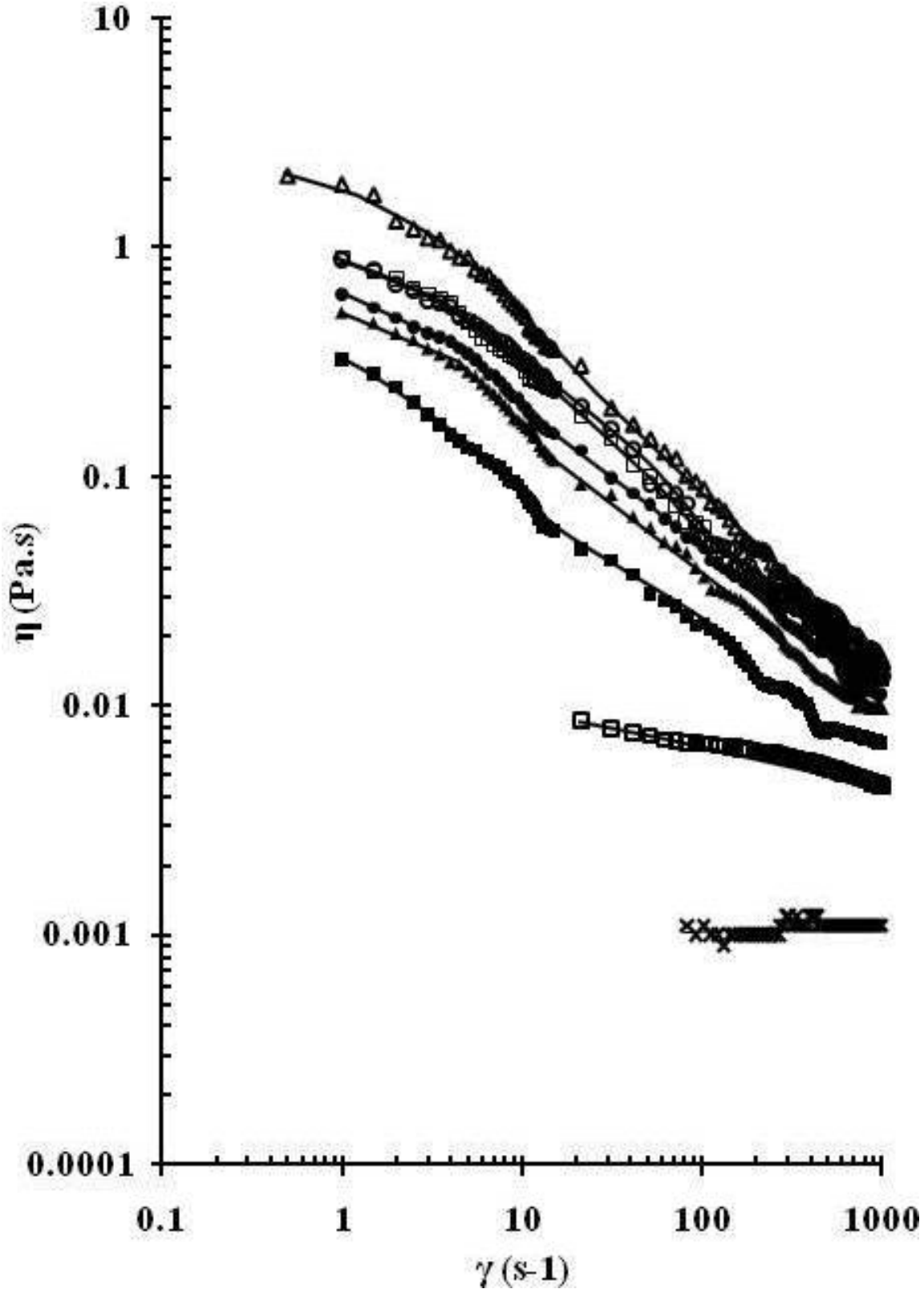

Figure 3.17. Rheological behavior shown by samples of kinetic measurements with $[CTABr]_T$ = 0.015 M and [3-$BrC_6H_4CO_2Na$] = 0.01 M (×), 0.03 M (Δ), 0.04 M (○), 0.05 M (●), 0.06 M (▲), 0.08 M (■) and 0.1 M (□).

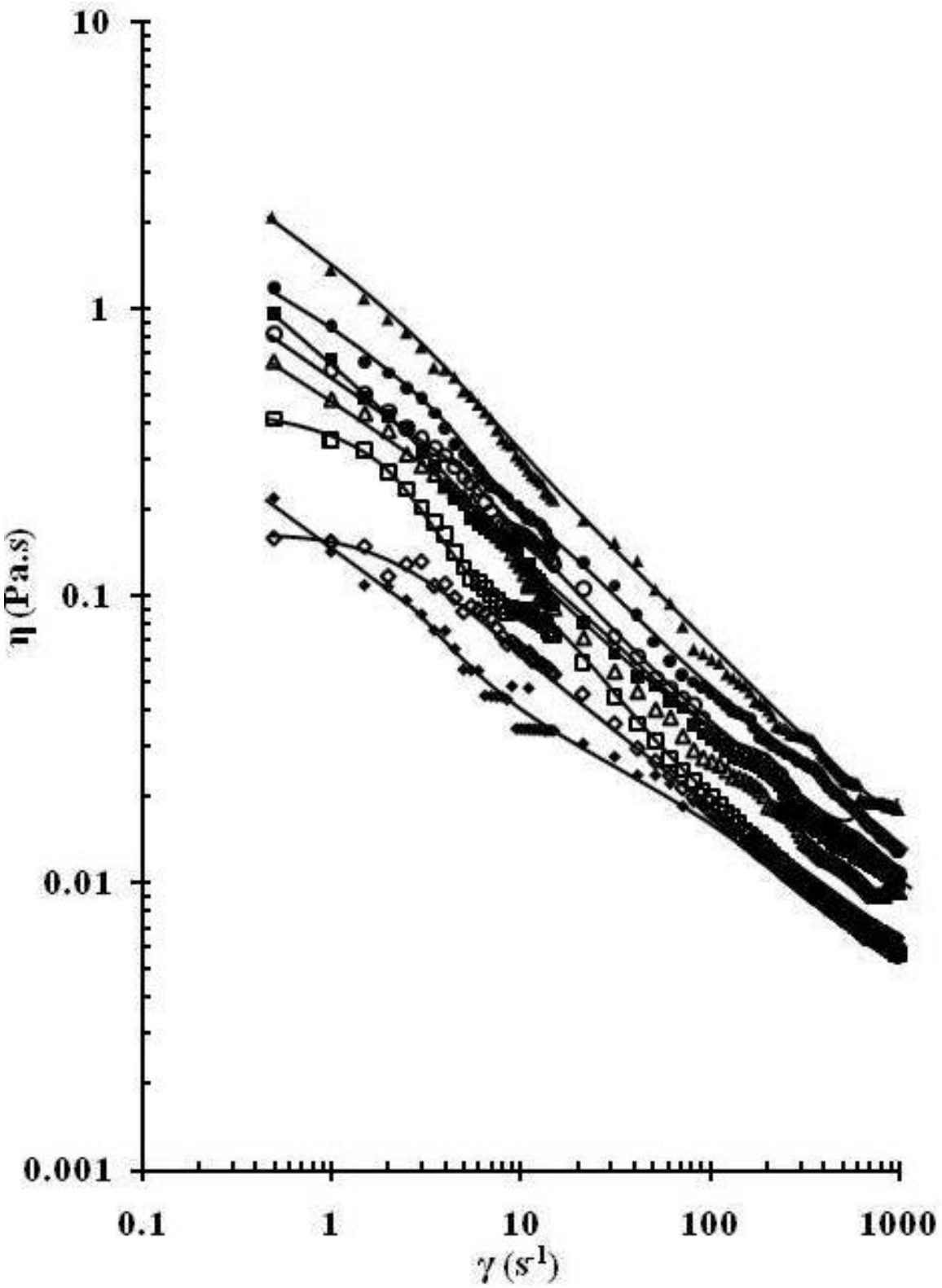

Figure 3.18. Rheological behavior shown by samples of kinetic measurements with $[CTABr]_T$ = 0.015 M and [4-$BrC_6H_4CO_2Na$] = 0.05 M (×), 0.01 M (♦), 0.02 M (■), 0.03 M (▲), 0.04 M (●), 0.05 M (○), 0.06 M (Δ), 0.08 M (□) and 0.1 M (◊).

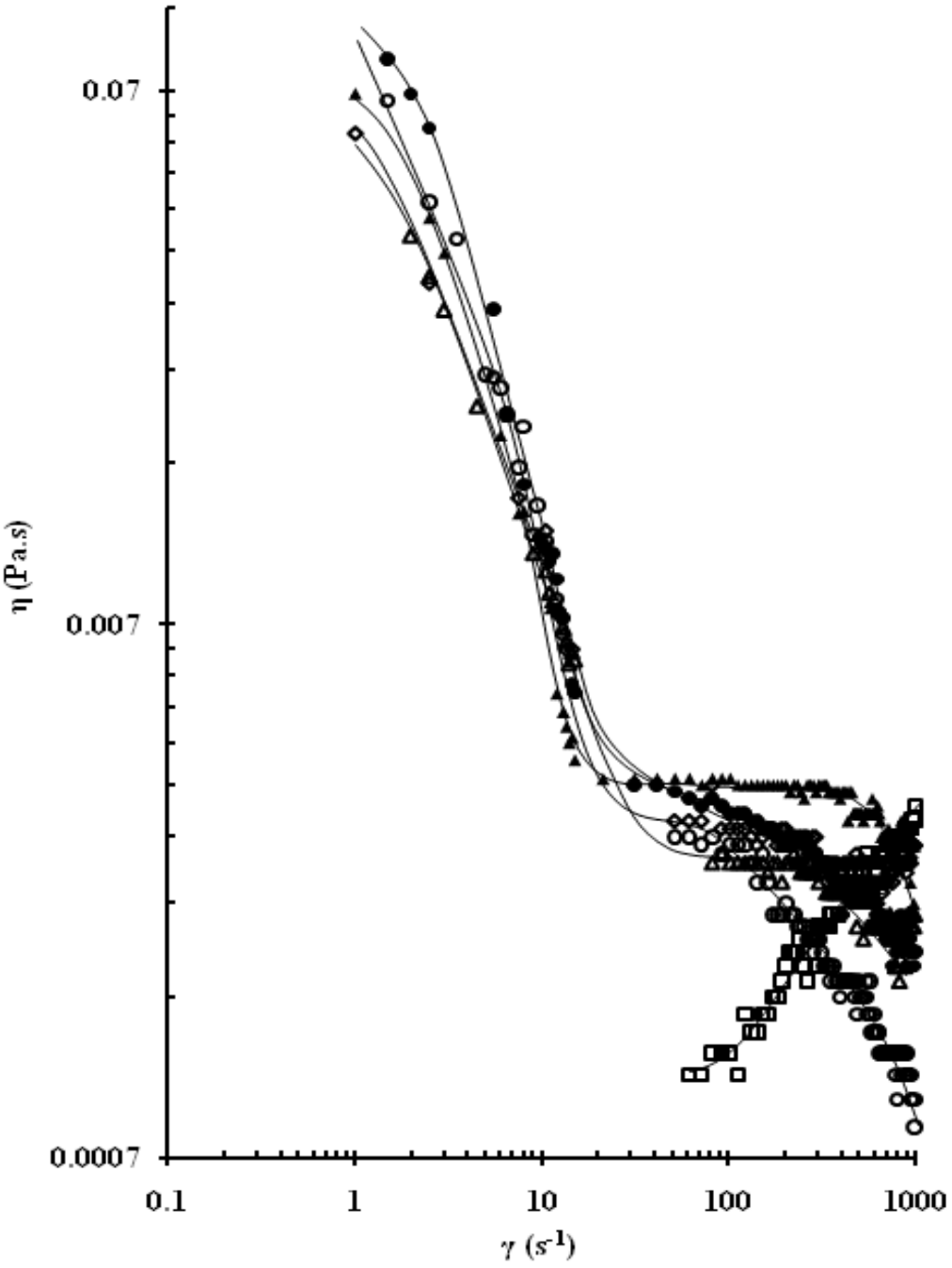

Figure 3.19. Rheological behavior shown by samples of kinetic measurements with $[CTABr]_T$ = 0.015 M and [2-$IC_6H_4CO_2Na$] = 0 M (×), 0.02 M (●), 0.05 M (▲), 0.07 M (Δ) and 0.1 M (◊).

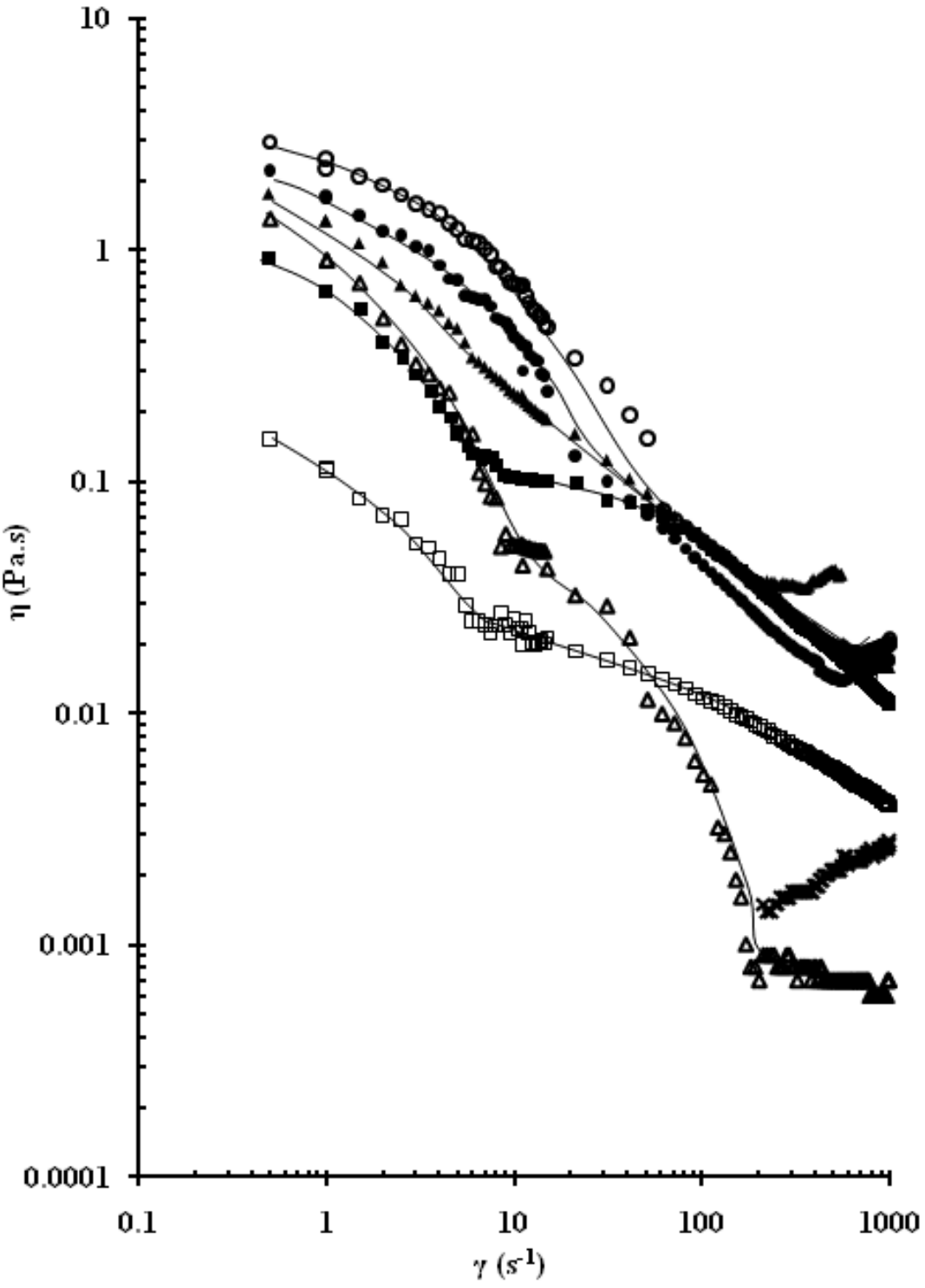

Figure 3.20. Rheological behavior shown by samples of kinetic measurements with $[CTABr]_T$ = 0.015 M and [4-$IC_6H_4CO_2Na$] = 0 M (×), 0.01 M (Δ), 0.015 M (●), 0.02 M (○), 0.03 M (▲), 0.05 M (■) and 0.1 M (□).

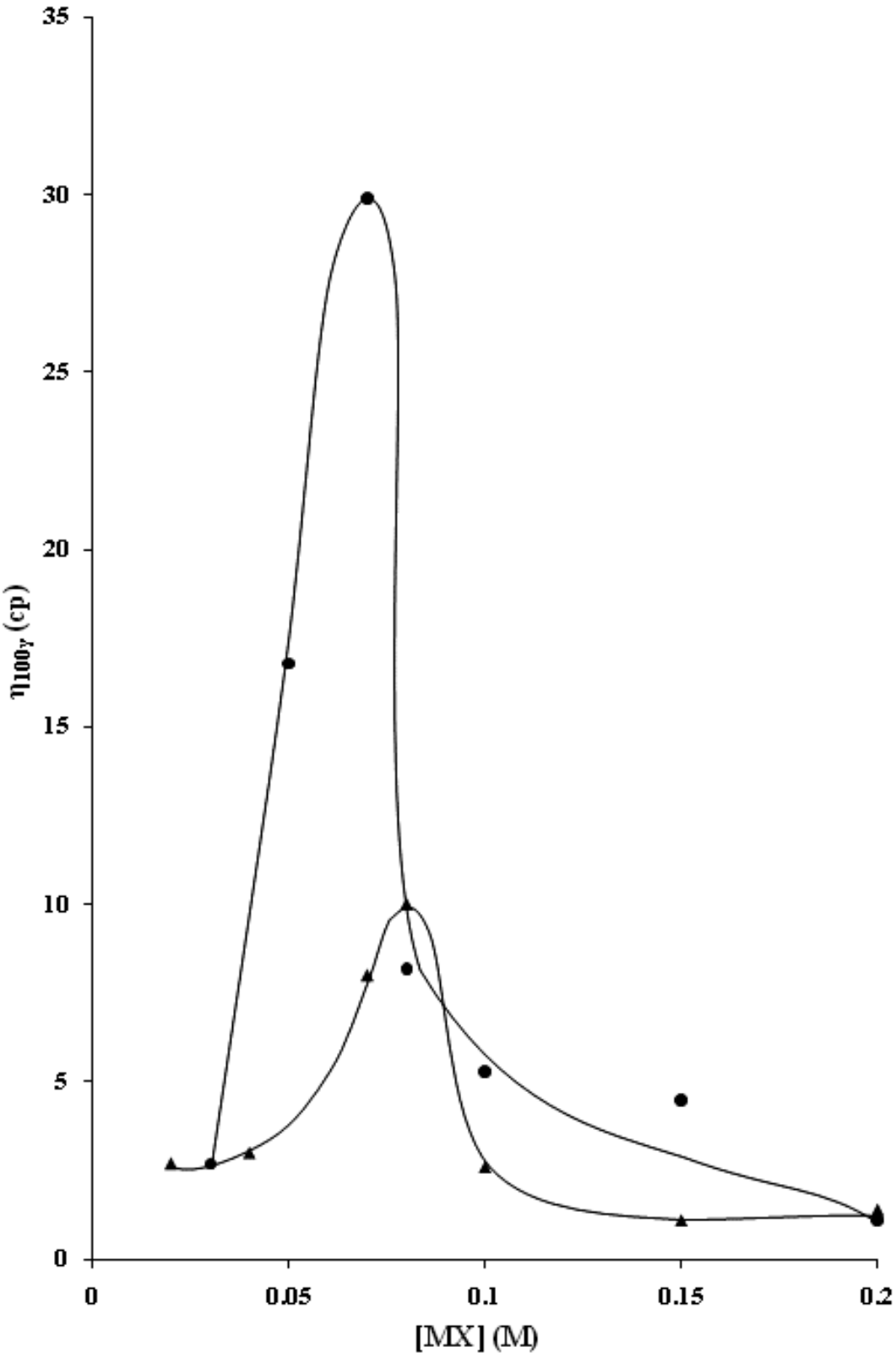

Figure 3.21. Plots of shear viscosity (η) at $\gamma = 100\ s^{-1}$ versus [MX] ([MX] = [3-FBzNa] (●) and [4-FBzNa] (▲)) at 15 mM CTABr, 0.2 mM PS^-, 0.03 M NaOH, 0.1 M Pip, and ~ 35 ^oC.

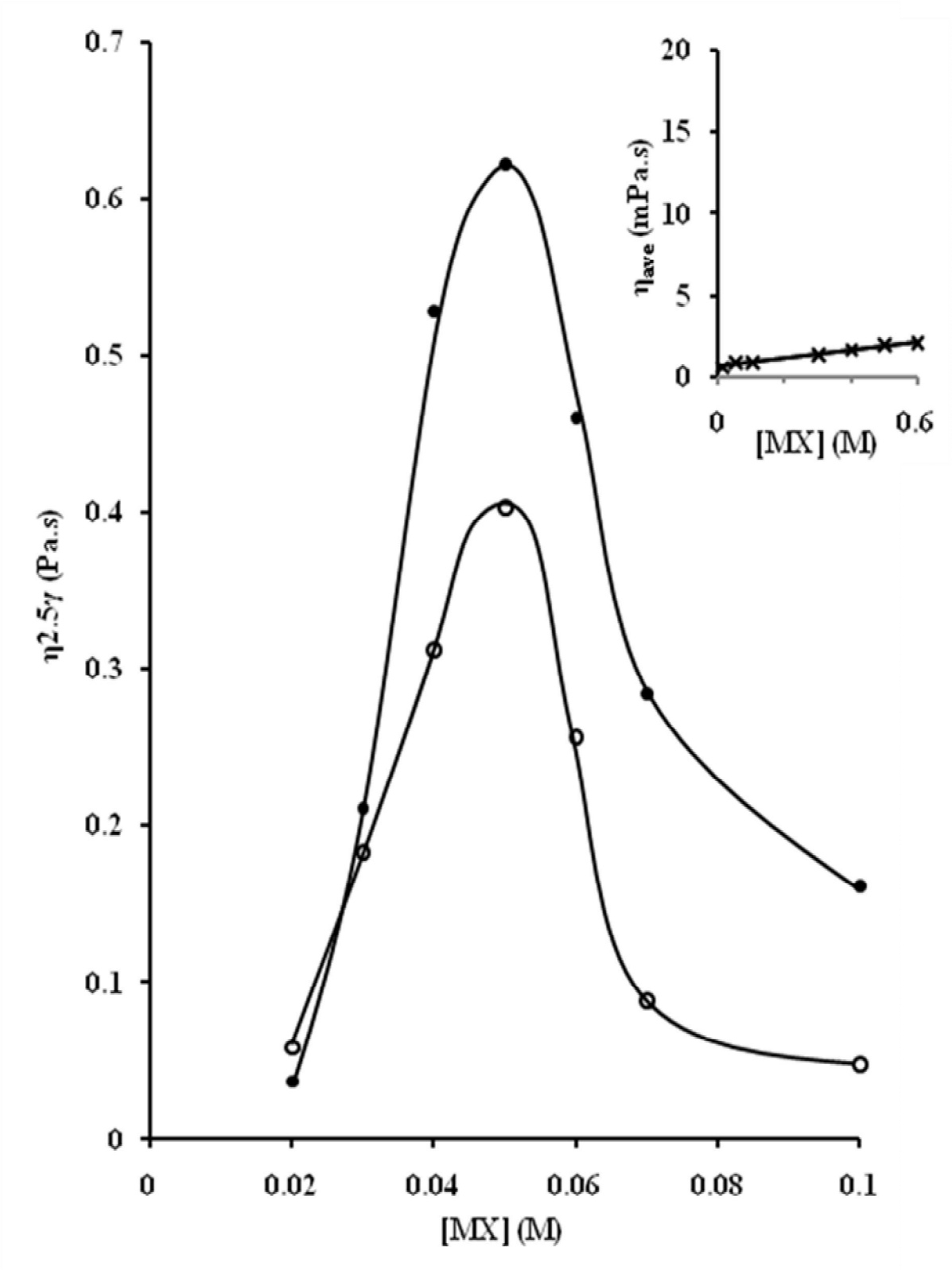

Figure 3.22. Plots of shear viscosity (η) at γ = 0.5 s^{-1} versus [MX] ([MX] = [2-ClBzNa] (×), [3-ClBzNa] (●) and [4-ClBzNa] (○)) at 15 mM CTABr, 0.2 mM PS^-, 0.03 M NaOH, 0.1 M Pip, and ~ 35 ^oC.

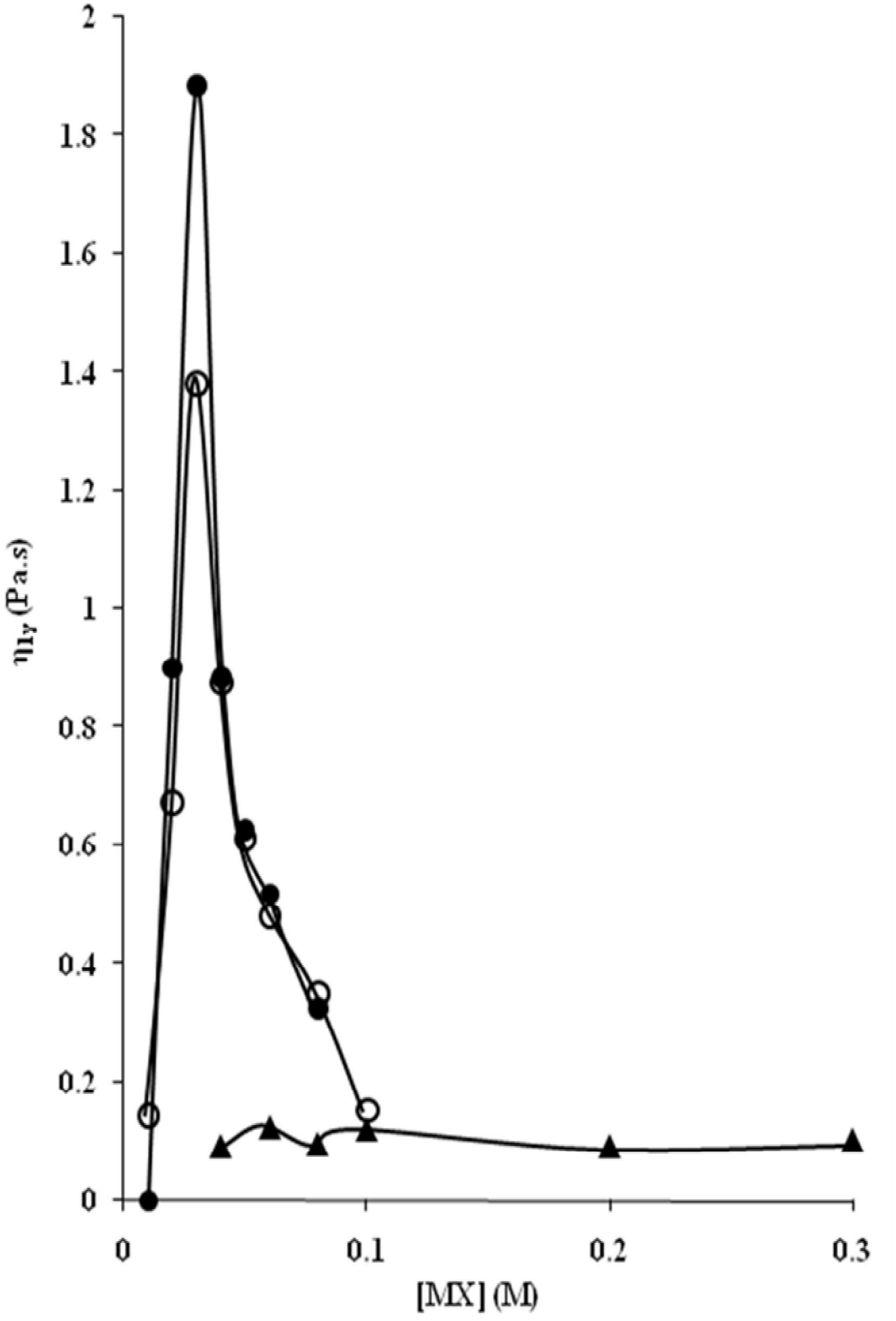

Figure 3.23. Plots of shear viscosity (η) at $\gamma = 1\ s^{-1}$ versus [MX] ([MX] = [2-BrBzNa] (■), [3-BrBzNa] (●) and [4-BrBzNa] (▲)) at 15 mM CTABr, 0.2 mM PS^-, 0.03 M NaOH, 0.1 M Pip, and ~ 35 ^oC.

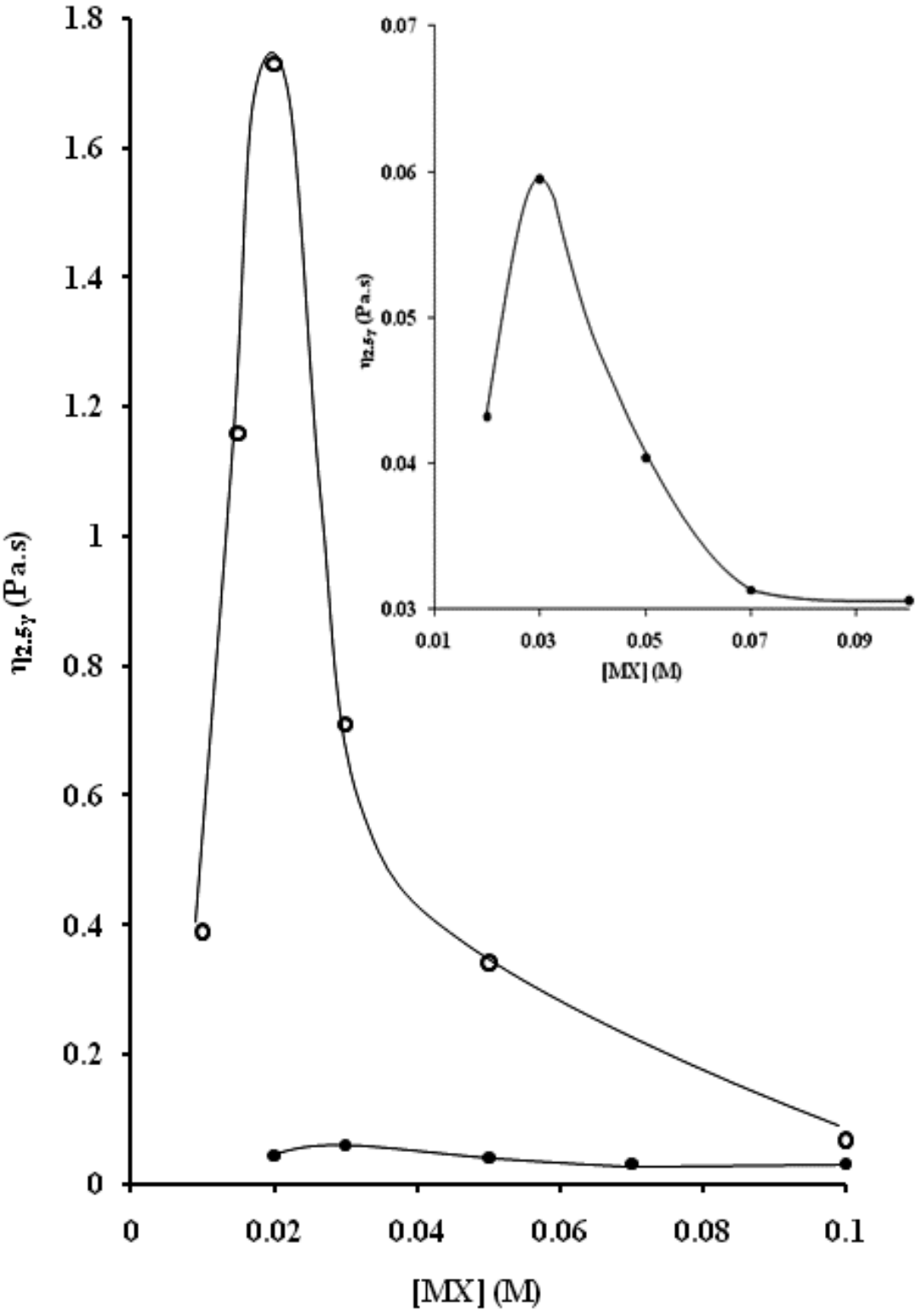

Figure 3.24. Plots of shear viscosity (η) at $\gamma = 2.5\ s^{-1}$ versus [MX] ([MX] = [2-IBzNa] (●) and [4-IBzNa] (▲)) at 15 mM CTABr, 0.2 mM PS^-, 0.03 M NaOH, 0.1 M Pip, and ~ 35 ^oC.

3.4 Reference(s)

(1) (a) Yusof, N. S. M.; Khan, M. N. *Langmuir* **2010**, *26*, 13, 10627-10635. (b) Yusof, N. S. M.; Khan, M. N. *J. Colloid Interface Sci* (2011), doi: 10.1016/j.jcis.2011.01.061.

(2) (a) Lin, Y.; Han, X.; Huang, J.; Fu, H.; Yu, C. *J. Colloid Interface Sci.* **2009**, *330*, 449–455. (b) Clausen, T. M.; Vinson, P. K.; Minter, J. R.; Davis, H. T.; Talmon, Y.; Miller, W. G. *J. Phys. Chem.* **1992**, *96*, 474–484. (c) Lu, T.; Huang, J.; Li, Z.; Jia, S.; Fu, H. *J. Phys. Chem. B* **2008**, *112*, 2909–2914. (d) Shrestha, R. G.; Aramaki, K. *J. Nepal Chem. Soc.* **2008/2009**, *23*, 65–73. (e) Raghavan, S. R.; Kaler, E. W. *Langmuir* **2001**, *17*, 300-306.

Chapter 4 : DISCUSSION

The nucleophilic reaction between piperidine and anionic phenyl salicylate (PS^-) occurs through an intramolecular general base assistance and results in two products, *N*-piperidinylsalicylamide and phenol.[1,2,3] The existence of the micelles in the aqueous reaction system has generally no effect on the products as well as the mechanism of the reaction. But, the observed pseudo-first-order rate constants for reaction at 0.1 M piperidine (Pip), 0.2 mM phenyl salicylate (PS^-), absence of [MX] and $[CTABr]_T$ range 5 to 15 mM were found to decrease by about 10-fold as compared to the pseudo-first-order rate constant of the reaction in the absence of CTABr. This is due to the distribution of reactants in the aqueous phase and micellar pseudophase.[2] This leads to the conclusion that the CTABr micelles act as a medium inhibitor of such a reaction. This means that the rate of reaction between micellized piperidine (Pip_M) and anionic phenyl salicylate (PS^-_M) is significantly slower than the reaction when both exist in aqueous phase (Pip_W and PS^-_W).

Under the experimental condition of entire kinetic runs of present study, phenyl salicylate (PSH) is deprotonated forming ionized phenyl salicylate (PS^-) completely (i.e. $[PSH]_T = [PS^-]_T$). This is clearly proven when the initial absorbance values (A_0) were found to be independent of $[CTABr]_T$ and $[^-OH]$ in the present study and the fact that ionized phenyl salicylate (PS^-) absorbs strongly, whilst the non-ionized phenyl salicylate (PSH) does not absorb to a detectable level at 350 nm.[2a] Also noted that the rates of uncatalyzed and hydroxide ion-catalyzed hydrolysis of PS^- are insignificant compared to the rate of piperidinolysis of PS^-.[2] The existence of protonated Pip ($PipH^+$) is also possible for such system, but since the concentration is very low as compared to the concentration of nonprotonated piperidine ([Pip]) in the presence of the present kinetic conditions. Thus, it is reasonable to assume that $[Pip]_T = [Pip] + [PipH^+] \approx [Pip]$. This is also evident from the values of k_{obs} listed in **Tables 3.1** to **3.4**.

The observations explained above for the reaction between piperidine and PS^- under the condition of the present study reveal a brief reaction scheme as represented by **Figure 4.1**.

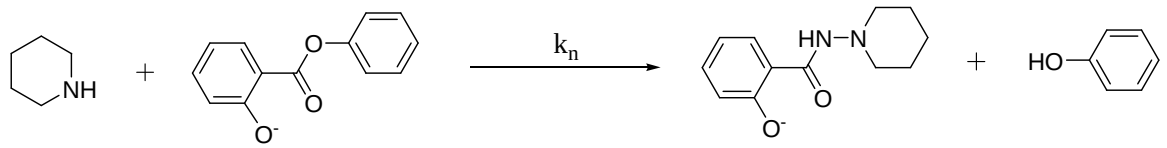

Piperidine PS^- Ionized N-piperidinylsalicylamide Phenol

Figure 4.1. Reaction scheme between piperidine and PS^- under the condition of the present study.

where k_n is the nucleophilic second-order rate constant. Therefore, a fixed and known concentration of piperidine was added in excess ($[Pip]_T/[PS^-]_T$ = 500) to assure pseudo-first-order reaction between piperidine and PS^- where $k_{obs} = k_n [Pip]_T$ with $[Pip]_T$ representing total concentration of Pip.

4.1 Theory of an Empirical Kinetic Approach to Study the Occurrence of Ion-Exchange between Counterions of CTABr Micelles.

Micelle formation such as the aggregation of CTABr surfactant molecules in the case of this study, has the ability to create multiphases medium of reactions and reducing the observed rate constant due to lower rate of reaction in micellar pseudophase.[3,4] The effects of CTABr micelles on the rate of reaction of piperidine with PS^- in the absence and presence of an inert salt is explained according to the Pseudophase Micellar (PM) model[5] by considering the micellization of both reactant species as shown in **Figure 4.2**.[2a,3a,c] Such a bimolecular reaction does not involve any cross-interface reaction.[1b] Thus such a reaction occurs simultaneously in both phases: aqueous phase and micellar pseudophase resulting in

the same products, P_1 and P_2 but at different rates of formation: i.e. with different rate constants (k^n_M and k^n_W).

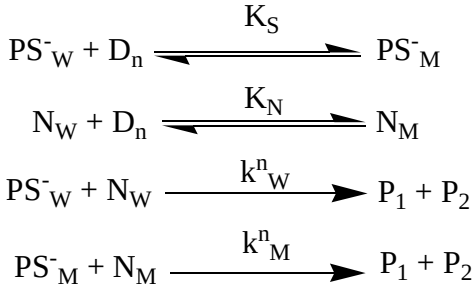

Figure 4.2 The effects of CTABr micelles on the rate of reaction of piperidine and PS^-.

In **Figure 4.2**, D_n represents CTABr micelle and K_S and K_N are the CTABr micellar binding constants of PS^- and piperidine, respectively. Symbols k^n_W and k^n_M represent nucleophilic second-order rate constants for the reactions of piperidine with PS^- in the respective aqueous phase and micellar pseudophase. Subscripts W and M stand for water phase and micellar pseudophase respectively. The observed rate law is

$$\text{rate} = k_{obs}\,[PS^-]_T \qquad \textbf{Eq. 4.1}$$

where $[PS^-]_T = [PS^-_W] + [PS^-_M]$.

The observed rate law for the reaction (i.e. **Eq. 4.1**) and **Figure 4.2** can lead to **Eq. 4.2.**

$$k_{obs} = \frac{(k^n_W + k^{mr}_M K_N K_S\,[D_n])[Pip]_T}{(1 + K_S\,[D_n])(1 + K_N[D_n])} \qquad \textbf{Eq. 4.2}$$

In **Eq. 4.2**, $k^{mr}_M = k^n_M / V_M$ where V_M is the micellar molar volume in M^{-1}, $[Pip]_T = [Pip_W] + [Pip_M]$ under the typical reaction conditions, $[D_n] = [CTABr]_T - cmc$,[3] K_S and K_N represent micellar binding constant of respective PS^- and piperidine and k^n_W and k^n_M

represent nucleophilic second-order rate constant for the reaction of piperidine with PS^- in the aqueous and micellar pseudophase respectively. As the cmc for CTABr has been reported to be $< 1 \times 10^{-4}$ M in the presence of 0.2 mM PS^- and in the absence of any inert salt[6], and the cmc value is expected to be reduced by the addition of an inert salt[6,7], therefore $[D_n] \approx [CTABr]_T$ under this condition of the present kinetic study.

It has been reported that the value of micellar binding constant of piperidine, K_N for tetradecyltrimethylammonium bromide (TTABr) micelle is about 0.3 M^{-1}.[8,9] The value of K_N should not be significantly altered when CTABr micelle is used.[10] In addition to that, the existence of different concentration of MX will not affect the value of K_N due to the nonionic highly hydrophilic behavior of piperidine. Thus, it is apparent that $1 >> K_N[D_n]$ at $[CTABr]_T$ used in this study (5, 6, 7, 10 and 15 mM) and under such condition, **Eq. 4.2** can be reduced to **Eq. 4.3**.

$$k_{obs} = \frac{(k^n_W + k^{mr}_M K_N K_S [D_n])\,[Pip]_T}{1 + K_S [D_n]} \qquad \textbf{Eq. 4.3}$$

In the aqueous system of the present study, the anions that exist are PS^-, Br^-, HO^-, and X^- (from the organic inert salt MX). Thus, the possible ion-exchange processes that occur at the cationic micellar surface are X^-/PS^-, X^-/Br^-, X^-/HO^-, Br^-/PS^-, Br^-/HO^- and HO^-/PS^-. But the most effective is the occurrence of X^-/PS^- ion-exchange.[3] The occurrence of ion-exchange has been discovered to decrease CTABr micellar binding constant of PS^- (K_S) with the increase of [MX] due to X^-/PS^- ion-exchange through an empirical relationship, **Eq. 4.4**[1b]

$$K_S = K_S^0 / (1 + K_{X/S} [MX]) \qquad \textbf{Eq. 4.4}$$

where $K_S^0 = K_S$ at [MX] = 0 and $K_{X/S}$ is an empirical constant with a magnitude that represents the ability of counterion X^- to expel S^- from a cationic micellar pseudophase.

Since the reaction between piperidine and the PS^- occurred under the condition of pseudo-first-order rate law ($[Pip]_T/[PS^-] = 500$) and the concentration of piperidine remains constant ($[Pip]_T = [Pip] + [PipH^+] \approx [Pip]$) whilst phenyl salicylate exists in complete ionized form (i.e. $[PS^-]$) with charge similar to the charge on counterions of ionic micelles, **Eqs. 4.3** and **4.4** lead to **Eq. 4.5**,

$$k_{obs} = \frac{k_0 + \theta K^{X/S}[MX]}{1 + K^{X/S}[MX]} \qquad \textbf{Eq. 4.5}$$

with k_0, θ and $K^{X/S}$ given by respective **Eqs. 4.6, 4.7** and **4.8**.

$$k_0 = \frac{(k_W + k^{mr}{}_M K_N K_S{}^0 [D_n])[Pip]_T}{1 + K_S{}^0 [D_n]} \qquad \textbf{Eq. 4.6}$$

where $k_W = k^n{}_W [Pip]_T = k_{obs}$ at $[D_n]$ and $[MX] = 0$ with the assumption that K_N is independent of $[MX]$

$$\theta = \frac{F_{X/S}\, k^n{}_W{}^{MX} [Pip]_T}{1 + K_N [D_n]} \qquad \textbf{Eq. 4.7}$$

where $k^n{}_W{}^{MX}[Pip]_T = k_{obs}$ at the respective values of $[MX]$, $[D_n] = 0$, and $F_{X/S}$ ($= \theta/(k^n{}_W{}^{MX}[Pip]_T)$) is an empirical constant whose magnitude should vary $\leq$ 1.0 to > 0, and

$$K^{X/S} = \frac{K_{X/S}}{1 + K_S{}^0 [D_n]} \qquad \textbf{Eq. 4.8}$$

where $[D_n] \approx [CTABr]_T$. Under the experimental conditions of this study where $1 >> K_N[D_n]$, **Eq. 4.7** is reduced to **Eq. 4.9**.

$$\theta = F_{X/S}\, k^n{}_W{}^{MX} [Pip]_T \qquad \textbf{Eq. 4.9}$$

The relationship of the variation of rate constants (k_{obs}) with the concentration of inert salts as presented by **Eq. 4.5** has been used repetitively and proven to be applicable in studying the effects of various inert inorganic and organic salts on pseudo-first-order rate constants (k_{obs}) for alkaline hydrolysis and the aminolysis of phthalimide[1b,c], phenyl salicylate[1b,2a,3a,b,c], phenyl benzoate[1b,3d] and *N*-benzylphthalimide[1b] obtained at a constant concentration of cationic micelles, amine nucleophiles such as piperidine and NaOH.

In view of **Eq. 4.9**, the $F_{X/S}$ value represents the fraction of the expulsion of micellized counterions PS^-_M to the bulk aqueous phase by the optimum concentration values of MX through ion exchange X^-/PS^-. The value of $F_{X/S}$ is 1 if the limiting concentration of X^- can induce 100% transfer of PS^-_M from the micellar pseudophase to the bulk aqueous phase. The limiting concentration of an organic salt MX is defined as the optimum value of [MX] at which the values of k_{obs} become independent of [MX] (i.e. at the optimum value of [MX], $K^{X/S}[MX] >> 1$ and $\theta K^{X/S}[MX] >> k_0$ in **Eq. 4.5**). Counterions HO^- and Br^- are species with moderate hydrophilicity whilst PS^- is a species with moderate hydrophobicity. Thus, it is impossible for counterions HO^- and Br^- to completely expel PS^-_M even when $[HO^-]_T/[PS^-]_T$ and $[Br^-]_T/[PS^-]_T$ are very large. Therefore the value of $F_{X/S}$, in **Eq. 4.7** must be within the range of > 0 to ≤ 1.0. It can be concluded that the value of $F_{X/S}$, under the condition of $1 >> K_N[D_n]$, may also be considered as the measure of the micellar penetration of X^- relative to that of PS^- where the hydrophobicity of PS^- is larger than that of X^-.[3a,b,c,4d]

4.2 Effects of the Concentrations of Various Halo-Substituted Benzoate Salts on k_{obs} for the Reaction of Pip with PS^- at a Constant Concentration of CTABr Micelles and 35°C.

4.2.1 The Nonlinear Increase of k_{obs} with [MX]

Plots of **Figures 3.1** to **3.10** in Chapter 3 revealed the nonlinear increase of k_{obs} upon increasing concentration of MX. There are three possibilities of such nonlinear increase which are:

i) The existence if ionic strength or the specific ion effect contributed by the organic salt used,

ii) nucleophilic cleavage of PS^- by X^-,[3a] and

iii) the occurrence of ion exchange processes in aqueous micellar system.[3,4a]

All these possibilities will be explained in the following text.

i) Effects of ionic strength or the specific ion effect on k_{obs}.

The organic salts added to the reaction mixtures of the kinetic runs may be thought of affecting k_{obs} by merely ionic strength/specific salt effect. To investigate such a possibility, kinetic runs were carried out at different [MX] in the absence of CTABr. As shown in **Tables 3.1 - 3.4** of Chapter 3, the values of k_{obs} are almost independent of MX in the range studied kinetically with the presence of CTABr micelles. Therefore, the nonlinear increase, shown in **Figures 3.1** to **3.10,** could not be attributed to the salt or specific salt effect.

ii) Nucleophilic reaction of X^- ions with PS^-.

The anions X^- of the organic salts (MX) used in this study are extremely weak nucleophiles with pK_a of conjugate acids of X^- of ~2-4.[11] Therefore, they are unable to act as nucleophiles in the nucleophilic cleavage of PS^-. In addition to that, it is a necessity that the nucleophile must possess a proton at its nucleophilic site in order to become effective in the nucleophilic reaction with PS^- through intramolecular general base assistance.[3b] Unfortunately, X^- ions of the organic salts used lack of this characteristic. Therefore, nucleophilic reaction of X^- with PS^- does not occur.

iii) The occurrence of ion-exchange processes in aqueous micellar system.

As discussed above in (i) and (ii), the nonlinear increase of k_{obs} with the increase of [MX] cannot be attributed to either the salt effect or nucleophilic reaction of X^- with PS^-. This led to the last possible reason (i.e (iii)) that probably more than one independent ion-exchange processes occurred at the CTABr micellar surface in the present reaction system.[3,4a] Therefore, the rates of ionic micellar-mediated reactions involving ionic reactants with charges similar to the charge possessed by the counterions of the ionic micelles are expected to be influenced by the occurrence of ion-exchange between different types of counterions. As mentioned earlier in the text, possible ion-exchange processes in the present reaction system are X^-/PS^-, X^-/Br^-, X^-/HO^-, Br^-/HO^-, Br^-/PS^- and HO^-/PS^- with varying effectiveness depending on two major factors which are the hydrophobicity difference and relative concentrations of the exchanging ions.[1b]

In cases where many simultaneous ion-exchange processes occur, the less effective ion-exchange is usually ignored when compared to the most effective ion-exchange. A highly hydrophilic counterion cannot efficiently expel a highly hydrophobic counterion from the ionic micellar surface to the aqueous phase due to the fact that hydrophilic ions

will prefer to get the most contact with water whilst the more hydrophobic ions will prefer to be away from water. Thus, the effectiveness of an ion-exchange process decreases with the increase in the difference of hydrophobicity of exchanging ions.[1b]

It is also important to note that the concentration of the three anions exist in the kinetic condition of this study (PS^-, Br^- and HO^-) were kept constant but the concentration of X^- were varied and found to be affecting the observed rate constant, k_{obs} of the reaction. The ion-exchange HO^-/Br^-, X^-/HO^- and HO^-/PS^- remained kinetically insignificant because the rate of hydrolysis was independent of $[HO^-]$ within the $[HO^-]$ range in the present study and $[HO^-]_T/[PS^-]_T > 100$. The same goes to ion-exchange of X^-/Br^-. The ion-exchange Br^-/PS^- may also be ignored as compared to the ion-exchange X^-/PS^- for the fact that either the values of $[X^-]$ is many fold larger than that of $[Br^-]$ or the hydrophobicity of X^- is much larger than that of Br^-. Therefore, the most effective and plausible ion-exchange occurrence that affects k_{obs} is the transfer of micellized anionic phenyl salicylate (PS^-_M) to aqueous phase through X^-/PS^- ion-exchange. As higher concentration of inert organic salts added to the system, more counterions X^- penetrates into the micellar pseudophase, and more PS^- are expelled to the aqueous phase. This agrees with the increasing k_{obs} values and the fact that the rate of reaction in aqueous phase is about 10 times faster than in micellar phase.

4.2.2 The Existence of Systematic Negative Deviations of Observed as Compared to Calculated Rate Constants at Low Concentration Values of Organic Salts.

In **Section 4.2.1**, it has been explained that the less significant ion-exchange processes (i.e. X^-/HO^- and X^-/Br^-) do not have a direct effect to the rate of reaction when compared to the more significant ion-exchange process (i.e. X^-/PS^-). However, the ion-

exchange processes of X^-/HO^- and X^-/Br^- might as well affect the occurrence of X^-/PS^- ion-exchange process indirectly by reducing the effective concentration of MX required for it. This indirect effect is prominent in the kinetic reaction system involving 3-FBzNa (**Figure 3.1**), 4-FBzNa (**Figure 3.2**), 3-ClBzNa (**Figure 3.4**), 4-ClBzNa (**Figure 3.5**), 2-BrBzNa (**Figure 3.6**), 3-BrBzNa (**Figure 3.7**), 4-BrBzNa (**Figure 3.8**), 2-IBzNa (**Figure 3.9**) and 4-IBzNa (**Figure 3.10**). In these figures, there exist systematic negative deviations of k_{obs} as compared to k_{calc} (dashed lines) at low concentration of added organic salts. The magnitudes of these negative deviations get smaller as the values of the concentration of organic salt get larger as well by the decreasing total concentration of CTABr values. Such observations may be explained as follows.

As counterions (X^-) penetrate into CTABr micellar pseudophase, the counterions HO^-, Br^- and PS^- in micellar pseudophase will be expelled to the bulk aqueous phase according to their relative hydrophilicity. Anion HO^- is the most hydrophilic species among these three anions, followed by Br^- and PS^-. Thus, addition of MX at low concentration will result in the expulsion of HO^- to the aqueous phase from micellar pseudophase up to a point in which further addition of [MX] were no longer affecting such ion-exchange process. By further addition of [MX], anion Br^- is expelled in the same manner. Once the optimum value of [MX] needed to expel anions HO^- and Br^- from micellar pseudophase by ion-exchange processes X^-/HO^- and X^-/Br^- is achieved, further increase in [MX] will cause the occurrence of ion-exchange X^-/PS^-. This will eventually increase the value of k_{obs} due to the ~10 times faster reaction between PS^- and piperidine in aqueous phase as compared to the micellar pseudophase. The optimum point of the concentration of MX at which further increase of [MX] is effective to expel PS^- from micellar pseudophase to aqueous phase is

termed as the effective concentration of MX ($[MX]_S^{ef}$) . This relation is represented by **Eq. 4.10**.

$$[MX]_S^{ef} = [MX] - ([MX]_{OH}^{op} + [MX]_{Br}^{op}) \qquad \textbf{Eq. 4.10}$$

where $[MX]_0^{op}$ ($\approx [MX]_{OH}^{op} + [MX]_{Br}^{op}$) is the optimum concentration of MX needed to expel both HO^- and Br^- ions from micellar pseudophase to aqueous phase.

Thus, when $[MX]_0^{op}$ is very low compared to [MX] ($[MX] >> [MX]_0^{op}$), $[MX]_S^{ef}$ can be considered as the [MX] ($[MX]_S^{ef} \approx [MX]$). This is evident in case such as when MX = 2-ClBzNa (**Figure 3.3**) in which the nonlinear least-squares data treatment were done by considering only $[MX]_0^{op} = 0$ and the least-squares fitting were found to be satisfying. But, for cases as shown by all of the reaction sets with different MX except MX = 2-ClBzNa, the treatment with $[MX]_0^{op} = 0$ is no longer giving the satisfying observed data fitting, indicating that the X^-/HO^- and X^-/Br^- ion-exchange processes are no longer negligible as compared to X^-/PS^-. The values of $[MX]_0^{op}$ were calculated using an iterative technique. In doing so, the empirical parameters θ and $K^{X/S}$ were determined twice: the first was by fixing the $[MX]_0^{op} = 0$ M and the second was by choosing the most reliable $[MX]_0^{op} \neq 0$ by iterative technique.[1b] The value of $\sum di^2$ for both cases were also determined when calculating the values of θ and $K^{X/S}$ by **Eq. 4.11**.

$$di = k_{obs\ i} - k_{calc\ i} \qquad \textbf{Eq. 4.11}$$

In **Eq. 4.11**, $k_{obs\ i}$ and $k_{calc\ i}$ are the rate constants determined by experiment and by least-squares calculation at the i-th value of [MX]. The values of $\sum di^2$, calculated at different presumed values of $[MX]_0^{op}$, were compared and $[MX]_0^{op}$ value at which $\sum di^2$ value turned out to be minimum will be the best $[MX]_0^{op}$. At this value, the calculated θ and $K^{X/S}$ will be chosen for further calculation in determining the ion-exchange constant. The reliability of the calculation when $[MX] \neq 0$ as compared to when $[MX] = 0$ is proven by

the low values of $\sum di^2$ given (**Table 4.1** and **4.2**). This can also be observed by the nicely fitted k_{calc} when [MX] $\neq$ 0 which is represented by solid lines and deviating k_{calc} when [MX] = 0 which is represented by dashed lines in **Figures 3.1** to **3.10**.

4.2.3 Determination of Ion-Exchange Constant, K_X^{Br} Under the Reaction Conditions with the Absence and Presence of Maximum in the Plot of k_{obs} versus [MX].

The values of k_{obs} at different [MX] and at a constant $[CTABr]_T$ were treated with **Eq. 4.5** using nonlinear least-squares technique and the deviation of calculated rate constants are represented by solid and dashed lines in **Figures 3.1** until **3.10**. All the figures except **Figures 3.7** and **3.8** were showing k_{obs} independent region upon addition of [MX] at high concentration. This agrees with **Eq. 4.5** and proving that the salt effect contributed by the organic salts used is either none or negligible under the concentration range of present study. The values of $F_{X/S}$, $K^{X/S}$ and $\sum di^2$ at different $[CTABr]_T$ calculated by nonlinear least-squares technique for these cases are presented in **Table 4.1** with respective nonzero and zero $[MX]_0^{op}$ values.

Table 4.1 : Values of the Empirical Constants θ and $K^{X/S}$, Calculated from **Eq. 4.5** (where [MX] = $[MX]_S^{ef}$ with Zero and Nonzero $[MX]_o^{op}$ values) in CTABr Micelles

$[CTABr]_T$[a] mM	$10^4 k_o$[b] s^{-1}	$[MX]_o^{op}$ mM	$10^4 \theta$ s^{-1}	$K^{X/S}$ M^{-1}	$K_{X/S}$ M^{-1}	$F_{X/S}$	$K_{X/S}^n$ M^{-1}	K_X^{Br}	$10^8 \sum di^2$
				3-FBzNa					
5	29.5	5.9	254 ± 8[c]	12.8 ± 1.1[c]	461[d]	0.78[e]	358[f]	14.3[g]	219.5
5	29.5	0	275 ± 14	9.37 ± 1.15	337	0.84	284	11.3	579.3
6	28.8	7.3	229 ± 6	10.1 ± 0.60	434	0.70	304	12.2	74.68
6	28.8	0	256 ± 16	6.92 ± 0.95	298	0.78	233	9.32	385.9
7	27.9	9.4	241 ± 7	8.18 ± 0.53	409	0.74	301	12.1	63.09
7	27.9	0	283 ± 24	5.09 ± 0.87	255	0.87	220	8.81	460.4
10	27.4	13.1	219 ± 6	6.76 ± 0.38	480	0.67	321	12.9	24.98
10	27.4	0	284 ± 37	3.47 ± 0.80	246	0.87	214	8.56	411.9
15	26.0	18.8	209 ± 23	4.59 ± 0.91	487	0.64	311	12.4	40.91
15	26.0	0	897 ± 1280	0.54 ± 0.86	57.2	2.74	157	6.28	255.2
				4-FBzNa					
5	29.9	4.5	269 ± 6	11.9 ± 0.7	428	0.82	352	14.1	154.6
5	29.9	0	289 ± 12	9.15 ± 0.92	329	0.88	291	11.6	507.6
6	29.1	4.7	266 ± 3	9.76 ± 0.26	420	0.81	341	13.7	26.80
6	29.1	0	289 ± 11	7.44 ± 0.64	320	0.88	283	11.3	285.2
7	28.5	5.2	263 ± 9	8.28 ± 0.63	414	0.80	333	13.3	155.6
7	28.5	0	288 ± 17	6.25 ± 0.76	313	0.88	275	11.0	433.4
10	26.6	7.3	253 ± 10	6.23 ± 0.53	442	0.77	342	13.7	109.2
10	26.6	0	294 ± 24	4.23 ± 0.64	300	0.90	270	10.8	362.8
15	25.2	9.8	254 ± 27	3.76 ± 0.65	399	0.78	310	12.4	60.57
15	25.2	0	472 ± 191	1.39 ± 0.71	147	1.44	213	8.51	224.8
				2-ClBzNa					
5	27.6	0	224 ± 6.9	6.56 ± 0.6	236.2	0.69	163.0	6.52	290.4
6	27.3	0	218 ± 6.7	5.25 ± 0.5	225.8	0.67	151.3	6.05	206.8
7	26.8	0	219 ± 8.8	4.18 ± 0.4	209	0.67	140.0	5.60	207.5

10	25.3	0	213 ± 7.2	2.97 ± 0.2	210.9	0.65	137.1	5.48	246.1
15	24.6	0	214 ± 15	1.71 ± 0.2	181.3	0.65	117.8	4.71	404.8
				3-ClBzNa					
5	30.7	6.0	266 ± 2.5	40.7 ± 1.4	1465	0.81	1192	47.7	107.0
5	30.7	0	285 ± 10	25.4 ± 2.8	914.4	0.87	795.5	31.8	1211
6	29.1	6.8	250 ± 4.3	38.5 ± 2.0	1656	0.76	1266	50.6	275.9
6	29.1	0	271 ± 12	20.6 ± 2.7	885.8	0.83	735.2	29.4	1349
7	28.3	7.1	244 ± 1.8	35.2 ± 0.7	1760	0.75	1313	52.5	42.11
7	28.3	0	267 ± 1.1	17.6 ± 2.11	880.0	0.82	721.6	28.9	1013
10	27.8	10.8	236 ± 3.7	25.1 ± 1.17	1782	0.72	1286	51.4	119.6
10	27.8	0	265 ± 15	13.0 ± 1.9	923.0	0.81	747.6	29.9	1038
15	25.0	13.3	228 ± 4.3	16.6 ± 0.7	1760	0.70	1227	49.1	90.78
15	25.0	0	300 ± 36	5.97 ± 1.4	627.5	0.92	577.3	23.1	1454
				4-ClBzNa					
5	29.1	5.6	223 ± 4.1	49.6 ± 2.7	1786	0.68	1214	48.9	86.35
5	29.1	0	240 ± 11	31.3 ± 4.1	1127	0.73	822.7	32.9	548.5
6	26.6	6.3	212 ± 2.2	45.4 ± 1.6	1952	0.65	1269	50.8	36.63
6	26.6	0	243 ± 21	22.5 ± 5.0	967.5	0.74	716.0	28.6	1820
7	26.6	6.6	205 ± 2.0	36.4 ± 1.3	1820	0.63	1147	45.9	26.13
7	26.6	0	238 ± 23	19.1 ± 4.5	955.0	0.73	697.2	27.9	1685
10	25.3	9.2	222 ± 8.3	23.5 ± 2.2	1669	0.67	1118	44.7	20.14
10	25.3	0	263 ± 30	11.5 ± 2.8	816.5	0.80	653.2	26.1	1157
15	24.9	14.8	216 ± 4.9	17.6 ± 1.2	1866	0.66	1232	49.3	77.24
15	24.9	0	290 ± 48	7.32 ± 2.3	775.9	0.89	690.6	27.6	1525
				2-BrBzNa					
5	29.3	6.3	206 ± 3.8	9.33 ± 0.49	335.9	0.63	211.6	8.46	84.37
5	29.3	0	219 ± 7.8	7.17 ± 0.70	258.1	0.67	172.9	6.92	297.5
6	28.8	6.6	199 ± 4.3	8.37 ± 0.50	359.9	0.61	219.5	8.78	92.93
6	28.8	0	213 ± 8.6	6.40 ± 0.65	275.2	0.65	178.9	7.16	307.6
7	27.7	6.7	199 ± 5.0	7.20 ± 0.48	360	0.61	219.6	8.78	101.6
7	27.7	0	213 ± 9.3	5.56 ± 0.58	278	0.65	180.7	7.23	253.9

10	26.2	8.8	206 ± 6.3	4.97 ± 0.36	352.9	0.63	222.3	8.89	71.71
10	26.2	0	228 ± 13	3.65 ± 0.45	259.2	0.70	181.4	7.26	223.3
15	25.8	9.4	212 ± 4.5	3.34 ± 0.15	354	0.65	230.1	9.20	16.75
15	25.8	0	241 ± 16	2.41 ± 0.30	255.5	0.74	189.1	7.56	142.4
				2-IBzNa					
5	29.3	4.5	254 ± 2.4[d]	9.78 ± 0.24[d]	352[e]	0.78[f]	275[g]	11.0[h]	13.21
5	29.3	0	274 ± 12	7.56 ± 0.75	272	0.84	228	9.12	210.4
6	28.8	5.6	261 ± 6.5	8.51 ± 0.52	366	0.80	293	11.8	66.11
6	28.8	0	286 ± 16	6.39 ± 0.82	275	0.87	239	9.56	272.9
7	27.9	7.8	246 ± 7.3	7.96 ± 0.57	398	0.75	299	12.0	62.90
7	27.9	0	278 ± 22	5.49 ± 0.89	275	0.85	234	9.36	286.4
10	27.1	9.7	229 ± 8	5.88 ± 0.45	417	0.70	292	11.7	38.30
10	27.1	0	274 ± 32	3.72 ± 0.78	264	0.84	222	8.88	240.0
15	26.2	14.0	220 ± 17	3.42 ± 0.44	363	0.67	243	9.72	9.651
15	26.2	0	587 ± 533	0.79 ± 0.84	83.7	1.80	151	6.04	96.44
				4-IBzNa					
5	30.9	4.4	293 ± 2.4	115 ± 4.0	4140	0.90	3726	149	72.38
5	30.9	0	335 ± 25	51.2 ± 11	1843	1.02	1880	75.2	3452
6	29.3	4.8	284 ± 5.0	105 ± 7.6	4515	0.87	3928	157	278.9
6	29.3	0	333 ± 31	44.0 ± 12	1892	1.02	1930	77.2	4373
7	27.2	5.5	289 ± 8.5	78.4 ± 8.3	3920	0.88	3450	138	500.0
7	27.2	0	333 ± 30	37.3 ± 9.0	1865	1.02	1902	76.1	2746
10	26.2	9.4	262 ± 0.2	56.1 ± 0.1	3983	0.80	3186	127	0.075
10	26.2	0	361 ± 30	37.2 ± 9.0	2641	1.10	2905	116	2380

[a] Total concentration of CTABr. [b] $k_0 = k_{obs}$ at [MX] = 0. [c] Error limits are standard deviation. [d] $K_{X/S} = K^{X/S}_{X} (1 + K_S^{o} [CTABr]_T)$ where K_S^{o} = 7000 M^{-1}. [e] $F_{X/S} = \theta / k_w$ where $k_w = k_{obs}$ at $[CTABr]_T = 0$, $[Pip]_T = 0.1$ M and the value of k_w, under such conditions is 32.7 x 10^{-3} s^{-1} at 35°C. [f] $K_{X/S}^{n} = F_{X/S}K_{X/S.}$ [g] $K_X^{Br} = K_{X/S}^{n}/K_{Br/S}^{n}$, where $K_{Br/S}^{n}$ = 25 M^{-1}.

A closer look at **Figures 3.7** and **3.8** revealed the presence of maxima on the k_{obs} values upon [MX]. Such plotted behavior may be attributed to the significant negative salt effect of 3-BrBzNa and 4-BrBzNa when [3-BrBzNa] and [4-BrBzNa] > 0.1 M as shown in **Table 3.3** in Chapter 3. Thus, in the kinetic study under the presence of CTABr at concentration range 0.0 to 0.5 M for 3BrBzNa and 4-BrBzNa, the salt effect is no longer negligible.

In order to deal with the significant salt effect towards the observed rate constants, the data treatment, using nonlinear least-squares technique, was slightly different from the other sets. **Eq. 4.5** was used by replacing θ with $F_{X/S}k_{obs}^{MX}$ where $F_{X/S}$ represents an empirical constant whose magnitude should be in the range of ≤ 1.0 from > 0 and k_{obs}^{MX} = k_{obs} at a typical value of [MX] and $[CTABr]_T = 0$. For the region in which k_{obs} values are independent of [MX], average value was taken to simplify the calculation. The values are 31.8×10^{-3} s^{-1} for 3-BrBzNa and 31.9×10^{-3} s^{-1} for 4-BrBzNa within [3-BrBzNa] or [4-BrBzNa] = 0.0 – 0.1 M. The values of k_{obs}^{MX}, for subsequent [MX], were taken directly from the experimental values.

The values of $F_{X/S}$, $K^{X/S}$ and $\sum di^2$, at different $[CTABr]_T$, were calculated by the nonlinear least-squares technique for MX = 3-BrBzNa and 4-BrBzNa and these results are summarized in **Table 4.2**. **Figures 3.7** and **3.8** represent the extent of satisfactory observed data fit to **Eq. 4.5** by replacing θ with $F_{X/S}k_{obs}^{MX}$ where solid and dashed lines are drawn through calculated rate constants with parameters $F_{X/S}$ and $K^{X/S}$ at respective nonzero and zero $[MX]_0^{op}$.

Table 4.2 : Values of the Empirical Constants θ and $K^{X/S}$, Calculated from **Eq. 4.5** by replacing θ with $F_{X/S}k_{obs}^{MX}$ (where $[MX] = [MX]_S^{ef}$ with Zero and Nonzero $[MX]_o^{op}$ values) for 3-BrBzNa and 4-BrBzNa in CTABr Micelles.

$[CTABr]_T$[a] mM	$10^4\ k_o$[b] s^{-1}	$[MX]_o^{op}$ mM	$K^{X/S}$ M^{-1}	$K_{X/S}$ M^{-1}	$F_{X/S}$	$K_{X/S}^n$ M^{-1}	K_X^{Br}	$10^8\ \sum di^2$
			3-BrBzNa					
5	29.8	4.0	51.3 ± 2.7	1847	0.97 ± 0.01	1792	71.7	216.6
5	29.8	0	34.8 ± 4.4	1253	1.02 ± 0.04	1291	51.6	1477
6	29.2	4.1	46.6 ± 1.0	2004	0.96 ± 0.06	1924	77.0	61.20
6	29.2	0	33.4 ± 3.1	1436	1.00 ± 0.03	1436	57.4	1409
7	28.5	5.7	42.1 ± 1.7	2105	0.90 ± 0.01	1895	75.8	237.9
7	28.5	0	27.3 ± 2.9	1365	0.96 ± 0.03	1310	52.4	1886
10	27.5	6.8	27.3 ± 1.1	1938	0.88 ± 0.01	1706	68.2	69.35
10	27.5	0	17.7 ± 2.4	1257	0.94 ± 0.04	1182	47.3	944.0
15	25.2	15.9	16.8 ± 0.7	1781	0.89 ± 0.01	1585	63.4	133.4
15	25.2	0	8.28 ± 1.5	878	1.03 ± 0.08	904.0	36.2	1994
			4-BrBzNa					
5	29.4	3.6	44.6 ± 1.8	1606	0.99 ± 0.01	1590	63.6	321.3
5	29.4	0	32.5 ± 2.7	1170	1.04 ± 0.03	1217	48.7	1577
6	29.3	4.6	36.6 ± 1.2	1574	0.97 ± 0.01	1527	61.1	171.5
6	29.3	0	25.1 ± 2.7	1079	1.04 ± 0.04	1122	44.9	2059
7	28.9	5.3	31.7 ± 1.8	1585	0.97 ± 0.02	1537	61.5	528.2
7	28.9	0	21.4 ± 1.0	1070	1.06 ± 0.03	1134	45.4	1369
10	27.4	10.2	24.7 ± 0.8	1736	0.99 ± 0.01	1736	69.4	123.8
10	27.4	0	14.5 ± 1.6	1030	1.09 ± 0.05	1123	44.9	1695
15	26.6	14.4	13.2 ± 0.6	1399	0.98 ± 0.02	1371	54.8	192.5
15	26.6	0	6.91 ± 1.2	732.5	1.15 ± 0.10	842.4	33.7	2602

[a] Total concentration of CTABr. [b] $k_0 = k_{obs}$ at [MX] = 0. [c] Error limits are standard deviation. [d] $K_{X/S} = K^{X/S}{}_X\ (1 + K_S^o\ [CTABr]_T)$ where $K_S^o = 7000\ M^{-1}$. [e] $F_{X/S} = \theta / k_w$ where $k_w = k_{obs}$ at $[CTABr]_T = 0$, $[Pip]_T = 0.1$ M and the value of k_w, under such conditions is 32.7 x $10^{-3}\ s^{-1}$ at 35°C. [f] $K_{X/S}^n = F_{X/S}K_{X/S}$. [g] $K_X^{Br} = K_{X/S}^n/K_{Br/S}^n$, where $K_{Br/S}^n = 25\ M^{-1}$.

The values of calculated $K_{X/S}$, in **Tables 4.1** and **4.2**, were found to be almost independent of $[CTABr]_T$ range within 5 to 15 mM CTABr. Empirically, the value of $K_{X/S}$ is proportional to K_X (ionic micellar binding constant of counterion X) and inversely proportional to K_S (ionic micellar binding constant of another counterion S). Thus, with Ω_S representing the proportionality constant, $K_{X/S} = \Omega_S K_X/K_S$, where Ω_S is assumed to be

dependent only upon molecular characteristics of counterion S and independent of counterion X. Similarly, for ion-exchange of Y^-/S^-, $K_{Y/S} = \Omega_S K_Y/K_S$. Thus,

$$\frac{K_{X/S}}{K_{Y/S}} = \frac{K_X}{K_Y} \qquad \textbf{Eq. 4.11}$$

where K_X/K_Y represents the thermodynamic ion-exchange constant for ion-exchange process X^-/Y^- occurring at cationic micellar surface, i.e. $K_X^Y = ([X_M][Y_W])/([X_W][Y_M])$. If $K_{X/S}$ and $K_{Y/S}$ were determined experimentally by the use of **Eq. 4.4** where the optimum values of [X] or [Y] has caused >90% expulsion of counterion S to the aqueous phase, the use of **Eq. 4.11** is correct. But, if $K_{X/S}$ and $K_{Y/S}$ values were determined using **Eq. 4.5**, then the values need to be normalized, $K_{X/S}^n = F_{X/S}K_{X/S}$ and $K_{Y/S}^n = F_{Y/S}K_{Y/S}$ where $F_{X/S} = \theta/k^n{}_W{}^{MX}[Pip]_T$ and $F_{Y/S}^n = \theta/k^n{}_W{}^{MY}$ with $1 >> K_N[Dn]$ (where N = Pip). Thus, under such conditions, the ratio $K_{X/S}/K_{Y/S}$ should be replaced by the ratio $K_{X/S}^n/K_{Y/S}^n$ in **Eq. 4.11**. Since the value of $K_{X/S}$ were determined using **Eq. 4.5**, it was normalized and treated according to **Eq. 4.11** with a known value of $K_{Br/S}^n$ ($S = PS^-$) = 25 M^{-1}.These results are summarized in **Tables 4.1** and **4.2** as well.

4.3 Discussion on the Values of Ion-Exchange Constants.

It has been almost certain by direct and indirect investigations on the micellar environment that the micellized solubilizates of different hydrophobicity and steric requirements is not homogeneous in term of water concentration, polarity, relative permittivity, and even its molecular fluidity.[4b,12] From the exterior regions of the headgroups to the interior of the core of a micelle, the hydrophobicity is increased whilst the hydrophilicity is decreased continuously. A solubilizate molecule in a micellar

pseudophase is expected to occupy a micellar location where various hydrophilic, electrostatic, hydrophobic and steric interactions gave the most stable state.

It is evident from **Eq. 4.9**, that θ is actually independent of $[CTABr]_T$. In agreement with this prediction, we observe from **Tables 4.1** and **4.2** that the θ values, for all of the organic salt used, remain independent of $[CTABr]_T$. The values of $F_{X/S}$ were calculated from **Eq. 4.9** where $1 >> K_N[D_n]$, $k^n_W = 32.7 \times 10^{-2}\ M^{-1}s^{-1}$,[4(d)], and $[Pip]_T = 0.1$ M. The average calculated values of $F_{X/S}$ and K_X^{Br} are shown in **Table 4.3**.

Table 4.3: Average Values of $F_{X/S}$ and K_X^{Br} for Different MX in the Presence of CTABr Micelles.

X	$[MX]_0^{op}$	$10^2 F_{X/S}$	K_X^{Br}
3-FBz^-	Nonzero	71 ± 6	12.8 ± 0.9
	Zero	122 ± 85	8.85 ± 1.8
4-FBz^-	Nonzero	80 ± 2	13.4 ± 0.6
	Zero	100 ± 25	10.6 ± 1.2
2-$ClBz^-$	Zero	67 ± 2	5.67 ± 0.7
3-$ClBz^-$	Nonzero	75 ± 4	50.3 ± 2.0
	Zero	85 ± 5	28.6 ± 3.3
4-$ClBz^-$	Nonzero	66 ± 2	47.9 ± 2.5
	Zero	78 ± 7	28.6 ± 2.6
2-$BrBz^-$	nonzero	63 ± 2	8.82 ± 0.3
	zero	68 ± 4	7.23 ± 0.2
3-$BrBz^-$	nonzero	92 ± 4	71.2 ± 5.6
	zero	100 ± 4	49.0 ± 8.0
4-$BrBz^-$	nonzero	98 ± 1	62.1 ± 5.2
	zero	108 ± 5	43.5 ± 5.7
2-IBz^-	nonzero	74 ± 5	11.2 ± 0.9
	zero	104 ± 43	8.59 ± 1.4
4-IBz^-	nonzero	87 ± 4	144 ± 12
	zero	104 ± 4	83.9 ± 18

The values of the ion-exchange constant, K_X^{Br} (**Table 4.3**) for the organic salts (MX) of this study decrease in the following order.

$4\text{-}IC_6H_4CO_2Na > 3\text{-}BrC_6H_4CO_2Na > 4\text{-}BrC_6H_4CO_2Na > 3\text{-}ClC_6H_4CO_2Na > 4\text{-}ClC_6H_4CO_2Na > 4\text{-}FC_6H_4CO_2Na > 3\text{-}FC_6H_4CO_2Na > 2\text{-}IC_6H_4CO_2Na > 2\text{-}BrC_6H_4CO_2Na > 2\text{-}ClC_6H_4CO_2Na$.

Scheme 4.1

Several studies have been carried out earlier to investigate the effect of mono-substituted halo-benzoates towards the structural features of the cationic micelles.[4d,13,14]. These studies involved physical methods such as ^1H NMR measurement and revealed that such counteranions are localized in the Stern layer and intercalated among the positively charged micellar head.[15] The counterions are also known to be affecting micellar aggregation by increasing the aggregation number due to a more efficient packing of surfactant chains as resulted from the reduced unfavorable head group-head group repulsion by the counterions' intercalation.[14]

Zakin and his coworkers[15] has studied the effect of addition of *o*-, *m*- and *p*-chlorobenzoates on the aqueous cationic micellar system and concluded that *m*- and *p*-$ClC_6H_4CO_2^-$ interaction with cationic micelles will result to viscoelastic micellar system whilst the same micellar aggregation system with *o*-$ClC_6H_4CO_2^-$ addition remained spherical, thus nonviscoelastic. Number of researches has eventually led us to the conclusion that the key to such viscoelasticity is the nature of counterion adsorption due to the counterion penetration beyond the surfactant headgroups,[15,16] thus counterion such as salicylate as compared to counterions such as chloride may be a wise choice in promoting micellar growth.[17,18]

Magid et al.[18] have strongly suggested that the counterion hydration and the strength of dispersion interaction or known as van der Waals forces between the counterions and

surfactant headgroups are the major players in determining the penetration ability of the counterions into micellar pseudophase. The less hydrated counterion posses greater ability in shielding the charge of the surfactant aggregates, thus become more effective in penetrating into greater depth and having higher ion-exchange constant. The same goes to aromatic counterions with the need to focus on its substituent group(s) as well as its position on the aromatic ring.[15a,19] Thus, in such cases as this study, the focus of discussion should be on the behavior originated from the different substituent on the aromatic benzoates. The relationship of the ion-exchange constants (K_X^{Br}) involving the counterions from such organic salts may also be described in the following manner.

$$3\text{-}FC_6H_4CO_2^- \approx 4\text{-}FC_6H_4CO_2^-,$$

$$2\text{-}ClC_6H_4CO_2^- < 3\text{-}ClC_6H_4CO_2^- \approx 4\text{-}ClC_6H_4CO_2^-,$$

$$2\text{-}BrC_6H_4CO_2^- < 3\text{-}BrC_6H_4CO_2^- \approx 4\text{-}BrC_6H_4CO_2^-$$

$$\text{and } 2\text{-}IC_6H_4CO_2^- < 4\text{-}IC_6H_4CO_2^-$$

Scheme 4.2

To discuss such order, we have to understand the structure and the possible position of such compounds in the micellar pseudophase and bulk aqueous phase in the previously studied system as shown in **Figure 4.3** where X is the halogen attached to the benzene ring.

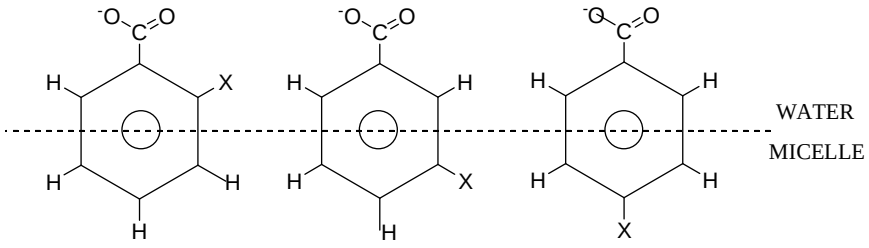

Figure 4.3: Orientations of monosubstituted halo benzoates at *o*-, *m*- and *p*- position in aqueous micellar system.

Figure 4.3 illustrates the orientation of 3 different position of halo-substituted benzoates at the micelle-water interface proven using NMR studies by Smith et al.[20] Halogen species are hydrophobic substituent, therefore prone to stay on the hydrocarbon part of the micelle aggregation.[15a] The position of halogen at 3- and 4-carbon on the aromatic ring gave them the advantage to penetrate deeper, thus become the favorable substituted counterions in promoting micellar growth. On the other hand, when the halogen substituent is placed on the 2-carbon position, the penetration towards the hydrophobic part of micelle become harder, thus unfavorable in producing wormlike micellar aggregation.[15] This agrees with the experimental result as represented by **Scheme 4.2** where 3- and 4-substituted halobenzoates gave larger values of ion-exchange constant, K_X^{Br}, compared to the halobenzoate at 2-position. It is also observable by rheological measurements that in general, the viscosities observed were higher for 3- and 4-halobenzoates as compared to 2-halobenzoate. Another possible phenomenon exhibited upon 2-ClBzNa addition was proposed in which such counterions do not even penetrate into micellar aggregation, instead they are just tilted in the orientation that their loci is tangentional to the micellar interface.[21] On the other hand, the situation with the addition of 3- and 4-ClBzNa proposed were in agreement with Smith et al. discussed before.[20]

Another factor, other than the different position of halogen substituent, the hydrophobicity possessed by the halogen itself is one of the major factor towards counterion penetration as well. This can be discussed in terms of the charge and softness of the counterions. Comparing the four halogens, the softness varies in the following manner: F < Cl < Br < I. The results of ion-exchange constants of this study can also be generally represented in such manner that FBzNa < ClBzNa < BrBzNa < IBzNa. The generalization of this order is that as the softness of the counterion increases, the ion-exchange constant

will also increase. Thus, the viscoelasticity is also expected to be in the same behavior. This has been proposed by Subramaniam and Ducker[22] that soft mono- and dianions are more effective in inducing growth of micelle than hard anions in terms of their polarizability ability. Vermathen and his coworkers[14] have also concluded the same thing because with the increase of anions' softness, there will be higher tendency of those anions to intercalate among the headgroups, which decreases headgroup repulsions and increase the possibility of inducing micellar growth.

The relatively more reliable average values of $F_{X/S}$ and K_X^{Br} as well as some reported values of K_X^{Br} are summarized in **Table 4.4**.[3c]

Table 4.4 The Average Values of $F_{X/S}$ and K_X^{Br} for Different MX in the Presence of CTABr Micelles[a]

X	$[MX]_o^{op}$	$10^2 F_{X/S}$	K_X^{Br}	cmc_2
3-FBz^-	nonzero	71 ± 6[b]	12.8 ± 0.9[b]	~12.9 mM[c]
4-FBz^-	nonzero	80 ± 2	13.4 ± 0.6	~13.8 mM[c]
2-$ClBz^-$	zero	67 ± 2	4.67 ± 0.7	
2-$ClBz^-$	-	-	4.0[d]	
3-$ClBz^-$	nonzero	75 ± 4	50.3 ± 2.0	
3-$ClBz^-$	nonzero	72	50[e]	
4-$ClBz^-$	nonzero	66 ± 2	47.9 ± 2.5	
2-$BrBz^-$	nonzero	63 ± 2	8.82 ± 0.3	
3-$BrBz^-$	nonzero	92.4 ± 4	71.2 ± 5.6	
4-$BrBz^-$	nonzero	98 ± 1	62.1 ± 5.2	
2-IBz^-	nonzero	74 ± 5	11.2 ± 0.9	
4-IBz^-	nonzero	87 ± 4	144 ± 12	
Bz^-	zero	70	5.8[f]	200 mM CTACl + ≥ 50 mM BzK[g]
2,6-Cl_2Bz^-	-	-	5.0[h]	
2-CH_3Bz^-	nonzero	43	4.9[i]	
3-CH_3Bz^-	Nonzero	50	17.7[i]	
4-CH_3Bz^-	Nonzero	48	16.7[i]	

[a] Unless otherwise noted cationic micelles are CTABr. [b] Error limits are standard deviations. [c] Ref 14, cmc_2 values are for TTAX micelles. [d] Ref. 13. [e] Ref. 23. [f] Ref. 24. [g] Ref. 25. [h] Ref. 21. [i] The values of K_X^{Br} were recalculated from the observed data published as Ref. 26.

If the $F_{X/S}$ values of 2-, 3- and 4-CH_3Bz^- are compared with the $F_{X/S}$ values of the halo-benzoate salts used in this study, it can be clearly seen that all the halo-benzoates

posses much higher magnitudes and this has been discussed in one of recent study[3c] that such observation is due to the significantly larger hydrophobicity and molecular size of substituent CH_3 as compared to the halogen-substituents. For 2-$ClBz^-$ and 3-$ClBz^-$, the ion-exchange constant, K_X^{Br} has been determined before and the values for the same organic salt in this study seem to be satisfyingly repeatable The same goes for the $F_{X/S}$ values of 3-$ClBz^-$ that the value determine from this study agrees with the one determined by Ducker and coworkers.[22] If we compare the $F_{X/S}$ values for X = 3-FBz^-, 3-$ClBz^-$ and 4-$ClBz^-$ with X = Bz^-, the values are actually comparable indicating the quite similar micellar penetration behavior of these counterions. But when X = 3-$BrBz^-$, 4-$BrBz^-$ and 4-IBz^- the $F_{X/S}$ values are quite high indicating a deeper penetration of such counterions. This might be due to the highly hydrated fluoro- atom on 3-FBz^- as well as chloro- atom on 3- and 4-$ClBz^-$, thus weakly micellar penetrating compared to the weakly hydrated bromo- atom in 3- and 4-$BrBz^-$ as well as the iodo- atom in 4-IBz^- which showed strong penetration towards the cationic micellar pseudophase. The $F_{X/S}$ values of 2-$BrBz^-$ and 2-IBz^- were found to be low. These are explainable if we refer to the illustration of counterion penetration proposed by Smith[21] (**Figure 4.2**). The substitution at 2-position in the aromatic ring will make it harder for the counterion to penetrate towards the hydrophobic region in the micelle due to the very close position with the CO_2^- group, thus restricted from penetrating very deep.

It is also worthwhile to compare the ion-exchange constant values between those such as Bz^-, 2-$ClBz^-$, 2-$BrBz^-$, 2,6-Cl_2Bz^- and 3-CH_3Bz^- which are known to produce only spherical micelles at ≤ 20 mM CTABr[15a,16,19a,27] with those such as 3- and 4-$BrBz^-$ as well as 4-IBz^- from this study which have been observed to be very viscoelastic. The difference of their K_X^{Br} is ~ 44 to 140 indicating the different effect brought by different counterion in terms of their penetration and binding towards the cationic micelles and thus can be

predicative towards their aggregation behavior. Ge et al.[28] has studied the effect of chemical structures of *p*-halobenzoates on micelle CTAC nanostructure at 5 mM. The 4 *p*-halobenzoates seem to have almost similar $F_{X/S}$ values, thus expected to have a similar penetration depth but the K_X^{Br} values determined by this study for 4-FBz^-, 4-$ClBz^-$, 4-$BrBz^-$ and 4-IBz^- increases from 13.4, 47.2, 62.1 and 144 respectively. According to the investigation of Ge et al.[28], the chemical shift from the ^1H NMR study was significantly affected by the insertion of *p*-fluorobenzoate, followed by *p*-chlorobenzoate and *p*-bromobenzoate and the most for *p*-iodobenzoate. This is due to their increasing ability to donate electrons by resonance effect to the benzene ring. The structures of micellar aggregation investigated by cryo-TEM have shown increasing micellar length and entanglement from the system of 4-FBzNa/CTACl to 4-ClBzNa/CTACl to 4-BrBzNa/CTACl and to 4-IBzNa/CTACl. It is logically concluded that the increasing influence of halobenzoates counterions into the hydrocarbon core of the micelles may be related to their increasing size and molecular volume, hydrophobicity, polarizability and associated free energy of dehydration. These increasing factors lead to the formation of longer and more entangled wormlike micelles. The K_X^{Br} values for the halo-substitution of benzoate at 2- and 3- positions in CTABr aqueous micellar system were also showing the same pattern of order. This is illustrated by **Scheme 4.3**.

$$\underset{(4.67)}{2\text{-}ClC_6H_4CO_2Na} < \underset{(8.82)}{2\text{-}BrC_6H_4CO_2Na} < \underset{(11.2)}{2\text{-}IC_6H_4CO_2Na}$$

$$\underset{(12.8)}{3\text{-}FC_6H_4CO_2Na} < \underset{(50.3)}{3\text{-}ClC_6H_4CO_2Na} < \underset{(71.2)}{3\text{-}BrC_6H_4CO_2Na}$$

Scheme 4.3 : The order of K_X^{Br} values for X = 2-, 3- or 4-halobenzoates and Br is the counterion of CTABr micelle where parenthesized values represent K_X^{Br}.

4.4 Rheological Measurement that Support the Proposed Kinetic Approach in Relating Ion-Exchange Constant to the Structure of the Micellar Aggregation.

Micellar aggregation has been termed as "living polymer" due to its ability to deform and reform accordingly to the different situation.[29] Plenty attempts has been continuously done to investigate micellar structural behavior by different methods such as drag reducing measurement, flotation technique, florescence quenching method, cryo-TEM and ^{1}H NMR measurements.[30] One of the well known method is the rheological study of the different micellar condition. The existence of N1 values and high zero-shear viscosity (η_0) are good indicators in proving the existence of long and entangled wormlike micelles. The aggregation of wormlike micelles instead of normal spherical micelles is indicated by the visibility of viscosity maxima as a function of the concentration of the counterionic salt which has been known to be a characteristic feature of such micellar solution in previous studies.[17,27,31]

Figures 3.11 - 3.20 except **Figure 3.13** illustrated the apparent viscosity (η) behavior in response to the shear rate (γ) applied. A typical shear thinning were observed upon the increase of γ indicating the alignment of micellar structure according to the rotation of the mobile part in the rheometer. For wormlike micellar solutions, it has been previously discovered that the plot of viscosity values at specific shear rate as a function of the concentration of the counterionic salt will show at least one maximum where the viscosity seem to be highest at that specific [counterionic salt]:[surf] ratio.[25,27,31] **Figures 3.21** to **3.24** revealed a maximum for [MX]/$[CTABr]_T$ system for all organic salts used except for 2-ClBzNa (**Figure 3.22**). The apparent viscosity, η showed an almost unchanged values upon the increase of shear rate. Thus, no maximum can be observed as the solution acted as water-like solution. This agreed with the expected result as compared to its

determined K_X^{Br} value which is 4.67 in this study. Shear thinning behavior was observed for 2-, 3- and 4-BrBzNa (**Figures 3.16 -3.18).** But only 3- and 4-$BrC_6H_4CO_2Na$ exhibit a concentration of MX which gave the significant maximum viscosity (**Figure 3.23**). However, under magnification, the plot of viscosity at 0.5 s^{-1} shear rate versus salt concentration for [2-BrBzNa]/$[CTABr]_T$ system revealed a maximum at [2-BrBzNa]/$[CTABr]_T$ = 4. This is shown by **Figure 4.4**. This is explainable by its low K_X^{Br} value (8.82). However, the value is almost double as compared to the K_X^{Br} value when X^- = 2-$ClBz^-$, thus it is predicted that there are spherical and vesicles micellar aggregation in this system.

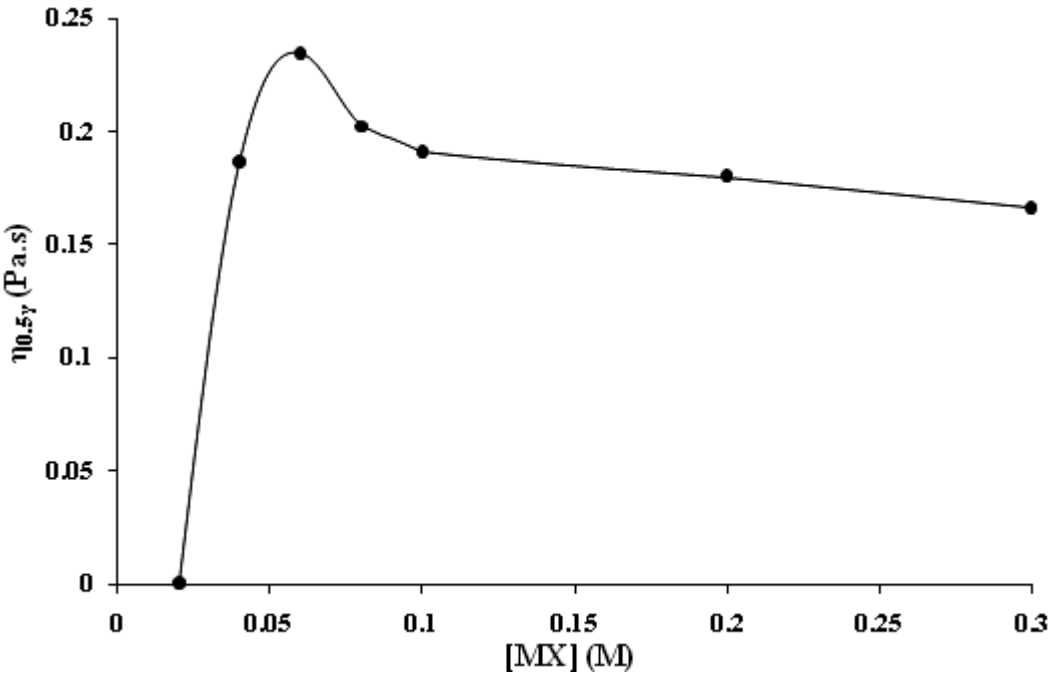

Figure 4.4 : Plot of shear viscosity (η) at γ = 0.5 s^{-1} versus [MX] ([MX] = [2-$BrC_6H_4CO_2Na$]) at 0.015 M CTABr, 2.0×10^{-4} PS^-, 0.03 M NaOH, 0.1 M Pip and ~ 35°C.

Despite the fact that it is common to observe the viscosity maxima in the plots of shear viscosity value, at fixed shear rate (η_γ), versus [MX] for viscoelastic micellar system, the causes and reasons are still unclear. However, the proposed possibilities are:

(a) A transition from linear to branched micelles or a maximum in micellar contour length[32], and

(b) the increase of viscosity is attributed by the process of micellar growth whilst the decrease of the viscosity is attributed by micellar breaking. [33]

When the concentration of MX, added to CTABr aqueous micellar system, is too low or too high, the plot of apparent viscosity versus shear rate were showing shear thickening instead of shear thinning. Since the shear thinning is explainable by the alignment of the micelles, shear thickening is expected to be due to the further entanglement of the micelles as more and more disruption occurs by rotational rheometer. This has been detected by a number of previous study at dilute solution of micellar system.[34] The optimum addition of MX is achieved at the point of viscosity maxima where the penetration of X^- into CTABr micelles optimized the elongation and entanglement of the micelles. Above the optimum point it is expected that further X^- added force the micelle to form ring-like micellar aggregation. This way, more X^- counterions can bind at the outer as well as the inner side of the ring-like micelle.[35] However, the physical characteristic of the aqueous micellar system changes due to the lack of viscoelasticity of the ring-like micelle.

References

(1) Khan, M. N. *J. Chem. Soc. Perkin Trans II* **1989**, 199-208. (b) Khan, M. N. Micellar Catalysis: Surfactant Science Series; CRC Taylor & Francis; Boca Raton, FL. 2007; Vol 133. (c) Khan, M. N.; Ahmad, F. B. H. *Reaction Kinetics, Mech. And Catal.* **2001**, *72*, 321-329.

(2) (a) Khan, M. N.; Arifin, Z.; Lasidek, M. N.; Hanifiah, M. A. M.; Alex, G. *Langmuir* **1997**, *13*, 3959-3964. (b) Khan, M. N. *J. Org. Chem.* **1997**, *62*, 3190-3193.

(3) (a) Khan, M. N.; Ismail, E.; Yusof, N. S. M. *Colloid and Surfaces A* **2010**, *361*. 150-161. (b) Khan, M. N.; Ismail, E. *Indian Journal of Chemistry* **2009**, *48A*, 781-787. (c) Yusof, N. S. M.; Khan, M. N. *Langmuir* **2010**, 26, 10627-10635. (d) Khan, M. N.; Ismail, E.; Misran, O. *J. Mol. Liq.* **2002**, *95*, 75-86. (e) Yusof, N. S. M.; Khan, M. N. *J. Colloid Interface Sci.* **2011**. Online

(4) Khan, M. N.; Ismail, E. *J. Chem. Research(s)* **2001**, 143-145. (b) Khan, M. N.; Naaliya, J.; Dahiru, M. *J. Chem. Research(s)* **1988**, 116-117. (c) Khan, M. N.; Arifin, Z.; Yusuff, M. R., Ismail, E. *J. Colloid Interface Sci.* **1999**, *220*, 474-476.

(5) (a) Cordes, E. H.; Gitler, C.; *Prog. Bioorg. Chem.* **1973**, 2, 1-53. (b) Bunton, C. A.; Savelli, G. *Adv. Phys. Org. Chem.* **1986**, 22, 213-309. (c) Rathman, J. F. *Curr. Opin. Colloid Interface Sci.* **1996**, *4*, 1, 514-518.

(6) (a) Sotgiu, G.; Schirone, L.; Rallo, F. *Il Nuovo Cimento D* **1996**, *18*, 1179-1186. (b) Modaressi, A.; Sifaoi, H.; Grzesiak, B.; Solimando, R.; Domanska, U.; Rogalski, M. *Coll. Surf. A* **2007**, *296*, 104-108. (c) Chaimovich, H.; Blanco, A.; Chayet, L.; Costa, L. M.; Monteiro, P. M.; Bunton, C. A.; Paik, C. *Tetrahedron* **1975**, *31*, 1139-1143.

(7) (a) Liu, J.-F.; Min, G.; Ducker, W. A. *Langmuir* **2001**, *17*, 4895-4903. (b) Para, G.; Jarek, E.; Warszynski, P. *Coll. Surf. A* **2004**, *261*, 65-73.

(8) Iglesias, E.; Leis, J. R.; Pefia, M. E. *Langmuir* **1994**, *10*, 662-669.

(9) Fernandez, A.; Iglesias, E.; Garcia-Rio, L.; Leis, J. R. *Langmuir* **1995**, *11*, 1917-1924.

(10) Bravo, C.; Herves, P.; Leis, J. R.; Pena, M. F. *J. Colloid Interface Sci.* **1992**, *153*, 529-536.

(11) (a) Deavers, K.; Macek. T.; Karlson, U. G.; Trapp, S. *Environ. Sci. Pollut. Res.* **2010**, *17*, 1355-1361. (b) Hirokawa, T.; Tsuyoshi, T.; Kiso, Y. *J. Chrom. A* **2002**, *408*, 27-41. (c) Tao, L.; Han, J.; Tao, F-M. *J. Phys. Chem. A* **2008**, *112*, 775-782.

(12) (a) Shobha, J.; Balasubramaniam, D. J. *Chem. Sc.* **1987**, *98*, 469-478. (b) McCarroll, M.; Toerhe, K.; Wandruszka, R. *Langmuir* **1998**, *14*, 2965-2969.

(13) Khan, M. N.; Yusoff, M. R. *J. Phys. Org. Chem.* **2001**, *14*, 74-80.

(14) Vermathen, M.; Stiles, P.; Bachofer, S. J.; Simonis, U. *Langmuir* **2002**, *18*, 1030-1042.

(15) (a) Lu, B.; Li, X.; Scriven, L. E.; Davis, H. T.; Talmon, Y.; Zakin, J. L. *Langmuir* **1998**, *14*, 8-16. (b) Qi, Y.; Zakin, L. Z. *Ind. Eng. Chem. Res.* **2002**, *41*, 6326-6336.

(16) Magid, L. J.; Han, Z.; Warr, G. G.; Cassidy, M. A.; Butler, P. D.; Hamilton, W. A. *J. Phys. Chem. B* **1997**, 101, 7919-7927.

(17) (a) Raghavan, S. R.; Kaler, E. W. *Langmuir* **2001**, *17*, 300-306. (b) Magid, L. J. *J. Phys. Chem. B* **1998**, *102*, 4064-4074.

(18) Magid, L. J.; Han, Z.; Li, Z. *J. Phys. Chem. B* **2000**, *16*, 149-156.

(19) (a) Gravsholt, S. *J. Colloid Interface Sci.* **1976**, *57*, 575-577. (b) Kreke, P. J.; Magid, L. J.; Gee, J. C. *Langmuir* **1996**, *12*, 699-705.

(20) Smith, B. C.; Chou, L. C.; Zakin, J. L. *J. Rheol*. **1994**, *38*, 73-83.

(21) Bachofer, S. J.; Turbitt, R. M. *J. Colloid Interface Sci.* **1989**, *135*, 325-334.

(22) Subramaniam, V.; Ducker, W. A. *Langmuir* **2000**, *16*, 4447-4454.

(23) Khan, M. N.; Ismail, E. *J. Phys. Chem. A* **2009**, *113*, 6484-6488.

(24) Khan, M. N.; Ismail, E. *J. Dispersion Sci. Technol.*, in press.

(25) Ali, A. A.; Makhloufi, R. *Colloid Polym. Sci.* **1999**, *277*, 270-275.

(26) Khan, M. N.; Ismail, E. *J.Mol. Liq.* **2007**, *136*, 54-63.

(27) Rao, U. R. K.; Manohar, C.; Valaulikar, B. S.; Iyer, R. M. *J. Phys. Chem.* **1987**, *91*, 3286-3291.

(28) Ge, W.; Kesselman, E.; Talmon, Y.; Hart, D. J.; Zakim, J. L. *J. Non-Newtonian Fluid Mech.* **2008**, *154*, 1-12.

(29) Yang, J. *Current Opinion in Colloid and Interface Science* **2002**, *7*, 276-281.

(30) (a) Bahri, M. A.; Hoebeke, M.; Grammenos, A.; Delanaye, L.; Vandewalle, N.; Seret, A. *Coll. Surf. A* **2006**, 290, 206-212. (b) Kuperkar, K.; Abezgauz, L.; Danino, D.; Verma, G.; Hassan, P. A.; Aswal, V. K.; Varade, D.; Bahadur, P. *PRAMANA-J. Phys.* **2008**, *71*, 5, 1003-1008. (c) Brown, E. F.; Burghardt, W. R. *Langmuir* **1997**, *14*, 13, 3902-3904. (d) Vasquez, P. A.; McKinley, G. H.; Cook, L. P. *J. Non-Newtonian Fluid Mech*. **2007**, 144, 122-139.

(31) (a) Clausen, T. M.; Vinson, P. K.; Minter, J. R.; Davis, H. T.; Talmon, Y.; Miller, W. G. *J. Phys. Chem.* **1992**, *96*, 474-484. (b) Shubert, B. A.; Wagner, N. J.; Kaler, E. W. *Langmuir*, **2004**, *20*, 3564-3573. (c) Aswal, V. K.; Goyal, P. S.; Thiyagarajan, P. *J. Phys. Chem. B* **1998**, *102*, 2469-2473. (d) Ali, A. A.;Makhloufi, R. *Phys. Rev. E.* **1997**, *56*, 4474-4478.

(32) Lu, T.; Huang, J.; Li, Z.; Jia, S.; Fu, H. *J. Phys. Chem. B* **2008**, *112*, 2909-2914.

(33) Shrestha, R. G.; Aramaki, K. *J. Nepal Chem. Soc.* **2008/2009**, *23*, 65-73.

(34) (a) Berret, J.-F.; Gamez-Corrales, R.; Lerouge, S.; Decruppe, J.-P. *J. Eur. Phys.* **2000**, 343-350. (b) Goveas, J. L.; Pine, D. J. *Europhysics Letters* **1999**, *48*, 6, 706-712.

(35) Davies, T. S.; Ketner, A. M.; Raghavan, R. *J. Am. Chem. Soc*. **2006,** *128*, 6669-6675.

CONCLUSION

This study has achieved its main purpose which is to provide a quantitative insight of micellar structural aggregation behavior through the determination of thermodynamic ion-exchange constant involving different halo-substituted organic salts (MX) and cetyltrimethylammonium bromide (CTABr) micelles. The values of ion-exchange constants, K_X^{Br}, are listed in **Table 4.1**. Another useful parameter is the $F_{X/S}$ which represents the fraction of the expulsion of micellized counterion PS^-_M to the bulk aqueous phase by the optimum concentration of MX through ion-exchange X^-/PS^-. The values are also listed in **Table 4.1**. The K_X^{Br} values were found to be related to the rheological behavior of the micellar systems. Hence, it can be concluded that these values are better indication towards the viscoelasticity of micelles. This gives a strong and quantitative support to the assumption that the strength of micellar binding by certain counterions is contributing to the process of micellar structural transition from spherical to wormlike micelle.

APPENDICES

APPENDIX A (TABLES I – X)

Table I: Pseudo-First-Order Rate Constants (k_{obs}) for the Reaction of Piperidine with Anionic Phenyl Salicylate (PS^-) at a Constant $[CTABr]_T$ and Different [3-FBzNa].[a]

$[CTABr]_T$ /M	0.005			0.006			0.007			0.010			0.015		
10^2 [MX]	$10^4 k_{obs}$	RE_1[b]	RE_2[c]	$10^4 k_{obs}$	RE_1[b]	RE_2[c]	$10^4 k_{obs}$	RE_1[b]	RE_2[c]	$10^4 k_{obs}$	RE_1[b]	RE_2[c]	$10^4 k_{obs}$	RE_1[b]	RE_2[c]
M	s^{-1}			s^{-1}			s^{-1}			s^{-1}			s^{-1}		
0.0	29.5 ± 0.2[d]			28.8 ± 0.3[d]			27.9 ± 0.1[d]			27.4 ± 0.1[d]			26.0 ± 0.3[d]		
0.2	28.4 ± 0.6			27.2 ± 0.2			27.8 ± 0.2			27.3 ± 0.3			25.0 ± 0.2		
0.5	31.4 ± 0.2			28.7 ± 0.3			27.5 ± 0.2			27.5 ± 0.5			25.1 ± 0.2		
1.0	43.0 ± 0.2	-18	5.4	35.3 ± 0.4	-24	3.4	30.8 ± 0.2	-31	6.0	26.9 ± 0.3			26.4 ± 0.4		
1.5	55.0 ± 0.9	-9.2	3.7	42.9 ± 0.4	-17	-0.8	39.2 ± 0.1	-18	5.0	32.1 ± 0.3	-26	7.0	28.4 ± 0.1		
2.0	60.8 ± 0.5	-13	-5.0	52.7 ± 0.2	-7.5	2.2	43.4 ± 0.4	-19	-3.5	34.7 ± 0.4	-28	-3.6	28.9 ± 0.3	-23	6.6
3.0	81.2 ± 0.8	-3.2	-1.6	66.3 ± 0.4	-2.8	0.3	56.2 ± 0.4	-10	-4.4	47.6 ± 1.1	-9.2	1.0	34.7 ± 0.1	-16	-0.7
4.0	99.4 ± 2.5	2.5	1.6	74.0 ± 0.2	-5.9	-6.1	68.6 ± 0.1	-3.9	-2.9	55.3 ± 0.2	-6.9	-3.0	40.6 ± 0.1	-11	-4.0
5.0	105 ± 0.9	-3.2	-5.8	89.4 ± 0.5	2.1	0.3	81.2 ± 0.9	1.6	0.2	64.7 ± 1.2	-1.8	-1.6	48.5 ± 0.8	-2.3	-0.9
7.0	126 ± 0.7	-1.0	-3.6	106 ±0.4	2.5	-0.1	96.7 ± 0.7	1.6	-1.9	79.5 ± 0.6	1.7	-1.6	59.2 ± 0.6	1.0	-2.7
10	159 ± 2.7	6.5	4.2	125 ± 1.2	2.3	-0.9	121 ± 0.6	5.6	1.7	100 ± 1.2	5.9	-1.5	75.7 ± 0.5	5.4	0.1
15	183 ± 1.8	5.4	4.2	151 ± 1.5	4.1	2.4	143 ± 1.2	3.2	1.0	120 ± 1.2	3.6	0.6	99.5 ± 1.7	7.5	5.0
20	190 ± 3.4	0.2	0.2	166 ± 1.4	3.0	2.3	162 ± 1.3	3.3	2.5	137 ± 0.7	3.2	1.5	106 ± 0.6	-4.9	-2.9
30	201 ± 1.5	-4.7	-3.0	174 ± 1.8	-4.8	-2.5	174 ± 1.7	-4.5	-2.3	152 ± 1.1	-3.8	-1.3			
$10^{-1}\delta_{app}^{av}/M^{-1}cm^{-1}$ [e] =	684 ± 12			682 ± 6			679 ± 9			686 ± 10			690 ± 12		

[a] $[phenyl\ salicylate]_0$ = 0.2 mM, 35 °C, λ = 350 nm, $[piperidine]_T$ = 0.1 M, $[\ ]_T$ represents total concentration and the aqueous reaction mixture for each kinetic run contained 2 % v/v CH_3CN. The required amounts of 3-$FC_6H_4CO_2Na$ ([MX]) were generated into the reaction mixture by using the stock solution (w M) of 3-$FC_6H_4CO_2H$ prepared in (w + 0.05) M aqueous NaOH. The stock solution of NaOH was used to produce a fixed known concentration (0.03 M) of NaOH into the reaction mixture for each kinetic run. Thus, the maximum concentration of added NaOH was 0.06 M. [b] $RE_1 = 100\times(k_{obs} - k_{cald1})/k_{obs}$ where k_{cald1} values were calculated

from **Eq. 4.5** with kinetic parameters (k_0, θ and $K^{X/S}$) listed in **Table 4.1**. [c] $RE_2 = 100\times(k_{obs} - k_{cald2})/k_{obs}$ where k_{cald2} values were calculated from **Eq. 4.5** with [MX] replaced by [MX] – $[MX]_0^{op}$ and $[MX]_0^{op}$ = 5.9, 7.3, 9.4, 13.1 and 18.8 mM at 5, 6, 7, 10 and 15 mM CTABr, respectively, as well as kinetic parameters listed in **Table 4.1**. [d] Error limits are standard deviations. [e] Mean value of δ_{app} (= δ_{app}^{av}) obtained within [MX] range shown in the **Table 3.1** and the error limits are standard deviations.

Table II: Pseudo-First-Order Rate Constants (k_{obs}) for the Reaction of Piperidine with Anionic Phenyl Salicylate (PS^-) at a Constant $[CTABr]_T$ and Different [4-FBzNa].[a]

$[CTABr]_T$ /M	0.005			0.006			0.007			0.010			0.015		
10^2 [MX] M	$10^4 k_{obs}$ s^{-1}	RE_1[b]	RE_2[c]	$10^4 k_{obs}$ s^{-1}	RE_1[b]	RE_2[c]	$10^4 k_{obs}$ s^{-1}	RE_1[b]	RE[c]	$10^4 k_{obs}$ s^{-1}	RE_1[b]	RE_2[c]	$10^4 k_{obs}$ s^{-1}	RE_1[b]	RE_2[c]
0.0	29.9 ± 0.2[d]			29.1 ± 0.1[d]			28.5 ± 0.2[d]			26.6 ± 0.2[d]			25.2 ± 0.1[d]		
0.2	29.5 ± 0.2			29.1 ±0.1			28.8 ± 0.2			26.8 ± 0.1			25.5 ± 0.3		
0.5	32.3 ± 0.2	-26	3.1	31.3 ± 0.1	-23	4.1	29.6 ± 0.2			28.1 ±0.5			25.9 ± 0.2		
0.8	42.1 ± 0.4	-12	6.3	35.7 ± 0.2	-22	-2.8	36.2 ± 0.6	-13	6.6	29.5 ± 0.1	-20	6.5	26.2 ±0.2		
1.0	45.7 ±0.3	-12	2.5	41.3 ± 0.2	-14	0.9	38.7 ± 0.4	-13	3.2	32.7 ± 0.1	-15	7.2	27.1 ± 0.2	-16	6.4
1.5	55.9 ± 0.2	-8.9	-0.9	50.5 ± 0.1	-9.4	-0.8	45.9 ±0.6	-11	-6.4	37.1 ± 0.5	-15	0.4	29.9 ± 0.1	-15	1.1
2.0	66.1 ± 0.7	-5.6	-1.5	59.0 ± 0.8	-6.5	-1.7	52.5 ± 0.2	-9.5	-3.0	42.7 ± 0.2	-11	-1.1	32.9 ± 0.4	-14	-2.2
2.5	73.2 ± 0.1	-6.6	-4.8	67.5 ± 0.3	-3.6	-1.3	59.1 ± 0.3	-7.8	-4.1	48.4 ± 0.3	-7.9	-1.3	36.1 ± 0.2	-12	-4.0
3.0	84.2 ± 0.2	-1.7	-1.5	77.4 ± 0.1	1.0	1.6	65.7 ± 0.6	-6.0	-4.1	53.1 ± 0.7	-6.9	-2.8	40.3 ± 0.4	-7.3	-2.5
4.0	95.6 ± 0.8	-3.9	-5.5	90.1 ± 0.2	1.5	0.2	78.2 ± 0.2	-3.1	-3.5	62.9 ± 0.4	-3.9	-3.1	46.6 ± 0.3	-5.0	-4.0
5.0	111 ± 0.2	-0.3	-3.0	99.9 ±0.5	0.2	-1.9	89.1 ± 0.6	-1.6	-3.2	71.9 ± 0.8	-2.0	-3.1	53.5 ± 0.1	-1.8	-3.1
7.0	140 ± 0.2	6.3	3.5	122 ± 0.1	3.1	0.6	110 ± 0.2	2.1	-0.1	86.8 ± 0.7	-1.1	-3.9	65.5 ± 0.1	0.7	-2.8
10	162 ± 0.1	5.0	3.2	144 ± 1.0	2.7	0.3	135 ± 0.2	4.8	2.3	111 ± 0.5	4.4	1.1	87.1 ± 0.2	8.2	4.7
15	185 ± 0.9	2.8	2.0	168 ± 0.8	1.0	-0.4	163 ± 0.2	5.4	3.9	140 ± 0.2	6.9	4.7	108 ± 0.2	5.2	3.4
20	198 ± 0.8	0.4	0.5	188 ± 0.2	1.8	1.8	177 ± 0.1	2.4	2.1	153 ± 0.6	2.6	1.8	117 ± 0.2	-4.5	-.28
30	211 ± 0.2	-4.0	-2.5	203 ± 1.2	-2.8	-1.1	188 ± 0.3	-5.1	-3.5	168 ± 0.2	-4.7	-2.8			

$10^{-1}\delta_{app}{}^{av}/M^{-1}cm^{-1}$ [e] =	**688 ± 23**	**681 ± 19**	**687 ± 10**	**704 ± 15**	**703 ± 10**

[a] $[\text{phenyl salicylate}]_0$ = 0.2 mM, 35 °C, λ = 350 nm, $[\text{piperidine}]_T$ = 0.1 M, $[\ ]_T$ represents total concentration and the aqueous reaction mixture for each kinetic run contained 2 % v/v CH_3CN. The required amounts of 4-$FC_6H_4CO_2Na$ ([MX]) were generated into the reaction mixture by using the stock solution (w M) of 4-$FC_6H_4CO_2H$ prepared in (w + 0.05) M aqueous NaOH. The stock solution of NaOH was used to produce a fixed known concentration (0.03 M) of NaOH into the reaction mixture for each kinetic run. Thus, the maximum concentration of added NaOH was 0.06 M. [b] $RE_1 = 100\times(k_{obs} - k_{cald1})/k_{obs}$ where k_{cald1} values were calculated from **Eq. 4.5** with kinetic parameters (k_0, θ and $K^{X/S}$) listed in **Table 4.1**. [c] $RE_2 = 100\times(k_{obs} - k_{cald2})/k_{obs}$ where k_{cald2} values were calculated from **Eq. 4.5** with [MX] replaced by $[MX] - [MX]_0^{op}$ and $[MX]_0^{op}$ = 4.5, 4.7, 5.2, 7.3 and 9.8 mM at 5, 6, 7, 10 and 15 mM CTABr, respectively, as well as kinetic parameters listed in **Table 4.1**. [d] Error limits are standard deviations. [e] Mean value of δ_{app} ($= \delta_{app}{}^{av}$) obtained within [MX] range shown in the **Table 3.1** and the error limits are standard deviations.

Table III: Pseudo-First-Order Rate Constants (k_{obs}) for the Reaction of Piperidine with Anionic Phenyl Salicylate (PS^-) at a Constant $[CTABr]_T$ and Different [2-ClBzNa].[a]

$[CTABr]_T$ /M	**0.005**		**0.006**		**0.007**		**0.010**		**0.015**	
10^2 [MX] M	**$10^4 k_{obs}$ s^{-1}**	**RE_1 [b]**	**$10^4 k_{obs}$ s^{-1}**	**RE_1 [b]**	**$10^4 k_{obs}$ s^{-1}**	**RE_1 [b]**	**$10^4 k_{obs}$ s^{-1}**	**RE_1 [b]**	**$10^4 k_{obs}$ s^{-1}**	**RE_1 [b]**
0.0	27.6 ± 0.5[c]		27.3 ± 0.7[c]		26.8 ± 0.4[c]		25.3 ± 0.6[c]		24.6 ± 0.3[c]	
0.2	28.9 ± 0.6	-4.3	28.7 ± 0.4	-2.0	27.9 ± 0.3	-1.8	26.1 ± 0.5	-1.2	25.9 ± 0.2	2.5
0.5	31.5 ± 0.3	-7.4	30.7 ± 0.3	-4.8	29.2 ± 0.3	-5.3	26.7 ± 0.4	-5.0	26.0 ± 0.3	-0.8
1.0	38.5 ± 0.3	-3.1	34.8 ± 0.2	-5.8	32.8 ± 0.2	-5.2	29.6 ± 0.4	-3.7	26.7 ± 0.3	-4.0
2.0	46.8 ± 0.3	-7.7	42.7 ± 0.3	-6.3	39.7 ± 0.3	-4.9	33.7 ± 0.1	-6.2	29.1 ± 0.2	-6.0
3.0	55.7 ± 0.3	-7.5	49.8 ± 0.2	-6.9	45.2 ± 0.7	-6.7	38.2 ± 0.4	-6.4	32.9 ± 0.3	-2.8
5.0	72.1 ± 0.5	-5.6	63.1 ± 0.6	-6.0	56.8 ± 0.5	-5.7	46.5 ± 0.4	-6.5	37.0 ± 0.5	-6.7
7.0	84.3 ± 0.5	-6.1	78.1 ± 0.6	-0.5	67.3 ± 0.5	-4.5	56.5 ± 0.3	-1.9	42.7 ± 0.3	-4.9
10	103 ± 0.5	-1.9	88.4 ± 0.4	-5.1	79.7 ± 0.7	-4.7	69.1 ± 0.3	1.3	51.5 ± 0.3	-1.3
15	130 ± 0.7	4.0	115 ± 0.5	2.9	100 ± 0.8	-0.8	81.0 ± 0.5	-2.6	64.1 ± 0.5	-1.3
20	147 ± 0.4	5.7	129 ± 0.6	2.9	120 ± 0.7	4.9	97.3 ± 0.5	2.2	76.7 ± 1.2	1.4

30	166 ± 1.1	5.1	150 ± 0.8	4.4	142 ± 0.7	6.0	118 ± 1.1	3.7	89.6 ± 0.6	5.1
40	169 ± 1.3	-0.5	160 ± 1.1	2.2	150 ± 0.4	1.9	128 ± 1.3	0.5	98.8 ± 0.4	1.0
50	175 ± 0.7	-2.1	164 ± 0.6	-0.7	156 ± 0.2	-6.5	139 ± 0.9	1.0	112 ± 0.6	-2.6
60	178 ± 1.8	-3.4	164 ± 1.2	-4.5	157 ± 1.4	-4.7	141 ± 0.7	-2.9		
$10^{-1}\delta_{app}^{av}/M^{-1}cm^{-1}$[d] =	**697 ± 9**		**707 ± 14**		**707 ± 12**		**703 ± 14**		**716 ± 11**	

[a] $[phenyl\ salicylate]_0$ = 0.2 mM, 35 °C, λ = 350 nm, $[piperidine]_T$ = 0.1 M, $[\ ]_T$ represents total concentration and the aqueous reaction mixture for each kinetic run contained 2 % v/v CH_3CN. The required amounts of 2-$ClC_6H_4CO_2Na$ ([MX]) were generated into the reaction mixture by using the stock solution (w M) of 2-$ClC_6H_4CO_2H$ prepared in (w + 0.05) M aqueous NaOH. The stock solution of NaOH was used to produce a fixed known concentration (0.03 M) of NaOH into the reaction mixture for each kinetic run. Thus, the maximum concentration of added NaOH was 0.06 M. [b] $RE_1 = 100\times(k_{obs} - k_{cald1})/k_{obs}$ where k_{cald1} values were calculated from **Eq. 4.5** with kinetic parameters (k_0, θ and $K^{X/S}$) listed in **Table 4.1**. [c] Error limits are standard deviations. [d] Mean value of δ_{app} (= δ_{app}^{av}) obtained within [MX] range shown in the **Table 3.3** and the error limits are standard deviations.

Table IV: Pseudo-First-Order Rate Constants (k_{obs}) for the Reaction of Piperidine with Anionic Phenyl Salicylate (PS^-) at a Constant $[CTABr]_T$ and Different [3-ClBzNa].[a]

$[CTABr]_T$ /M	**0.005**			**0.006**			**0.007**			**0.010**			**0.015**		
10^2 [MX] M	**$10^4\ k_{obs}$ s^{-1}**	**RE_1[b]**	**RE_2[c]**	**$10^4\ k_{obs}$ s^{-1}**	**RE_1[b]**	**RE_2[c]**	**$10^4\ k_{obs}$ s^{-1}**	**RE_1[b]**	**RE_2[c]**	**$10^4\ k_{obs}$ s^{-1}**	**RE_1[b]**	**RE_2[c]**	**$10^4\ k_{obs}$ s^{-1}**	**RE_1[b]**	**RE_2[c]**
0	30.7 ± 0.3[d]			29.1 ± 0.2[d]			28.3 ± 0.2[d]			27.8 ± 0.7[d]			25 ± 0.3[d]		
0.1	28.4 ± 0.2			28.1 ± 0.2			27.4 ± 0.4			25.6 ± 0.6					
0.2	30.7 ± 0.2									26.0 ± 0.1					
0.3	32.6 ± 0.3			29.5 ± 0.0			27.4 ± 0.8			26.6 ± 0.1			25.3 ± 0.7		
0.4	38.1 ± 0.7									27.0 ± 0.9					
0.5	39.4 ± 0.9			29.6 ± 0.1			29.3 ± 0.3						24.8 ± 0.7		
0.6	44.6 ± 0.1														
0.7										29.4 ± 0.1			25.0 ± 0.6		

0.8	52.3 ± 0.3	-41	7.5							29.8 ± 0.7					
0.9										29.8 ± 0.6					
1.0	64.8 ± 0.7	-27	1.9	52.1 ± 0.3	-35	3.0	45.1 ± 0.2	-42	0.8	33.3 ± 0.6			25.4 ± 0.8		
1.2				60.8 ± 0.2	-27	-1.9	54.5 ± 0.4	-29	-1.0						
1.5	92.9 ± 0.8	-8.5	-0.8	78.9 ± 0.4	-9.2	2.6	69.5 ± 0.6	-13	1.3	47.5 ± 0.1	-40	2.7	30.9 ± 0.9	-54	3.2
1.6													33.7 ± 0.7	-45	3.0
1.8													38.9 ± 0.8	-33	2.3
2.0	118 ± 0.7	1.4	1.8	98.0 ± 0.3	-1.6	1.0	88.7 ± 0.6	-2.2	1.5	65.0 ± 0.4	-18	1.0	44.9 ± 0.5	-21	4.1
2.5	135 ± 0.7	4.1	1.4	110 ± 0.7	-1.1	-2.7	105 ± 1.0	3.4	2.4	79.8 ± 0.5	-7.5	0.7	53.2 ± 0.8	-14	-2.6
3.0	144 ± 0.5	2.4	-1.9	124 ± 0.5	2.1	-1.5	112 ± 0.8	0.8	-2.7	90.1 ± 0.7	-4.5	-1.9	61.3 ± 0.8	-9.1	-5.6
3.5													73.7 ± 0.1	1.5	-7.5
4.0	160 ± 0.9	0.8	-4.3	138 ± 0.9	-0.2	-5.6	132 ± 0.9	3.6	-1.8	108 ± 1.0	-0.7	-3.4	79.5 ± 1.0	1.7	-2.9
5.0	183 ± 1.1	5.5	0.9	161 ± 1.1	5.8	0.6	149 ± 0.9	5.8	0.2	123 ± 0.7	1.6	-3.1	93.7 ± 1.1	5.7	-2.2
6.0	193 ± 1.3	4.6	0.5							138 ± 0.9	4.7	-0.4			
7.0				183 ± 0.9	6.1	2.0	167 ± 1.3	3.9	-0.8				118 ± 0.9	10	1.0
8.0										161 ± 0.2	7.8	3.1			
10	221 ± 1.9	3.6	1.9	208 ± 2.1	7.8	5.4	188 ± 1.1	3.8	-0.9	175 ± 0.8	7.6	4.0	145 ± 0.7	12	4.6
15	230 ± 1.5	-0.9	-0.6	220 ± 1.6	1.5	1.3	205 ± 0.7	1.5	1.1	185 ± 0.8	0.3	-0.9	159 ± 0.9	2.4	-0.7
20	240 ± 1.1	-1.2	0.4	229 ± 1.8	-3.5	-2.2	213 ± 0.9	-0.7	0.6	197 ± 0.4	-1.0	-0.1	175 ± 1.5	0.0	0.9
25													179 ± 1.4	-6.1	-1.9
30	246 ± 1.3	-3.7	-0.6	225 ± 1.2	-5.4	-2.2	219 ± 1.2	-4.7	-1.2	206 ± 0.7	-5.1	-1.4			
$10^{-1}\delta_{app}{}^{av}/M^{-1}cm^{-1}$ [e] =		**714 ± 10**			**709 ± 13**			**717 ± 7**			**718 ± 22**			**723 ± 21**	

[a] [phenyl salicylate]$_0$ = 0.2 mM, 35 ^{o}C, λ = 350 nm, [piperidine]$_T$ = 0.1 M, [ ]$_T$ represents total concentration and the aqueous reaction mixture for each kinetic run contained 2 % v/v CH_3CN. The required amounts of 3-$ClC_6H_4CO_2Na$ ([MX]) were generated into the reaction mixture by using the stock solution (w M) of 3-$ClC_6H_4CO_2H$ prepared in (w + 0.05) M aqueous NaOH. The stock solution of NaOH was used to produce a fixed known concentration (0.03 M) of NaOH into the

reaction mixture for each kinetic run. Thus, the maximum concentration of added NaOH was 0.06 M. [b] $RE_1 = 100\times(k_{obs} - k_{cald1})/k_{obs}$ where k_{cald1} values were calculated from **Eq. 4.5** with kinetic parameters (k_0, θ and $K^{X/S}$) listed in **Table 4.1**. [c] $RE_2 = 100\times(k_{obs} - k_{cald2})/k_{obs}$ where k_{cald2} values were calculated from **Eq. 4.5** with [MX] replaced by $[MX] - [MX]_0^{op}$ and $[MX]_0^{op}$ = 6.0, 6.8, 7.1, 10.8 and 13.3 mM at 5, 6, 7, 10 and 15 mM CTABr, respectively, as well as kinetic parameters listed in **Table 4.1**. [d] Error limits are standard deviations. [e] Mean value of δ_{app} ($= \delta_{app}^{av}$) obtained within [MX] range shown in the **Table 3.3** and the error limits are standard deviations.

Table V: Pseudo-First-Order Rate Constants (k_{obs}) for the Reaction of Piperidine with Anionic Phenyl Salicylate (PS^-) at a Constant $[CTABr]_T$ and Different [4-ClBzNa].[a]

$[CTABr]_T$ /M	**0.005**			**0.006**			**0.007**			**0.010**			**0.015**		
10^2 [MX] M	**$10^4 k_{obs}$ s^{-1}**	**RE_1[b]**	**RE_2[c]**	**$10^4 k_{obs}$ s^{-1}**	**RE_1[b]**	**RE_2[c]**	**$10^4 k_{obs}$ s^{-1}**	**RE_1[b]**	**RE_2[c]**	**$10^4 k_{obs}$ s^{-1}**	**RE_1[b]**	**RE_2[c]**	**$10^4 k_{obs}$ s^{-1}**	**RE_1[b]**	**RE_2[c]**
0	29.1 ± 0.6[d]			27.3 ± 0.7[d]			26.6 ± 0.2[d]			25.3 ± 0.4[d]			24.9 ± 0.3[d]		
0.1	28.4 ± 0.4			25.6 ± 0.5			26.2 ± 0.5			23.8 ± 0.8			23.3 ± 0.5		
0.2	28.3 ± 0.4			25.8 ± 0.3			23.7 ± 0.8			23.7 ± 0.7			22.6 ± 0.4		
0.3				26.1 ± 0.3			25.1 ± 0.3			24.4 ± 0.9			22.6 ± 0.6		
0.4	31.8 ± 0.5			30.1 ± 0.3			26.3 ± 0.9						22.8 ± 0.8		
0.5	33.5 ± 0.7			31.1 ± 0.4						26.2 ± 0.8			23.1 ± 0.6		
0.6				32.3 ± 0.5											
0.7				35.6 ± 0.5	-58	6.3	30.0 ± 0.2	-72	1.4						
0.8				41.7 ± 0.2	-44	0.9	36.7 ± 0.7	-49	0.4				23.4 ± 0.9		
0.9				47.2 ± 0.3	-34	-3.0	43.6 ± 0.6	-32	1.3				24.2 ± 0.8		
1.0	65.9 ± 0.7	-20	3.1	53.5 ± 0.1	-25	-3.4	47.2 ± 0.8	-28	-3.8	30.3 ± 0.9	-65	5.5	25.0 ± 0.9		
1.2													23.3 ± 1.0		
1.4													25 ± 0.7		
1.5	85.4 ± 0.4	-13	-6.3	79.1 ± 0.9	-2.8	-3.6	72.6 ± 0.2	-1.7	-1.6	49.6 ± 0.3	-22	4.9	27.7 ± 0.8	-85	7.4
2.0	107 ± 1.4	-3.1	-2.7	102 ± 1.5	8.0	1.1	91.7 ± 0.8	7.1	0.7	60.5 ± 0.9	-16	-3.3	43.4 ± 1.1	-35	1.9

2.5	129 ± 0.4	5.7	3.7	118 ± 1.8	1.1	2.6	105 ± 0.7	9.4	0.4	72.5 ± 1.0	-8.3	-3.9	54.9 ± 1.0	-20	-3.3
3.0	135 ± 2.0	2.8	-0.2	126 ± 2.3	9.7	0.1	115 ± 0.7	9.7	-0.2				66.2 ± 0.9	-9.7	-3.8
4.0	152 ± 2.3	3.7	0.4							99.1 ± 0.9	-1.3	-4.8	84.1 ± 0.6	-1.0	-4.7
5.0	166 ± 1.7	5.0	2.1	153 ± 4.0	7.8	0.3	144 ± 0.8	9.6	1.44	113 ± 1.2	0.6	-4.0	104 ± 1.2	7.7	1.1
6.0	168 ± 3.2	0.8	-1.5							129 ± 1.5	5.0	0.6	115 ± 1.3	8.0	0.4
7.0										141 ± 1.9	6.7	2.8			
8.0										149 ± 1.2	6.4	3.1	135 ± 1.5	9.0	2.2
10	190 ± 2.7	0.6	0.6	176 ± 1.9	-0.2	-1.4	165 ± 0.9	-0.4	-2.2	163 ± 1.6	6.3	4.5	148 ± 1.7	7.4	2.5
15													165 ± 1.9	0.8	0.9
20	203 ± 2.5	-3.9	-0.9	195 ± 2.3	-4.5	0.5	187 ± 1.4	-4.0	0.9	177 ± 1.8	-8.1	-3.9	170 ± 2.1	-7.3	-2.7
$10^{-1}\delta_{app}{}^{av}/M^{-1}cm^{-1}$ [e] =		**691 ± 24**			**702 ± 17**			**690 ± 31**			**719 ± 18**			**721 ± 33**	

[a] $[phenyl\ salicylate]_0$ = 0.2 mM, 35 °C, λ = 350 nm, $[piperidine]_T$ = 0.1 M, $[\ ]_T$ represents total concentration and the aqueous reaction mixture for each kinetic run contained 2 % v/v CH_3CN. The required amounts of 4-$ClC_6H_4CO_2Na$ ([MX]) were generated into the reaction mixture by using the stock solution (w M) of 4-$ClC_6H_4CO_2H$ prepared in (w + 0.05) M aqueous NaOH. The stock solution of NaOH was used to produce a fixed known concentration (0.03 M) of NaOH into the reaction mixture for each kinetic run. Thus, the maximum concentration of added NaOH was 0.065 M. [b] $RE_1 = 100\times(k_{obs} - k_{cald1})/k_{obs}$ where k_{cald1} values were calculated from **Eq. 4.5** with kinetic parameters (k_0, θ and $K^{X/S}$) listed in **Table 4.1**. [c] $RE_2 = 100\times(k_{obs} - k_{cald2})/k_{obs}$ where k_{cald2} values were calculated from **Eq. 4.5** with [MX] replaced by $[MX] - [MX]_0^{op}$ and $[MX]_0^{op}$ = 5.6, 6.3, 6.6, 9.2 and 14.8 mM at 5, 6, 7, 10 and 15 mM CTABr, respectively, as well as kinetic parameters listed in **Table 4.1**. [d] Error limits are standard deviations. [e] Mean value of δ_{app} ($= \delta_{app}{}^{av}$) obtained within [MX] range shown in the **Table 3.3** and the error limits are standard deviations.

Table VI: Pseudo-First-Order Rate Constants (k_{obs}) for the Reaction of Piperidine with Anionic Phenyl Salicylate (PS^-) at a Constant $[CTABr]_T$ and Different [2-BrBzNa].[a]

$[CTABr]_T$ /M	**0.005**			**0.006**			**0.007**			**0.010**			**0.015**		
10^2 [MX] M	**$10^4\ k_{obs}$ s^{-1}**	**RE_1 [b]**	**RE_2 [c]**	**$10^4\ k_{obs}$ s^{-1}**	**RE_1 [b]**	**RE_2 [c]**	**$10^4\ k_{obs}$ s^{-1}**	**RE_1 [b]**	**RE_2 [c]**	**$10^4\ k_{obs}$ s^{-1}**	**RE_1 [b]**	**RE_2 [c]**	**$10^4\ k_{obs}$ s^{-1}**	**RE_1 [b]**	**RE_2 [c]**
0	29.3 ± 0.2[d]			28.8 ± 0.3[d]			27.7 ± 0.4[d]			26.2 ± 0.3[d]			25.8 ± 0.4[d]		

0.2	30.1 ± 0.3			27.7 ±0.6			27.8 ± 0.5			26.4 ± 0.2			24.2 ± 0.3		
0.5	31.9 ± 0.4			30.2 ± 0.2			27.9 ± 0.2			26.5 ± 0.6			25.2 ± 0.4		
0.8	34.2 ± 0.1	-16	6.2	32.5 ± 0.3	-16	5.3	30.8 ± 0.2	-16	4.9	27.7 ± 0.3			25.4 ± 0.5		
1.0	36.3 ± 0.2	-16	3.0	34.1 ± 0.4	-17	1.7	33.3 ± 0.2	-13	4.9	29.9 ± 0.7	-12	7.8	27.8 ± 0.4	-11	5.9
1.5	42.7 ± 0.3	-12	0.3	40.9 ± 0.1	-10	2.2	38.2 ± 0.1	-10	2.1	32.8 ± 0.6	-12	2.8	29.9 ± 0.6	-12	2.3
2.0	49.7 ± 0.4	-7.0	0.7	45.3 ± 0.3	-10	-1.5	43.0 ± 0.2	-7.8	0.7	35.8 ± 0.5	-12	-0.5	31.9 ± 0.4	-12	-0.8
2.5	55.1 ± 0.2	-5.7	-0.9	51.1 ± 0.8	-6.2	-0.8	47.2 ± 0.8	-6.9	-1.0	39.0 ± 0.8	-11	-2.3	34.4 ± 0.1	-11	-1.8
3.0	60.4 ± 0.5	-4.3	-1.6	56.0 ± 0.5	-4.6	-1.2	51.7 ± 0.5	-5.1	-1.3	42.8 ± 0.8	-8.1	-1.9	37.1 ± 0.5	-8.8	-1.8
4.0	69.8 ± 0.1	-2.8	-2.7	64.4 ± 0.1	-3.1	-2.5	58.3 ± 0.9	-5.7	-4.5	49.2 ± 0.2	-5.8	-2.9	43.2 ± 0.7	-3.7	0.3
5.0	77.1 ± 0.2	-3.2	-4.5	72.3 ± 0.5	-1.7	-2.6	65.7 ± 0.2	-3.8	-4.3	55.5 ± 0.8	-3.7	-2.7	47.3 ± 0.5	-3.6	-1.6
7.0	93.5 ± 0.6	0.6	-1.9	86.8 ± 0.6	1.1	-1.2	80.5 ± 0.7	0.8	-1.2	67.7 ± 0.1	-0.3	-1.0	55.9 ± 0.7	-1.9	-2.2
10	113 ± 0.6	3.7	0.8	102 ± 0.7	1.3	-1.8	95.5 ± 0.9	1.4	-1.2	80.6 ± 0.7	0.3	-2.4	68.5 ± 0.9	1.2	-0.8
15	133 ± 0.6	3.8	1.8	124 ± 0.8	4.1	1.6	116 ± 0.3	3.2	0.8	100 ± 0.2	2.2	-0.2	84.4 ± 0.2	1.6	-1.0
20	149 ± 0.6	5.1	4.0	137 ± 0.5	3.6	2.4	132 ± 1.1	4.9	3.3	116 ± 0.3	3.9	2.1	100 ± 0.8	4.1	2.1
30	159 ± 1.1	-0.1	0.0	155 ± 1.2	3.5	3.4	149 ± 0.7	3.5	3.4	138 ± 0.1	4.6	4.1	119 ± 0.9	2.4	1.5
50	171 ± 2.6	-4.0	-2.3	160 ± 0.9	-5.4	-3.7	156 ± 1.7	-5.2	-3.7	150 ± 0.2	-4.2	-2.9	140 ± 0.3	-2.3	-1.1
$10^{-1}\delta_{app}^{av}/M^{-1}cm^{-1}$ [e] =		**725 ± 19**			**715 ± 30**			**729 ± 14**			**715 ± 6**			**717 ± 13**	

[a] $[phenyl\ salicylate]_0$ = 0.2 mM, 35 °C, λ = 350 nm, $[piperidine]_T$ = 0.1 M, $[\ ]_T$ represents total concentration and the aqueous reaction mixture for each kinetic run contained 2 % v/v CH_3CN. The required amounts of 2-$BrC_6H_4CO_2Na$ ([MX]) were generated into the reaction mixture by using the stock solution (w M) of 2-$BrC_6H_4CO_2H$ prepared in (w + 0.05) M aqueous NaOH. The stock solution of NaOH was used to produce a fixed known concentration (0.03 M) of NaOH into the reaction mixture for each kinetic run. Thus, the maximum concentration of added NaOH was 0.055 M. [b] $RE_1 = 100\times(k_{obs} - k_{cald1})/k_{obs}$ where k_{cald1} values were calculated from **Eq. 4.5** with kinetic parameters (k_0, θ and $K^{X/S}$) listed in **Table 4.1**. [c] $RE_2 = 100\times(k_{obs} - k_{cald2})/k_{obs}$ where k_{cald2} values were calculated from **Eq. 4.5** with [MX] replaced by $[MX] - [MX]_0^{op}$ and $[MX]_0^{op}$ = 6.3, 6.6, 6.7, 8.8 and 9.4 mM at 5, 6, 7, 10 and 15 mM CTABr, respectively, as well as kinetic parameters listed in **Table 4.1**. [d] Error limits are standard deviations. [e] Mean value of δ_{app} (= δ_{app}^{av}) obtained within [MX] range shown in the **Table 3.4** and the error limits are standard deviations.

Table VII: Pseudo-First-Order Rate Constants (k_{obs}) for the Reaction of Piperidine with Anionic Phenyl Salicylate (PS^-) at a Constant $[CTABr]_T$ and Different [3-BrBzNa].[a]

$[CTABr]_T$ /M	0.005			0.006			0.007			0.010			0.015		
10^2 [MX] M	$10^4 k_{obs}$ s^{-1}	RE_1[b]	RE_2[c]	$10^4 k_{obs}$ s^{-1}	RE_1[b]	RE_2[c]	$10^4 k_{obs}$ s^{-1}	RE_1[b]	RE_2[c]	$10^4 k_{obs}$ s^{-1}	RE_1[b]	RE_2[c]	$10^4 k_{obs}$ s^{-1}	RE_1[b]	RE_2[c]
0.0	29.8 ± 0.4[d]			29.2 ± 0.2[d]			28.5 ± 0.2[d]			27.5 ± 0.2[d]			25.2 ± 0.4[d]		
0.2	30.2 ± 0.5			29.3 ± 0.3			27.7 ± 0.4			27.2 ± 0.3			26.5 ± 0.2		
0.5	42.7 ± 0.2	-72	-1.5	40.2 ± 0.3	-76	-0.1	28.2 ± 0.3			38.5 ± 0.3			27.2 ± 0.3		
0.8							51.8 ± 0.9	-51	1.0						
1.0	96.2 ± 1.1	-9.7	1.1	89.7 ± 1.0	-14	1.5	70.7 ± 0.8	-25	3.7	45.3 ± 0.2	-51	-5.4	26.4 ± 0.2		
1.5	130 ± 2.2	-0.3	0.1	122 ± 2.2	-3.3	0.3	95.6 ± 0.1	14	-5.8	77.9 ± 1.3	-8.9	5.5	30.3 ± 0.4		
2.0	159 ± 1.8	5.5	2.6	147 ± 2.3	1.1	0.7	124 ± 0.8	-2.1	-1.2	93.9 ± 1.9	-5.3	-0.4	45.4 ± 0.8	-50	8.6
2.5				162 ± 0.3	0.5	-1.6	142 ± 0.2	0.5	-1.5				60.5 ± 0.7	-27	2.9
3.0	181 ± 1.6	0.7	-4.0	179 ± 1.3	2.6	-0.2	160 ± 0.7	4.0	0.6	122 ± 3.1	-0.2	-2.7	72.1 ± 0.2	-18	-2.2
3.5				191 ± 0.9	2.9	-0.1	172 ± 0.9	4.5	0.6				83.9 ± 0.9	-11	-3.4
4.0				201 ± 0.7	2.9	0.0	182 ± 0.3	4.6	0.5				95.2 ± 0.2	-5.3	-3.1
5.0	227 ± 1.3	4.8	1.1	216 ± 0.9	2.5	-0.1	201 ± 0.5	6.0	2.2	164 ± 1.6	5.1	0.1	114 ± 0.7	0.4	-3.0
6.0				227 ± 0.6	1.9	-0.2	216 ± 0.1	6.9	3.7				131 ± 0.4	4.3	-1.5
7.0	250 ± 0.5	4.9	2.4				223 ± 0.3	1.8	-0.5	187 ± 3.8	4.5	-0.1		8.6	1.6
8.0				244 ± 0.8	1.5	0.3	227 ± 0.7	-2.1	-3.4				159 ± 0.9	9.1	2.5
10	254 ± 4.1	-1.5	-2.5	256 ± 0.8	1.4	1.0	230 ± 0.9	-3.1	-2.4	209 ± 1.4	3.4	0.3	178 ± 0.8		
15													193 ± 0.4	6.0	2.0
20	246 ± 0.8	-3.7	-2.1	243 ± 0.7	-3.7	-1.8	232 ± 0.2	-1.2	0.7	218 ± 0.7	1.6	2.1	196 ± 0.4	2.6	1.3
30	232 ± 1.4	-1.1	1.6	229 ± 0.2	-0.8	1.9	212 ± 0.9	-2.7	0.6	195 ± 0.4	-4.1	-1.7	181 ± 0.4	-5.2	-2.4
50	171 ± 0.7	-1.0	2.6	162 ± 0.5	-5.1	-1.3	158 ± 1.0	-2.3	2.3	146 ± 0.5	-5.3	-1.0	138 ± 0.7	-10	-2.6

$10^{-1}\delta_{app}{}^{av}/M^{-1}cm^{-1}$ [e] =	**697 ± 36**	**701 ± 22**	**688 ± 18**	**695 ± 32**	**698 ± 17**

[a] $[phenyl\ salicylate]_0$ = 0.2 mM, 35 °C, λ = 350 nm, $[piperidine]_T$ = 0.1 M, $[\ ]_T$ represents total concentration and the aqueous reaction mixture for each kinetic run contained 2 % v/v CH_3CN. The required amounts of 3-$BrC_6H_4CO_2Na$ ([MX]) were generated into the reaction mixture by using the stock solution (w M) of 3-$BrC_6H_4CO_2H$ prepared in (w + 0.05) M aqueous NaOH. The stock solution of NaOH was used to produce a fixed known concentration (0.03 M) of NaOH into the reaction mixture for each kinetic run. Thus, the maximum concentration of added NaOH was 0.065 M. [b] $RE_1 = 100\times(k_{obs} - k_{cald1})/k_{obs}$ where k_{cald1} values were calculated from **Eq. 4.5** with kinetic parameters (k_0, $F_{X/S}$ and $K^{X/S}$) listed in **Table 4.2**. [c] $RE_2 = 100\times(k_{obs} - k_{cald2})/k_{obs}$ where k_{cald2} values were calculated from **Eq. 4.5** with [MX] replaced by $[MX] - [MX]_0{}^{op}$ and $[MX]_0{}^{op}$ = 4.0, 4.1, 5.7, 6.8 and 15.9 mM at 5, 6, 7, 10 and 15 mM CTABr, respectively, as well as kinetic parameters listed in **Table 4.2**. [d] Error limits are standard deviations. [e] Mean value of δ_{app} ($= \delta_{app}{}^{av}$) obtained within [MX] range shown in the **Table 3.4** and the error limits are standard deviations.

Table VIII: Pseudo-First-Order Rate Constants (k_{obs}) for the Reaction of Piperidine with Anionic Phenyl Salicylate (PS^-) at a Constant $[CTABr]_T$ and Different [4-BrBzNa].[a]

$[CTABr]_T$ /M	**0.005**			**0.006**			**0.007**			**0.010**			**0.015**		
10^2 [MX] M	**$10^4\ k_{obs}$ s^{-1}**	**RE_1[b]**	**RE_2[c]**	**$10^4\ k_{obs}$ s^{-1}**	**RE_1[b]**	**RE_2[c]**	**$10^4\ k_{obs}$ s^{-1}**	**RE_1[b]**	**RE_2[c]**	**$10^4\ k_{obs}$ s^{-1}**	**RE_1[b]**	**RE_2[c]**	**$10^4\ k_{obs}$ s^{-1}**	**RE_1[b]**	**RE_2[c]**
0	29.4 ± 0.2[d]			29.3 ± 0.2[d]			28.9 ± 0.2[d]			27.4 ± 0.2[d]			26.6 ± 0.2[d]		
0.2	30.0 ± 0.2			28.5 ± 0.2			27.9 ± 0.3			26.5 ± 0.3			27.5 ± 0.3		
0.5	43.6 ± 0.4	-65	-6.1	31.8 ± 0.2	-98	-4.8	30.2 ± 0.2			26.6 ± 0.2			27.9 ± 0.2		
0.8	74.8 ± 0.6	-23	-2.3	59.2 ± 0.2	-35	-1.9	50.2 ± 0.1	-47	-1.9	26.8 ± 0.2			28.3 ± 0.1		
1.0	96.0 ± 2.7	-8.0	2.9	79.7 ± 1.0	-13	5.2	67 ± 0.3	-24	2.3	35.5 ± 0.7			28.4 ± 0.2		
1.5	129 ± 0.7	0.3	2.2	107 ± 2.4	-4.4	0.4	94.5 ± 0.6	-9.7	-0.8	59.2 ± 0.5	-43	2.1	32.5 ± 0.7	-80	11
2.0	159 ± 0.7	6.5	5.2	130 ± 0.6	-0.0	-0.2	119 ± 0.3	-1.8	0.4	82.7 ± 1.0	-21	-1.1	47.5 ± 0.3	-43	2.8
2.5	171 ± 0.8	3.4	0.8	146 ± 0.7	0.3	-2.1	135 ± 0.2	-0.9	-1.7	103 ± 2.1	-9.7	-1.6	61.6 ± 0.9	-24	0.1
3.0	181 ± 0.8	1.1	-2.1	160 ± 0.8	0.7	-2.7	150 ± 0.7	0.5	-1.8	122 ± 0.7	-2.4	-0.1	72.2 ± 0.2	-17	-4.1
3.5	193 ± 0.9	1.2	-2.1	178 ± 0.9	4.3	0.6	165 ± 0.8	2.6	-0.4	134 ± 0.5	-1.3	-2.2	85.2 ± 0.4	-8.7	-2.6
4.0	206 ± 0.6	2.6	-0.6	190 ± 0.2	5.1	1.3	179 ± 0.1	4.6	1.3	150 ±0.8	3.0	0.2	94.9 ± 0.5	-5.4	-3.8

5.0	218 ± 1.2	0.5	-2.3	205 ± 0.9	3.8	0.4	200 ± 0.1	6.0	2.9	175 ± 0.8	7.1	2.6	115 ± 0.3	1.2	-2.2
6.0	237 ± 1.4	3.1	0.9	220 ± 0.8	4.3	1.4				191 ± 0.4	7.3	2.3	133 ± 0.4	5.3	-0.4
7.0							221 ± 0.7	3.4	1.1				148 ± 0.2	7.4	0.6
8.0	251 ± 1.2	1.1	-0.2	235 ± 0.7	1.9	-1.3				210 ± 0.9	4.7	-1.9			
10	257 ± 0.7	-1.6	-2.1	243 ± 1.1	-0.8	-1.7	242 ± 0.2	1.4	0.6	220 ± 0.4	1.0	-2.9	180 ± 0.6	8.3	1.3
15	258 ± 0.9	-1.2	-0.3				242 ± 0.3	-1.3	-2.6	231 ± 0.5	0.3	-1.1	200 ± 0.9	7.1	2.6
20	255 ± 1.5	2.8	-4.5	241 ± 2.0	1.1	3.1	241 ± 0.6	1.8	4.4	230 ± 0.9	1.5	2.0	202 ± 0.9	5.6	3.5
30	231 ± 1.2	-3.5	-0.8	219 ± 0.4	-6.1	-2.6	223 ± 0.5	-4.2	0.1	220 ± 1.0	-3.4	-0.3	192 ± 0.3	-5.2	-3.4
50	186 ± 1.1	-3.9	-0.3	181 ± 0.8	-3.1	0.0	184 ± 0.3	-3.7	2.0	181 ± 1.1	-5.3	0.2	164 ± 0.9	-9.3	-2.6
$10^{-1}\delta_{app}^{av}/M^{-1}cm^{-1}$ [e] =	**680 ± 20**			**680 ± 20**			**696 ± 19**			**691 ± 15**			**685 ± 18**		

[a] $[phenyl\ salicylate]_0$ = 0.2 mM, 35 °C, λ = 350 nm, $[piperidine]_T$ = 0.1 M, $[\ ]_T$ represents total concentration and the aqueous reaction mixture for each kinetic run contained 2 % v/v CH_3CN. The required amounts of 4-$BrC_6H_4CO_2Na$ ([MX]) were generated into the reaction mixture by using the stock solution (w M) of 4-$BrC_6H_4CO_2H$ prepared in (w + 0.05) M aqueous NaOH. The stock solution of NaOH was used to produce a fixed known concentration (0.03 M) of NaOH into the reaction mixture for each kinetic run. Thus, the maximum concentration of added NaOH was 0.055 M. [b] $RE_1 = 100\times(k_{obs} - k_{cald1})/k_{obs}$ where k_{cald1} values were calculated from **Eq. 4.5** with kinetic parameters (k_0, $F_{X/S}$ and $K^{X/S}$) listed in **Table 4.2**. [c] $RE_2 = 100\times(k_{obs} - k_{cald2})/k_{obs}$ where k_{cald2} values were calculated from **Eq. 4.5** with [MX] replaced by $[MX] - [MX]_0^{op}$ and $[MX]_0^{op}$ = 3.6, 4.6, 5.3, 10.2 and 14.4 mM at 5, 6, 7, 10 and 15 mM CTABr, respectively, as well as kinetic parameters listed in **Table 4.2**. [d] Error limits are standard deviations. [e] Mean value of δ_{app} (= δ_{app}^{av}) obtained within [MX] range shown in the **Table 3.4** and the error limits are standard deviations.

Table IX: Pseudo-First-Order Rate Constants (k_{obs}) for the Reaction of Piperidine with Anionic Phenyl Salicylate (PS^-) at a Constant $[CTABr]_T$ and Different [2-IBzNa].[a]

$[CTABr]_T$ /M	**0.005**			**0.006**			**0.007**			**0.010**			**0.015**		
10^2 [MX] M	**$10^4\ k_{obs}$ s^{-1}**	**RE_1[b]**	**RE_2[c]**	**$10^4\ k_{obs}$ s^{-1}**	**RE_1[b]**	**RE_2[c]**	**$10^4\ k_{obs}$ s^{-1}**	**RE_1[b]**	**RE_2[c]**	**$10^4\ k_{obs}$ s^{-1}**	**RE_1[b]**	**RE_2[c]**	**$10^4\ k_{obs}$ s^{-1}**	**RE_1[b]**	**RE_2[c]**
0.0	29.3 ± 0.4[d]			28.8 ± 0.5[d]			27.9 ± 0.5[d]			27.1 ± 0.2[d]			26.2 ± 0.5[d]		
0.2	28.7 ± 0.5			28.6 ± 0.3			27.2 ± 0.4			27.1 ± 0.2			26.3 ± 0.3		

0.5	31.5 ±0.4	-21	2.9	30.3 ± 0.7			27.5 ± 0.4			27.6 ± 0.2			26.0 ± 0.7		
0.7	34.0 ± 0.4	-22	-2.4	32.0 ± 0.5	-24	1.5	29.9 ±0.5			27.7 ± 0.3			25.9 ± 0.8		
1.0	40.0 ± 0.5	-16	-2.2	39.8 ± 0.6	-11	6.6	34.2 ± 0.6	-20	7.5	29.1 ± 0.3	-24	5.7	26.2 ± 0.5		
1.5	51.4 ± 0.3	-5.5	2.3	45.4 ± 0.3	-13	-1.3	40.7 ± 0.8	-15	2.6	34.0 ± 0.1	-18	2.3	27.1 ±0.6	-21	0.9
2.0	59.5 ± 0.7	-3.2	1.2	53.2 ± 0.8	-8.8	-1.7	45.8 ± 0.7	-15	-2.8	39.0 ±0.3	-13	0.9	30.9 ± 0.6	-13	2.6
3.0	73.4 ± 0.7	-1.5	-0.8	66.7 ± 0.7	-5.1	-3.0	58.6 ± 0.7	-7.9	-3.2	47.0 ± 0.5	-10	-3.6	36.2 ± 0.7	-8.5	-0.1
5.0	96.2 ± 0.9	-2.0	-2.1	90.3 ± 0.8	-0.7	-2.3	79.8 ±0.5	-2.4	-3.4	62.5 ± 0.5	-5.4	-5.4	45.5 ± 0.8	-4.7	-4.2
7.0	117 ± 0.9	2.6	-0.1	110 ± 0.3	1.7	-1.2	99.8 ± 1.1	2.6	-0.1	78.9 ± 0.5	0.9	-1.4	56.5 ± 0.9	1.3	-1.4
10	139 ± 1.1	3.2	0.8	133 ± 1.2	3.1	0.8	120 ± 1.0	3.0	-0.4	98.7 ± 0.6	4.7	1.5	71.5 ± 0.9	5.7	1.9
15	162 ± 0.9	1.7	0.7	159 ± 1.3	2.9	1.4	147 ± 0.9	4.3	2.4	121 ± 1.0	4.6	2.0	88.9 ± 0.10	3.5	1.5
20	177 ± 2.1	0.3	0.3	178 ± 1.4	2.9	2.8	163 ± 1.0	2.7	2.2	136 ± 1.5	2.6	1.5	100 ± 0.12	-2.8	-1.1
30	195 ± 1.6	-2.1	-0.6	190 ± 1.1	-4.0	-2.6	176 ± 1.2	-4.1	-2.3	152 ± 1.3	-3/6	-1.7			
$10^{-1}\delta_{app}^{av}/M^{-1}cm^{-1}$ [e] =		**689 ± 14**			**683 ± 20**			**687 ± 11**			**681 ± 15**			**685 ± 9**	

[a] $[phenyl\ salicylate]_0$ = 0.2 mM, 35 °C, λ = 350 nm, $[piperidine]_T$ = 0.1 M, $[\ ]_T$ represents total concentration and the aqueous reaction mixture for each kinetic run contained 2 % v/v CH_3CN. The required amounts of 2-$IC_6H_4CO_2Na$ ([MX]) were generated into the reaction mixture by using the stock solution (w M) of 2-$IC_6H_4CO_2H$ prepared in (w + 0.05) M aqueous NaOH. The stock solution of NaOH was used to produce a fixed known concentration (0.03 M) of NaOH into the reaction mixture for each kinetic run. Thus, the maximum concentration of added NaOH was 0.06 M. [b] $RE_1 = 100\times(k_{obs} - k_{cald1})/k_{obs}$ where k_{cald1} values were calculated from **Eq. 4.5** with kinetic parameters (k_0, θ and $K^{X/S}$) listed in **Table 4.1**. [c] $RE_2 = 100\times(k_{obs} - k_{cald2})/k_{obs}$ where k_{cald2} values were calculated from **Eq. 4.5** with [MX] replaced by $[MX] - [MX]_0^{op}$ and $[MX]_0^{op}$ = 4.5, 5.6, 7.8, 9.7 and 14.0 mM at 5, 6, 7, 10 and 15 mM CTABr, respectively, as well as kinetic parameters listed in **Table 4.1**. [d] Error limits are standard deviations. [e] Mean value of δ_{app} (= δ_{app}^{av}) obtained within [MX] range shown in the **Table 3.5** and the error limits are standard deviations.

Table X: Pseudo-First-Order Rate Constants (k_{obs}) for the Reaction of Piperidine with Anionic Phenyl Salicylate (PS^-) at a Constant $[CTABr]_T$ and Different [4-IBzNa].[a]

$[CTABr]_T$ /M	**0.005**			**0.006**			**0.007**			**0.010**		
10^2 [MX] M	**$10^4\ k_{obs}$ s^{-1}**	**RE_1[b]**	**RE_2[c]**	**$10^4\ k_{obs}$ s^{-1}**	**RE_1[b]**	**RE_2[c]**	**$10^4\ k_{obs}$ s^{-1}**	**RE_1[b]**	**RE_2[c]**	**$10^4\ k_{obs}$ s^{-1}**	**RE_1[b]**	**RE_2[c]**

0	30.9 ± 0.2[d]			29.3 ± 0.2[d]			27.2 ± 0.5[d]			26.2 ± 0.9[d]		
0.2	28.4 ± 0.3			28.6 ± 0.4			26.0 ± 0.4			25.9 ± 0.3		
0.5	51.2 ± 0.3	-81	6.7	35.2 ± 0.4	-139	1.8	27.0 ± 0.3			25.4 ± 0.3		
0.7	87.5 ± 0.7	-27	-4.0	76.4 ± 0.5	-32	-1.2	58.9 ± 0.5	-54	7.1	25.4 ± 0.3		
1.0	131 ± 0.8	-21	-1.7	124 ± 0.9	1.6	3.5	93.5 ± 0.7	-18	-2.1	37.6 ± 0.4	-100	9.9
1.5	175 ± 2.2	6.9	0.3	151 ± 2.1	0.7	-6.9	127 ± 0.9	-7.8	-9.3	76.7 ± 0.7	-23	-7.6
2.0	203 ± 3.0	9.1	2.1	185 ± 5.5	7.4	-0.7	162 ± 1.5	2.6	-2.7	110 ± 1.3	-1.1	-3.7
2.5	215 ± 2.8	6.3	0.1	211 ± 2.9	1.1	3.9	187 ± 9.4	6.5	0.9	135 ± 2.1	6.7	-0.9
3.0	226 ± 0.9	4.9	-0.1	221 ± 4.1	8.6	2.9	214 ± 9.9	12	6.9			
4.0	240 ± 0.7	2.1	-0.5	229 ± 1.3	2.7	-0.5	225 ± 0.9	6.5	3.0	183 ± 9.2	12	4.3
5.0	251 ± 1.1	0.7	0.1	234 ± 0.7	-1.7	-2.6	230 ± 0.7	1.6	-0.2	197 ±8.3	9.2	3.5
7.0	265 ± 1.1	-1.3	1.1	253 ± 2.1	-2.1	0.4	243 ± 0.7	-2.2	-1.0	208 ± 0.8	0.8	-0.2
10	267 ± 2.0	-6.8	1.4	261 ± 1.5	-6.0	-0.1	251 ± 1.3	-6.9	-2.6	216 ± 1.8	-8.4	-3.4
$10^{-1}\delta_{app}^{av}/M^{-1}cm^{-1}$ [e] =	**693 ± 23**			**678 ± 28**			**684 ± 35**			**691 ± 37**		

[a] [phenyl salicylate]$_0$ = 0.2 mM, 35 ^oC, λ = 350 nm, [piperidine]$_T$ = 0.1 M, [ ]$_T$ represents total concentration and the aqueous reaction mixture for each kinetic run contained 2 % v/v CH_3CN. The required amounts of 4-$IC_6H_4CO_2Na$ ([MX]) were generated into the reaction mixture by using the stock solution (w M) of 4-$IC_6H_4CO_2H$ prepared in (w + 0.05) M aqueous NaOH. The stock solution of NaOH was used to produce a fixed known concentration (0.03 M) of NaOH into the reaction mixture for each kinetic run. Thus, the maximum concentration of added NaOH was 0.04 M. [b] $RE_1 = 100\times(k_{obs} - k_{cald1})/k_{obs}$ where k_{cald1} values were calculated from **Eq. 4.5** with kinetic parameters (k_0, θ and $K^{X/S}$) listed in **Table 4.1**. [c] $RE_2 = 100\times(k_{obs} - k_{cald2})/k_{obs}$ where k_{cald2} values were calculated from **Eq. 4.5** with [MX] replaced by [MX] – $[MX]_0^{op}$ and $[MX]_0^{op}$ = 4.4, 4.8, 5.5 and 9.4 mM at 5, 6, 7 and 10 mM CTABr, respectively, as well as kinetic parameters listed in **Table 4.1**. [d] Error limits are standard deviations. [e] Mean value of δ_{app} (= δ_{app}^{av}) obtained within [MX] range shown in the **Table 3.5** and the error limits are standard deviations.

APPENDIX B (LIST OF PUBLICATION(S))

1. Determination of an Ion Exchange Constant by the Use of a Kinetic Probe: A New Semiempirical Kinetic Approach Involving the Effects of 3-F- and 4-F-Substituted Benzoates on the Rate of Piperidinolysis of Anionic Phenyl Salicylate in Aqueous Cationic Micelles. Yusof, N. S. M. and Khan, M. N., Langmuir, 2010, 26, 10627-10635.
2. Kinetic and Rheological Measurements of the Effects of Inert 2-, 3- and 4-Bromobenzoate Ions on the Cationic Micellar-Mediated Rate of Piperidinolysis of Ionized Phenyl Salicylate. Yusof, N. S. M.; Khan, M. N. J. Colloid Interface Sci (2011), doi: 10.1016/j.jcis.2011.01.061.
3. Kinetic and Rheological Measurements of the Effects of [2-$IC_6H_4CO_2Na$] and [4-$IC_6H_4CO_2Na$] on the Rate of Piperidinolysis of Anionic Phenyl Salicylate. Yusof, N. S. M. and Khan, M. N. Under communication.